

University of Windsor

## Scholarship at UWindor

---

Electronic Theses and Dissertations

Theses, Dissertations, and Major Papers

---

1-1-1971

### The effects of dislocations on the magnetic properties of grain-oriented silicon-steel.

Lakshmi N. Chaudhary  
*University of Windsor*

Follow this and additional works at: <https://scholar.uwindsor.ca/etd>

---

#### Recommended Citation

Chaudhary, Lakshmi N., "The effects of dislocations on the magnetic properties of grain-oriented silicon-steel." (1971). *Electronic Theses and Dissertations*. 6095.

<https://scholar.uwindsor.ca/etd/6095>

This online database contains the full-text of PhD dissertations and Masters' theses of University of Windsor students from 1954 forward. These documents are made available for personal study and research purposes only, in accordance with the Canadian Copyright Act and the Creative Commons license—CC BY-NC-ND (Attribution, Non-Commercial, No Derivative Works). Under this license, works must always be attributed to the copyright holder (original author), cannot be used for any commercial purposes, and may not be altered. Any other use would require the permission of the copyright holder. Students may inquire about withdrawing their dissertation and/or thesis from this database. For additional inquiries, please contact the repository administrator via email ([scholarship@uwindsor.ca](mailto:scholarship@uwindsor.ca)) or by telephone at 519-253-3000ext. 3208.

## INFORMATION TO USERS

This manuscript has been reproduced from the microfilm master. UMI films the text directly from the original or copy submitted. Thus, some thesis and dissertation copies are in typewriter face, while others may be from any type of *computer printer*.

**The quality of this reproduction is dependent upon the quality of the copy submitted.** Broken or indistinct print, colored or poor quality illustrations and photographs, print bleedthrough, substandard margins, and improper alignment can adversely affect reproduction.

In the unlikely event that the author did not send UMI a complete manuscript and there are missing pages, these will be noted. Also, if unauthorized copyright material had to be removed, a note will indicate the deletion.

Oversize materials (e.g., maps, drawings, charts) are reproduced by sectioning the original, beginning at the upper left-hand corner and continuing from left to right in equal sections with small overlaps.

ProQuest Information and Learning  
300 North Zeeb Road, Ann Arbor, MI 48106-1346 USA  
800-521-0600

UMI<sup>®</sup>



THE EFFECTS OF DISLOCATIONS ON THE MAGNETIC  
PROPERTIES OF GRAIN-ORIENTED  
SILICON-STEEL

by

LAKSHMI N. CHAUDHARY

A THESIS

SUBMITTED TO THE FACULTY OF GRADUATE STUDIES  
THROUGH THE DEPARTMENT OF ELECTRICAL  
ENGINEERING IN PARTIAL FULFILMENT OF  
THE REQUIREMENTS FOR THE DEGREE  
OF  
DOCTOR OF PHILOSOPHY

UNIVERSITY OF WINDSOR

1971

UMI Number: DC52675

### INFORMATION TO USERS

The quality of this reproduction is dependent upon the quality of the copy submitted. Broken or indistinct print, colored or poor quality illustrations and photographs, print bleed-through, substandard margins, and improper alignment can adversely affect reproduction.

In the unlikely event that the author did not send a complete manuscript and there are missing pages, these will be noted. Also, if unauthorized copyright material had to be removed, a note will indicate the deletion.

**UMI<sup>®</sup>**

---

UMI Microform DC52675  
Copyright 2009 by ProQuest LLC  
All rights reserved. This microform edition is protected against  
unauthorized copying under Title 17, United States Code.

---

ProQuest LLC  
789 East Eisenhower Parkway  
P.O. Box 1346  
Ann Arbor, MI 48106-1346

APX 5415

Approved by:

*A. Quasi*

*F. Kuffel*

*J. Lindner*

*F. J. Friedlaender*

*P. A. V. Thomas*

365787

## ABSTRACT

The effects of dislocations in grain-oriented silicon-steel on the coercive field strength  $H_c$ , the initial susceptibility  $\chi_i$  and their temperature dependence were investigated. Dislocations were introduced by plastic deformation in tension and their density and arrangement were varied by annealing. The dislocation density was determined by metallographic techniques and parallel measurements of the coercive field strength, the initial susceptibility and the mechanical hardness were made.

The results show that the coercive field strength varies directly and the initial susceptibility inversely, with the fourth root of the plastic tensile strain. The coercive field strength and the mechanical hardness are proportional directly and the initial susceptibility inversely to the square root of dislocation density.

On isochronal annealing, the coercive field strength of deformed specimens increases to a maximum with increasing annealing temperature and then drops steadily below its initial value, whereas the initial susceptibility drops initially and then steadily increases to much higher values. The coercive field strength  $H_c$  and the inverse initial susceptibility ( $\chi_i^{-1}$ ) increase on aging at lower temperatures (200°- 325°) and also during the initial stages of isothermal annealing at temperatures

550<sup>o</sup>- 630<sup>o</sup>C. However, at the later stages of annealing at these (550<sup>o</sup>- 630<sup>o</sup>C) and at higher temperatures (630<sup>o</sup>- 720<sup>o</sup>C), both decrease almost linearly with the logarithm of the annealing time achieving a constant value after prolonged annealing.

Measurements of the temperature dependence of the coercive field strength and the initial susceptibility were made between -196<sup>o</sup> and 750<sup>o</sup>C. The coercive field strength of undeformed specimens decreases monotonically as the temperature is increased from -196<sup>o</sup>C, whereas that of the deformed specimens first rises to a maximum at around 500<sup>o</sup>C and then drops steeply to zero at the Curie temperature.

The initial susceptibility of undeformed specimens decreases with rise of temperature from its value at -196<sup>o</sup>C, exhibits a minimum around room temperature, and increases sharply thereafter to a maximum at about 350<sup>o</sup>C; it steeply decreases again to a second minimum around 450<sup>o</sup>C and then increases to extremely high value slightly below the Curie temperature. With increasing strains, the first maximum is shifted towards lower temperature, is gradually flattened, and almost disappears for 7% deformed specimens.

The results are discussed in the light of various theories of the coercive field and the initial susceptibility and conclusions regarding the magnetization processes are drawn.



## ACKNOWLEDGEMENT

I wish to express my appreciation and sincere gratitude to Dr. A. H. Qureshi for his guidance in carrying out this research. Appreciation is also extended to Dr. J. G. Parr, Dr. E. Kuffel and Dr. P. A. V. Thomas for reviewing the thesis and levelling constructive criticisms.

I would like to thank many members of the departments of Electrical Engineering and Engineering Materials for helpful discussions and advice.

A special note of gratitude is expressed for my wife Krishna and my children Nilabh, Minni and Amitabh for their patient understanding and moral support over the many years of study leading towards the preparation of this thesis.

I am very grateful to the National Research Council of Canada for the financial support of this work.

## TABLE OF CONTENTS

ABSTRACT.....	ii
ACKNOWLEDGEMENT.....	iv
LIST OF FIGURES.....	v
Chapter	
I. INTRODUCTION.....	1
II. THEORETICAL CONSIDERATIONS.....	13
III. EXPERIMENTAL PROCEDURES.....	26
IV. EXPERIMENTAL RESULTS AND DISCUSSION.....	38
4.1 Introduction.....	38
4.2 Dependence of the Coercive Field Strength and the Initial Susceptibility on Deforma- tion and Density of Dislocations.....	45
4.3 Study of the Process of Thermal Recovery..	57
4.4 Temperature Dependence of the Coercive Field Strength.....	91
4.5 Temperature Dependence of the Initial Susceptibility.....	104
V. CONCLUSIONS.....	110
REFERENCES.....	114

## LIST OF FIGURES

Figure		Page
1.1-1	Variation of domain wall energy and restoring force on the wall with its displacement.....	6
3.3-1	Schematic diagram of the Forster Probe Coercimeter.....	29
4.1-1	Orientation of a typical grain in grain-oriented silicon steel.....	40
4.1-2	Surface domain pattern in grain-oriented silicon steel.....	42
4.1-3	Stereographic projection of a number of grains in grain-oriented steel.....	43
4.2-1	Dependence of the coercive field and initial susceptibility on tensile strain.....	48
4.2-2	Dependence of coercive field on the radius of curvature.....	52
4.2-3	Dependence of the coercive field and the initial susceptibility on the density of dislocations.....	54
4.2-4	Typical micrographs.....	55
4.3-1	Isochronal recovery of various deformed specimens of Fe-3.25%Si alloy.....	60
4.3-2	Isothermal recovery of the coercive field of 7% strained specimens.....	62
4.3-3	Isothermal recovery of the coercive field of 5% strained specimens.....	63
4.3-4	Isothermal recovery of the coercive field of 3% strained specimens.....	64
4.3-5	Isothermal recovery of the coercive field of 1% strained specimens.....	65

Figure		Page
4.3-6	Isothermal recovery of the initial susceptibility of 7% strained specimens.....	66
4.3-7	Isothermal recovery of the initial susceptibility of 5% strained specimens.....	67
4.3-8	Isothermal recovery of the initial susceptibility of 3% strained specimens.....	68
4.3-9	Isothermal recovery of the initial susceptibility of 1% strained specimens.....	69
4.3-10	Isothermal recovery of the coercive field and initial susceptibility of specimens with various degrees of deformation.....	71
4.3-11	Temperature dependence of the time of recovery of 7% deformed specimens.....	77
4.3-12	Temperature dependence of the time of recovery of 5% deformed specimens.....	79
4.3-13	Temperature dependence of the time of recovery of 3% deformed specimens.....	80
4.3-14	Temperature dependence of the time of recovery of 1% deformed specimens.....	81
4.3-15	Apparent activation energy as a function of the fractional recovery of $H_c$ and $\chi_i$ ...	82
4.3-16	Isothermal recovery of the microhardness of strained specimens.....	84
4.3-17	Isochronal recovery of the microhardness of strained specimens.....	86
4.3-18	Activation energy for 7% strained specimens at low temperatures.....	89
4.4-1	Temperature dependence of the coercive field strength of deformed Fe-3.25%Si alloy.....	94
4.4-2	Temperature dependence of the coercive field strength of undeformed Fe-3.25%Si and Fe-Cu alloys.....	95

Figure		Page
4.4-3	Variation of $H_C(\max) \cdot \lambda_{100}$ vs $K_1$ for the deformed specimens.....	102
4.5-1	Temperature dependence of the initial susceptibility of undeformed and deformed Fe-3.25%Si alloy.....	105

## CHAPTER I

### INTRODUCTION

In recent years, considerable progress has been made towards the understanding of the magnetization processes of ferromagnetic materials [1-6]. Many of the magnetic properties are known to be structure sensitive, i.e., they are drastically altered by the changes in microstructure and various structural defects. Many theoretical and experimental studies have been made on the influence of various lattice imperfections on the magnetization characteristic [5-20]. In the present work, the results of investigations on the effects of dislocations on the coercive field and the initial susceptibility are presented.

In the demagnetized state of an ideal crystal having no imperfections, the magnetization is uniform in zero field and is aligned almost everywhere, in one of the few crystallographic directions of "easy magnetization", the so-called "crystallographically preferred" directions. The regions in which the magnetization vector lies in one of these crystallographically preferred directions are called "domains" [2,3]. The sub-division of a ferromagnetic specimen into spontaneously magnetized domains, is a natural consequence of

the contributions of the various energies involved in the minimization of the total free energy of the ferromagnetic body [2,3] . The exchange interaction between neighbouring spins tends to align these spins parallel in order to lower the exchange energy. The magnetocrystalline interaction with the exchange energy. The magnetocrystalline interaction with the lattice tends to force the spins along one of the above mentioned crystallographically preferred directions, to minimize the magnetocrystalline anisotropy energy. However, the uniform magnetization of the specimen as a whole would create free pole density resulting in increased magnetostatic self energy. Consequently, to minimize the total free energy of the system, the ferromagnetic crystal divides itself into domains with uniform magnetization along one of the preferred directions.

The gradual transition between the magnetization direction in one domain and that in a neighbouring domain, takes place over a transition layer called domain wall or Bloch wall [2,3] . Inside a domain wall, the neighbouring spins are neither parallel nor oriented in the preferred direction. This involves work against both the exchange forces and the magnetocrystalline anisotropy. Therefore, the wall is a site of a certain amount of energy  $\gamma$  per unit area. The domain wall thickness  $\delta$  is determined by a detailed balance between the competing claims of the exchange and the anisotropy energies in the minimization of the wall energy  $\gamma$ ; the former tending to increase the thickness and the latter tending to decrease it. The domain wall thickness varies

from material to material and is temperature dependent; it decreases with decreasing temperature.

In a crystal having imperfections, the homogeneous magnetization pattern inside a domain is disturbed in the vicinity of various imperfections. The magnetization points locally in the direction of the "effective anisotropy" determined by a compromise between the anisotropy caused by stress field of the crystal defect and the magnetocrystalline anisotropy. The presence of cavities and nonmagnetic inclusions, causes additional distortion due to the creation of internal magnetic poles and associated magnetostatic energy. The inhomogeneities in the spacial distribution of magnetization are responsible for the interaction between the domain walls and the crystal defects. As a consequence, the wall energy varies with the position of the wall and depends on the number and the types of the crystal defects encompassed.

In general, the magnetization of a ferromagnetic body in an external field, may be changed by either or a combination of both of the following processes [2-5] : (i) by the domain wall displacement, i.e., the volume of the domains favourably oriented with respect to the applied field growing at the expense of the less favourably oriented domains or (ii) by the rotational process, i.e., the magnetization vectors inside the domains rotating towards the field direction.

It is now experimentally established [10-12] that in magnetically multiaxial crystals, (such as those of iron and



nickel having many directions of easy magnetizations, and large crystal anisotropy), the changes in magnetization in small magnetic fields and in the neighbourhood of the  $H_C$  point (i.e., the steep part of the virgin magnetization curve), take place mainly through the displacement of Bloch walls; predominantly  $180^\circ$  walls. The change in magnetization by the rotational process occurs only at much higher fields near saturation. Rotational processes are also responsible in cases where the domain structure breaks down; at higher temperatures when the crystalline anisotropy is vanishingly small (or in small particles). The contribution of these processes to the overall change in magnetization is affected greatly by the lattice defects. However, the displacement of the domain wall is much more impeded due to the lattice defects than the rotational process.

The magnetization of the ferromagnetic specimen could be reversible or irreversible (in thermodynamic sense). This is characterized by the phenomenon of hysteresis. The associated properties of technical importance are the coercive field strength and the initial susceptibility [1,2,4].

The coercive field strength of a specimen is defined as the negative magnetizing field required to bring the remanent induction to zero after the specimen has been magnetized to saturation [1,2]. The coercive field strength is an important parameter due to the fact that the energy dissipated in going once around the hysteresis loop is equal

to the area of the loop, and is of the order of the product of the saturation induction  $B_s$  and the coercive field  $H_c$  [1,2]. The initial susceptibility is a measure of the magnetizability of a demagnetized ferromagnetic specimen in small fields and is given by the slope of the virgin magnetization curve in its initial linear and reversible part (at the origin). This is of importance in communication circuits where the material is usually subjected to low magnetizing fields.

Any theory of coercive field strength and initial susceptibility must provide a mechanism whereby, in passage through the crystal, the energy  $E_w$  of the domain wall or the total restoring force  $P$  ( $= \frac{dE_w}{dz}$ , the gradient of the wall energy) must vary with the position of the wall as shown in fig. (1.1-1). There are then, positions of energy minima and the walls will take up these positions. In order to displace the walls and with that increase the magnetization, it is necessary to apply an external field which in effect exerts a pressure on the walls. For small fields and displacements up to the point B, the magnetization is continuous and reversible. This determines the initial susceptibility. As the field strength is increased beyond point B, the walls move in steps, i.e., jump further until halted by a greater hindrance which can be overcome by a further increase in the applied field ( Barkhausen jumps ) [1, 2] . These uneven volume changes of domains can only be reversed by the application of negative magnetizing field. Therefore, in the thermo-

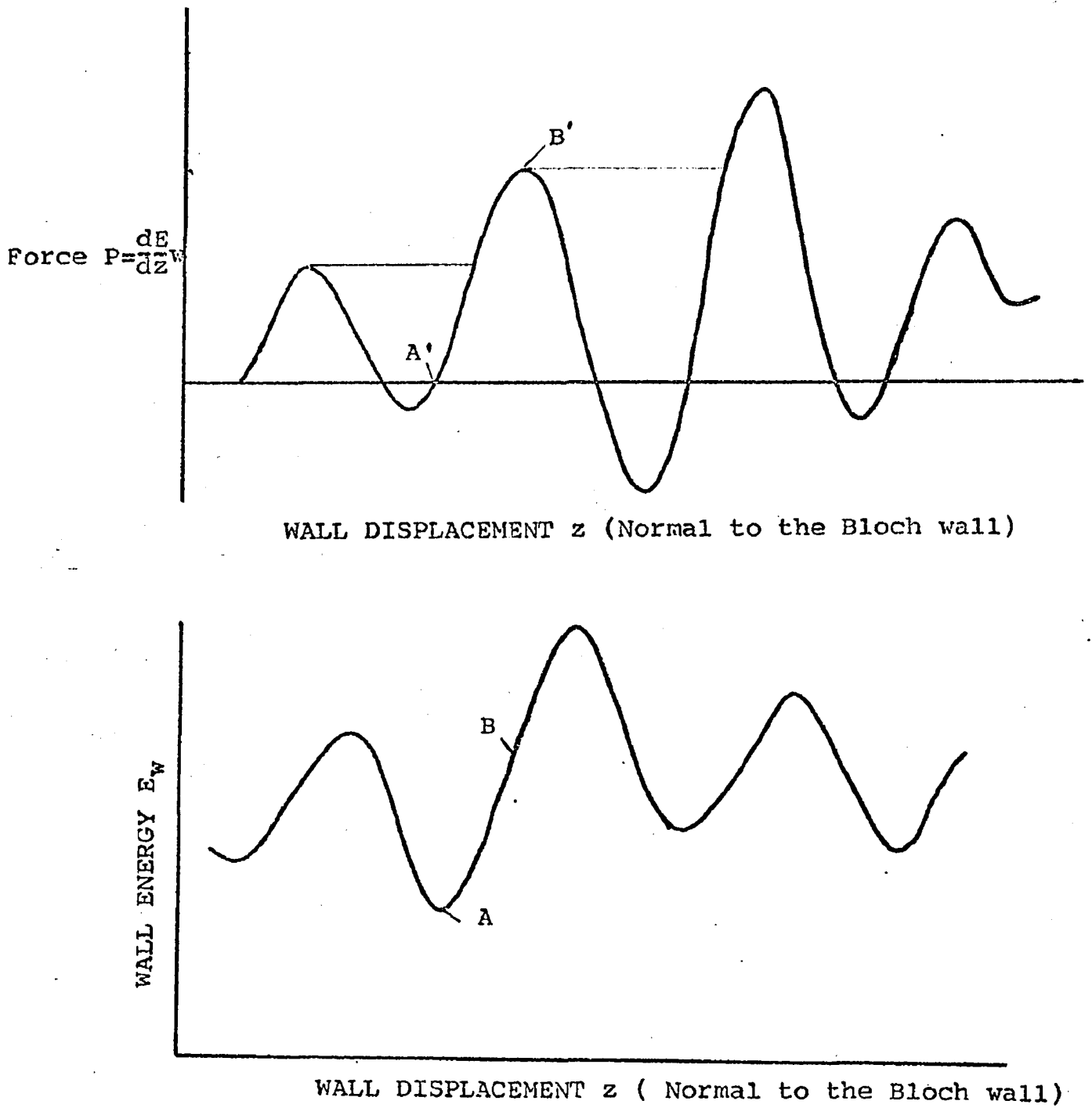


Fig. 1.1-1. Variation of the domain wall energy and the restoring force on the wall with displacement normal to the wall

dynamic sense, they are irreversible.

The matrix disturbances hindering the wall movement are known to be internal stresses and dislocations, nonmagnetic inclusions, cavities and inhomogeneities in composition resulting in local fluctuations in the magnetization. The relation between the coercive field strength, the initial susceptibility and the matrix disturbances can be evaluated if the kind, intensity, and space distribution of the disturbances as well their specific interaction with the Bloch walls, i.e., their effectiveness as hindrances for the wall movement, are known quantitatively. For the quantitative understanding of the coercive field strength and the initial susceptibility, various theories have been proposed. However, they differ from one another because each one of them is related in a special way to one of the above mentioned disturbances (e.g. stress theory [21-24], foreign body theory [23], stray field theory [25], dislocation theory [6-9]).

Each theory assumes the influence of a single type of disturbance on the domain wall movement and neglects all the others present in the material. Furthermore, in the absence of a detailed knowledge of the internal structure of the material, each theory makes special assumptions about the distribution of the disturbances inside the material to avoid complications in calculations.

The role of internal inhomogeneous stresses, which always exist in a material, in impeding the magnetization

process was first suggested by Bloch [2] and this idea was further developed by Kondorski [21] and Kersten [22, 23] (stress theory). The energy of the Bloch wall varies with position as a consequence of the variation of the effective anisotropy resulting from its dependence on the internal stresses through magnetostriction [24]. Kersten [23] studied the effect of the amount and size of the non-magnetic inclusions on the coercive field and the initial susceptibility (foreign body theory or inclusion theory). According to Kersten, the change in the wall energy, caused by the presence of inclusions was a simple surface tension effect. The wall, in a position where it intersects a number of inclusions, will have smaller area, and therefore a lower energy, than in a position where no inclusions are intercepted. He used a highly simplified model in which the nonmagnetic inclusions are pictured as spheres arranged in a cubic lattice. Neel [20] criticized these theories and pointed out that implicit assumptions of rigid domain wall and regular distribution of inclusions, greatly overvalue the coercive field for actual materials where the perturbations might be more or less random. Furthermore, the magnetostatic energy associated with the presence of internal poles at the interface between the inclusion and the matrix far exceeds the changes in wall energy associated with the presence of inclusions. He extended these theories by taking into account the demagnetizing energy resulting from the inhomogeneities in the direction

of the magnetization produced by both internal stresses and inclusions. These theories were further developed by Kondorski [26] and Goodenough [25] .

Becker and Döring [24] have shown that the main contribution to the interaction between the internal stresses and spontaneous magnetization  $M_s$  is due to magnetostriction and that this interaction is described quantitatively by the magnetoelastic coupling energy which is a function of the direction of spontaneous magnetization, the magnetostrictive constants and the stress tensor of the structural defects. Another contribution arises from the fact that in the neighbourhood of the lattice defects, the crystal properties such as spontaneous magnetization, magnetocrystalline anisotropy etc. may be changed. Thus the magnetization distribution in the vicinity of the lattice defects is changed due to magnetoelastic interaction and change in the crystal properties. In the earlier theories [23,24], the internal stresses were characterized by an average stress amplitude, their source remaining unspecified. The modern theories [27-29] recognize that the internal stresses are associated with dislocations in the crystals. Dislocations are line defects in a crystal and cause internal stresses whose magnitude varies as the inverse of the distance 'r' from the dislocation line. Vicena [7], Kersten [8,9] and Trauble [6] have developed quantitative theories based on the dislocation model with different assumptions.

Systematic experimental studies on the quantitative relationship between a particular matrix disturbance, its distribution, size and shape, and particular magnetic properties are scarce. Experimental data on the influence of nonmagnetic inclusions on magnetic properties are due to Dijkstra and Wert [16] and Qureshi [17]. In [16] the influence of finely dispersed iron-carbide precipitates on the coercive field of iron was reported. In [17], the effects of volume, size and shape of randomly distributed copper precipitates on the coercive field and initial susceptibility were studied. Measurements on the effects of plastic deformation on the magnetic properties have been made on nickel single crystals by Dietrich & Kneller [12], Malek [18], Krause [58], Rieger [59] and Köster [60] and on iron single crystals by Malek [18] and Bilger and Träuble [10].

In these studies attempts were made to correlate the experimental data with the predictions of dislocation-theories of coercive field and initial susceptibility only indirectly--through plastic deformation and theories of work-hardening. Assumption was made that a given state of plastic deformation is uniquely associated with a certain density of dislocations. No attempt was made to determine the dislocation density. In most studies parallel measurements of  $H_c$  and  $\chi_i$  were not made.

Up to now, to the author's knowledge, there are no experimental data available on the quantitative relation between the coercive field, the initial susceptibility and dislocation density. The present investigations are an attempt to obtain reliable data and to compare these results with the theoretical statements in the literature.

It is difficult indeed to get complete and reliable information as to the internal state of the material and to devise a method by which only a single type of matrix disturbances (such as dislocations) are introduced. However, it is assumed for the present work that the dislocations are the dominant defects introduced by the plastic deformation, to which all the changes in the magnetic properties are attributed. The number of all other types of defects so developed or otherwise present is assumed to be small and their contribution to any change in the magnetic properties is considered as negligible.

In the present investigations the material used was Fe-3.25% Si grain-oriented transformer steel. The choice of this material was favoured by the fact that most of the physical constants of this alloy are known and available in the literature. Furthermore, quite reliable techniques for the etching of dislocations in this material have been established [31-36]. The dislocations were introduced in the specimens by plastic deformation by



tension and their density and geometrical arrangements were varied by annealing the specimens for various durations of time at different temperatures. The coercive field strength, the initial susceptibility and the mechanical hardness were measured. In parallel, the dislocation density was determined using metallographic techniques. The variation of the coercive field strength and the initial susceptibility as a function of temperature was also studied from  $-196^{\circ}\text{C}$  to the Curie temperature. Data were obtained using similar specimens of identical metallurgical and mechanical history.

In chapter II various dislocation theories of coercive field strength and initial susceptibility are discussed. In the subsequent chapters, the experimental data are obtained and the results are critically analysed and compared with the theories. Due to simplified models used as the basis of various theories, these results may not necessarily agree with any of them. However, it is expected that these results contribute towards further understanding of the process of magnetization and form a basis for a modified theory of hysteresis.

## CHAPTER II

### THEORETICAL CONSIDERATIONS

All modern theories of the coercive field strength  $H_c$  and the initial susceptibility  $\chi_i$  are based on simplified models which take into consideration the interaction of only one type of lattice defect with either of the magnetization processes e.g., the displacement of domain wall or the rotation of the magnetization vector inside the domains.

In general, the magnetization process is of a complex nature and both the processes may contribute towards the overall changes in magnetization; furthermore, lattice defects of more than one type are usually present.

In the simplest case, in magnetically multiaxial crystals of iron and nickel where crystal anisotropy is much larger than any stress anisotropy, the changes in magnetization take place predominantly by the displacement of domain walls. When the stress anisotropy is predominant, magnetization changes by rotational process.

In the following, the principles of calculations and final results of coercive field strength and the initial susceptibility based on various dislocation-models are discussed.

## CALCULATION OF THE COERCIVE FIELD STRENGTH

(a) The Change in Magnetization by Bloch Wall Displacement

It is assumed that the changes in magnetization are entirely due to the displacements of Bloch walls which are not strongly coupled to each other and no rotational process occurs. The restoring force opposing the displacement of a Bloch wall under the pressure of an external magnetic field is essentially due to its interaction with the lattice defects. For a random distribution of defects, the number of defects interacting with the wall will vary with the position of the wall ; also the interaction energy (or its gradient, the interaction force) due to a certain defect depends on its distance from the centre of the wall. Therefore, the total interaction potential of the wall (or the interaction force) during its movement through the network of defects depends on the position of the wall in the crystal; varying irregularly as shown in fig. (1.1-1). A domain wall occupying the position of minimum energy may be displaced by the action of an externally applied field. The motion of the wall goes on partially reversibly and partially by more or less large irreversible jumps. Then the coercive field is identified as that field at which these jumps are of the order of the domain diameter.

If  $E^{(i)}$  is the energy of interaction of the  $i$ -th wall separating domain '1' and domain '2', with the lattice defects

at a certain position of the wall, and the wall moves under the action of an externally applied field so that the volume of the domain 1 grows at the expense of domain 2 causing a change in the magnetic energy, then,

$$dE^{(i)} = H M_S (\cos \phi_1 - \cos \phi_2) dv^{(i)} \quad (2.1)$$

where

$dE^{(i)}$  = the increase in the energy of interaction of the  $i$ -th wall with the lattice defects at its new position after this movement

$H$  = the externally applied field

$M_S$  = the saturation magnetization

$\phi_1, \phi_2$  = the angles between the field  $H$  and the magnetization vectors of domain 1 and domain 2 respectively.

$dv^{(i)}$  = the increase in the volume of domain 1 due to the movement of the  $i$ -th wall.

The equilibrium value of the field is given by,

$$H = \frac{1}{M_S (\cos \phi_1 - \cos \phi_2)} \left| \frac{dE}{dv} \right| \quad (2.2)$$

Therefore, the coercive field strength corresponding to the  $i$ -th wall will be

$$H_C^{(i)} = \frac{1}{M_S (\cos \phi_1 - \cos \phi_2)} \left| \frac{dE}{dv} \right|_{\max}^{(i)}$$

and the coercive field strength for the whole specimen will be given by

$$H_C = \frac{1}{M_S} \left\langle \frac{1}{(\cos \phi_1 - \cos \phi_2)} \left| \frac{dE}{dv} \right|_{\max} \right\rangle \quad (2.3)$$

Where the average is over all the domain walls. This equation is the basis of all theoretical calculations of the coercive field strength.

For magnetically multiaxial crystals such as iron and nickel, the changes in magnetization in the neighbourhood of the  $H_c$  point are mainly through the displacement of  $180^\circ$  domain walls. On considering the displacement in the  $z$  direction--normal to the wall, in the  $x, y, z$  rectangular co-ordinate system, the coercive field is given by

$$H_c = \frac{1}{2M_s L_x L_y \cos \phi} \left\langle \left| \frac{dE}{dz} \right|_{\max} \right\rangle_{Av} \quad (2.4)$$

Where

- $L_x, L_y$  = the dimensions of an element of  $180^\circ$  wall in  $x$  and  $y$  directions respectively  
 $\phi$  = angle between the applied field and the magnetization vector in domain 1.  
 $dz$  = distance in the  $z$  direction, the wall has moved.

The gradient of the interaction energy of the wall is the interaction force, i.e.,  $\frac{dE}{dz} = P$ , the total force acting on the wall in the  $z$  direction due to all the defects.

Therefore from eqn. (2.4)

$$H_c = \frac{1}{2M_s L_x L_y \cos \phi} \left\langle \left| P_{\max} \right| \right\rangle_{Av} \quad (2.5)$$

Where  $P_{\max}$  is the total maximum force acting on the wall.

at location  $z$ .

If  $m_j$  = number of defects of type  $j$  interacting with the Bloch wall at location ' $z$ '

$p_j$  = force exerted by a defect of type ' $j$ '

Then the total force  $P$  acting on the wall at ' $z$ ' due to all the defects is given by

$$P = \sum m_j p_j$$

and therefore

$$H_C = \frac{1}{2M_S L_X L_Y \cos \phi} \left\langle \left| \sum (m_j p_j) \right|_{\max} \right\rangle_{Av} \quad (2.6)$$

The expression  $\left\langle \left| \sum (m_j p_j) \right|_{\max} \right\rangle$  has been evaluated by Trauble [6].

If  $N_j$  = average density of dislocation of type  $j$

$$\bar{m}_j = N_j L_X L_Y ;$$

the average number of dislocations interacting with the element of the wall of surface area  $L_X L_Y$ .

$d$  = average width of the domains in  $z$  direction

$\delta$  = thickness of the domain wall

$d/2\delta$  = the number of statistically independent positions, the wall can assume over a distance ' $d$ ' for which the  $H_C$  will have independent values.

The coercive field is evaluated as

$$H_C = \frac{[\ln (d/2\delta)]^{\frac{1}{2}}}{2M_S L_X L_Y \cos \phi} \left[ \sum \bar{m}_j P_j^2 \right]^{\frac{1}{2}}$$

using

$$m_j = N_j L_x L_y$$

$$H_C = \frac{(\ln d/2\delta)^{\frac{1}{2}}}{\sqrt{2} M_S \sqrt{L_x L_y} \cos \phi} \left[ \sum N_j P_j^2 \right]^{\frac{1}{2}} \quad (2.8)$$

The coercive field strength can thus be calculated from expression (2.4) by calculating the energy of interaction  $E$  between the domain wall and a dislocation or from (2.8) by calculating the force of interaction  $p_j$  exerted on the wall by a dislocation of type  $j$ .

Vicena [7] was the first to investigate the interaction between the Bloch wall and the dislocations. He assumed a plane  $180^\circ$  wall in a crystal of cubic symmetry, and a dislocation parallel to the wall. For this configuration he calculated the effects of the stress field of the dislocations on the Bloch wall and calculated the magneto-elastic coupling energy between them. By using statistical techniques of Neel [20], he found the value of the coercive field as

$$H_C = \frac{3|\lambda| bG}{8M_S d} \frac{1+\nu}{1-\nu} \left[ \delta^2 \ln \frac{d}{\delta} \right]^{\frac{1}{2}} N^{\frac{1}{2}} \quad (2.9)$$

Where

- $N$  = density of dislocations
- $\lambda$  = saturation magnetostriction constant
- $b$  = Burger's vector
- $\nu$  = Poisson's ratio
- $G$  = modulus of elasticity in shear

$d$  = average width of the domains

$\delta$  = thickness of the domain wall.

The expression (2.9) states a direct relationship between the coercive field strength and the square root of the density of dislocations. Rieder [13] on the other hand calculated the force of interaction between the domain wall and dislocation. For a [111] screw dislocation and a plane  $180^\circ$  wall, the interaction force is calculated to be

$$P_{111} = \frac{\sqrt{3}}{2} \pi \delta b \lambda_{100} (C_{11} - C_{12}) \quad (2-10)$$

where

$\delta$  = thickness of domain wall

$b$  = Burger's vector

$\lambda_{100}$  = magnetostriction constant

$C_{11}, C_{12}$  = coefficients of elasticity

According to Pfeffer [14] the expression gives the interaction force for all orientations of  $180^\circ$  and  $90^\circ$  walls and all types of dislocation provided the Bloch wall has a symmetrical spin arrangement along the direction normal to the wall which is always the case in iron [69]. If  $N$  = the density of all types of dislocations, the final expression for  $H_c$  in terms of the material constants and the density of dislocations according to Träuble [6] is given by

$$H_c = \frac{\pi \sqrt{3} \sqrt{d/2\delta}}{2 \sqrt{2} \sqrt{L_x L_y} \cos \phi} \frac{(C_{11} - C_{12}) b \delta \lambda_{100}}{M_s} N^{\frac{1}{2}} \quad (2.11)$$

Expression (2.11) also gives a direct proportionality between the coercive field strength and the square root of dislocation



density.

(b) Magnetization Changes by Irreversible Bending of Bloch Wall

Kersten [8] has calculated the expression for the coercive field with another assumption. Instead of considering a domain wall advancing rigidly through the network of dislocations, he considers a deformable wall so that under the pressure of an external field the wall bends about the dislocations. The value of the coercive field is given by the critical field necessary to bend the wall in the form of a semicircle; at this field the wall breaks away from the pinning points. He assumes the absence of any stray field and considers the over simplified model in which dislocations have a cubic distribution.

The expression for  $H_c$  in this situation is given by

$$H_c = \frac{1}{\mu_0 M_0} \sqrt{\frac{K_1 k T_c}{a}} \frac{1}{s} \quad (2.12)$$

$$= \frac{1}{\mu_0 M_0} \sqrt{\frac{K_1 k T_c}{a}} N^{\frac{1}{2}}$$

where

$M_0$  = saturation magnetization at  $0^\circ K$

$K_1$  = magnetocrystalline anisotropy constant

$k$  = Boltzmann constant

$T_c$  = Curie temperature

$a$  = lattice constant

$s$  = distance between pinning points.

$\mu_0$  = permeability of free space.

$N$  = density of dislocations; for regular arrangement of dislocations  $\frac{1}{S} = \sqrt{N}$

The expression (2.12) also shows that the coercive field is directly proportional to the square root of the dislocation density.

(c) Changes in Magnetization by Rotational Process

If the material is subjected to high internal stresses  $\sigma_i$  so that the stress anisotropy energy ( $\phi_s \sim \lambda \sigma_i$ ) is large compared to the crystal anisotropy energy ( $\phi_k \sim K_1$ ) the domain structure breaks down [61]. The magnetization points in the direction of the effective anisotropy determined by a compromise between the magnetoelastic interaction with the dislocations and the crystal anisotropy. Similar situation occurs also at higher temperatures when the crystal anisotropy is vanishingly small. The change in magnetization in this situation takes place essentially by rotational process against the effective anisotropy. The coercive field in this case is given by the expression, [6,24]

$$H_c = \frac{3|\lambda| |\sigma_i|}{M_s} - \frac{2|K_1|}{M_s} \quad (2.13)$$

and for the case when

$$\phi_s \gg \phi_k \quad \text{or} \quad |\lambda| |\sigma_i| \gg |K_1|$$

$$H_c = \frac{3 |\lambda| |\sigma_i|}{M_s} \quad (2.14)$$

Using  $\sigma_i \sim G$ , the modulus of elasticity in shear, the coercive field for strained specimens especially at higher temperature is given by [24]

$$H_c = \frac{\lambda G}{M_s} \quad (2.15)$$

The expressions derived in this section will be compared with experimental results when appropriate.

#### CALCULATION OF INITIAL SUSCEPTIBILITY

The initial susceptibility is a measure of the magnetizability of a demagnetized ferromagnetic specimen in small fields in the linear region of the magnetization curve and is defined as

$$\chi_i = \lim_{\Delta H \rightarrow 0} \left. \frac{\Delta M}{\Delta H} \right|_{\substack{M=0 \\ H=0}} \quad (2.16)$$

where  $\Delta M$  is the small change in magnetization caused by the application of small magnetic field  $\Delta H$  near the origin of the magnetization curve. The change in magnetization may be caused by domain wall displacement or magnetization rotation and therefore the expressions for  $\chi_i$  will again depend upon the mode of magnetization change.

(a) Change in Magnetization by 180° Bloch Wall Displacement

The equilibrium value of the field for a small displacement  $dz$  of the 180° wall may be written from eqn. (2.2) as

$$H = \frac{1}{2 M_S L_x L_y \cos \phi} \cdot |P| \quad (2.17)$$

Where  $P$  is the total force of interaction on the wall of surface area  $L_x L_y$ . From eqn. (2.16) one gets

$$\chi_i = \left. \frac{dM/dz}{dH/dz} \right|_{\substack{M=0 \\ H=0}} \quad (2.18)$$

Using eqn. (2.17) and (2.18) the expression for initial susceptibility is given by

$$\chi_i = \frac{4 M_S^2 \cos^2 \phi L_x L_y}{d} \left\langle \frac{1}{|dP/dz|} \right\rangle \quad (2.19)$$

where  $d$  is the average domain width.

The average  $\left\langle \frac{1}{|dP/dz|} \right\rangle$  is to be taken over all the zero points in the  $P(z)$  curve of fig. (1.1-1). For a crystal demagnetized by an alternating current the statistical calculations of Träuble gives

$$\chi_i = \frac{1.7 M_S^2 \delta \cos^2 \phi (L_x L_y)^{1/2}}{d} \left[ \sum N_j P_j^2 \right]^{-1/2} \quad (2.20)$$

Using the value of  $P$  from eqn. (2.10) the final expression

for  $\chi_i$  is obtained as

$$\chi_i = \text{const.} \frac{M_s^2}{d \lambda_{100} (C_{11} - C_{12})} N^{-\frac{1}{2}} \quad (2.21)$$

or

$$\chi_i \sim N^{-\frac{1}{2}} \quad (2.22)$$

According to eqn. (2.22) the initial susceptibility at constant temperature is inversely proportional to the square root of dislocation density.

(b) Magnetization Changes by Reversible Bending of Bloch Wall

Kersten [8] calculated the initial susceptibility with the assumption of a model in which the change in magnetization is caused by bending of the Bloch wall under the pressure of an external field. The pinning points are provided by the dislocations. He assumed a regular distribution of dislocations arranged in a cubic lattice, the edges of which are parallel to the wall. The effects of any stray field are neglected. The expression for  $\chi_i$  according to Kersten is

$$\chi_i = \frac{\mu_0 M_0}{6} \sqrt{\frac{a}{k T_c}} \frac{s^2}{d} \quad (2.23)$$

$$= \frac{\mu_0 M_0}{6} \sqrt{\frac{a}{k T_c}} \frac{1}{Nd} \quad (2.24)$$

where the symbols are essentially the same as in eqn. (2.12).

Finally

$$\chi_i = \text{const.} \frac{1}{N} \quad (2.25).$$

According to Kersten the initial susceptibility is inversely proportional to the density of dislocations.

(c) Change in Magnetization by Rotational Process

As mentioned before, when the stress anisotropy is large compared to the crystal anisotropy (  $|\lambda| |\sigma_i| \gg K_1$  ), the domain structure breaks down and the change in magnetization takes place by the rotation of the magnetization vector against the stress anisotropy. The initial susceptibility in this case is given by [6]

$$\begin{aligned} \chi_i &= (\text{const.}) \frac{M_s^2}{|\lambda| |\sigma_i|} \\ &= (\text{const.}) \frac{M_s^2}{\lambda G} \end{aligned} \quad (2.26)$$

The theories of coercive field and initial susceptibility discussed in this chapter will be compared with the experimental results in the subsequent chapters.

## CHAPTER III

### EXPERIMENTAL PROCEDURE

#### 3.1 SPECIMEN PREPARATION

The material used in the present investigations was grain-oriented silicon steel sheet of thickness 0.33 mm made by Westinghouse Company. The grain orientation in this material is (110) [100] so that the rolling plane is parallel to (110) plane and the rolling direction to the [100] direction. Specimens of 15 mm width were prepared with their length parallel to the rolling direction. In order to eliminate the effects of machining and previous workhardening the specimens were annealed in dry hydrogen atmosphere at 1000°C and subsequently furnace cooled at the rate of 50°C per hour.

The chemical composition of the specimen was as follows:

Si - 3.25%; Cr - 0.05%; Ni - 0.02%

Mn - 0.02%; Cu - 0.02%; Ti - 0.001%

C - 0.008%; other impurities 0.03% and the remainder iron.

The deformation of the specimens was done by a tensile machine (manufactured by Instron Co.). In all cases the specimens were strained at room temperature and at a strain rate of 0.2% per minute. The values of net plastic strain

were estimated to be within 4% of the nominal value (checked with a traveling microscope). The size of the undeformed and deformed specimens used for the measurement of the coercive field strength and the initial susceptibility was  $120 \times 15 \times 0.33 \text{ mm}^3$ .

The annealing of the specimens was done in a tube furnace in hydrogen atmosphere. The hydrogen was passed through a palladium diffusion cell to reduce the moisture content. For the specimens to be used for metallographic studies, the hydrogen was bubbled through n-heptane, a saturated hydrocarbon. This reduces the possibility of decarburization and helps to get reliable etching results.

### 3.2. MEASUREMENT OF HARDNESS

Diamond pyramid hardness measurements were made on the specimens after electropolishing with the Leitz miniload hardness tester. Because of the small thickness of the specimens a light load of 500 g was used. The values of hardness measured over the polished surface of the specimen varied from point to point and therefore, always 10 measurements were made on the same specimen and for each point on the curve, three specimens were used. Therefore, the values recorded on the hardness curves are an average of 30 measurements for the same metallographic history of the material.



### 3.3 MEASUREMENT OF COERCIVE FIELD STRENGTH

The measurement of the coercive field strength was made by a Forster probe pair coercimeter. The operation of the coercimeter is described here and the schematic diagram is shown in fig.(3.3-1). A field coil is mounted on a suitable stand. By proper orientation of the stand and the use of external magnets, the earth's field at the centre of the coil is virtually eliminated. A variable D. C. voltage is applied to the coil through a reversing switch. The sample is now placed inside the field coil and the field is increased to a maximum of 1400 Oe so as to saturate the sample and then slowly reduced to zero. The remanant magnetization intensity is indicated on a precision magnetic field meter using the Forster probe pair. The coil field is now increased in the opposite direction to a value  $H_c$  to make the readings on the field strength sensor zero. The coercive field strength is then directly read on the meter. Each of the Forster probe pair consists of two windings, a primary and a secondary winding around a high permeability core. The primary windings of the pair are connected in series opposition and the secondary windings in series addition. The output voltages of the secondary windings cancel when no magnetic field affects the probe cores. The high permeability cores are driven into saturation by a low frequency alternating current flowing through the primaries. If the

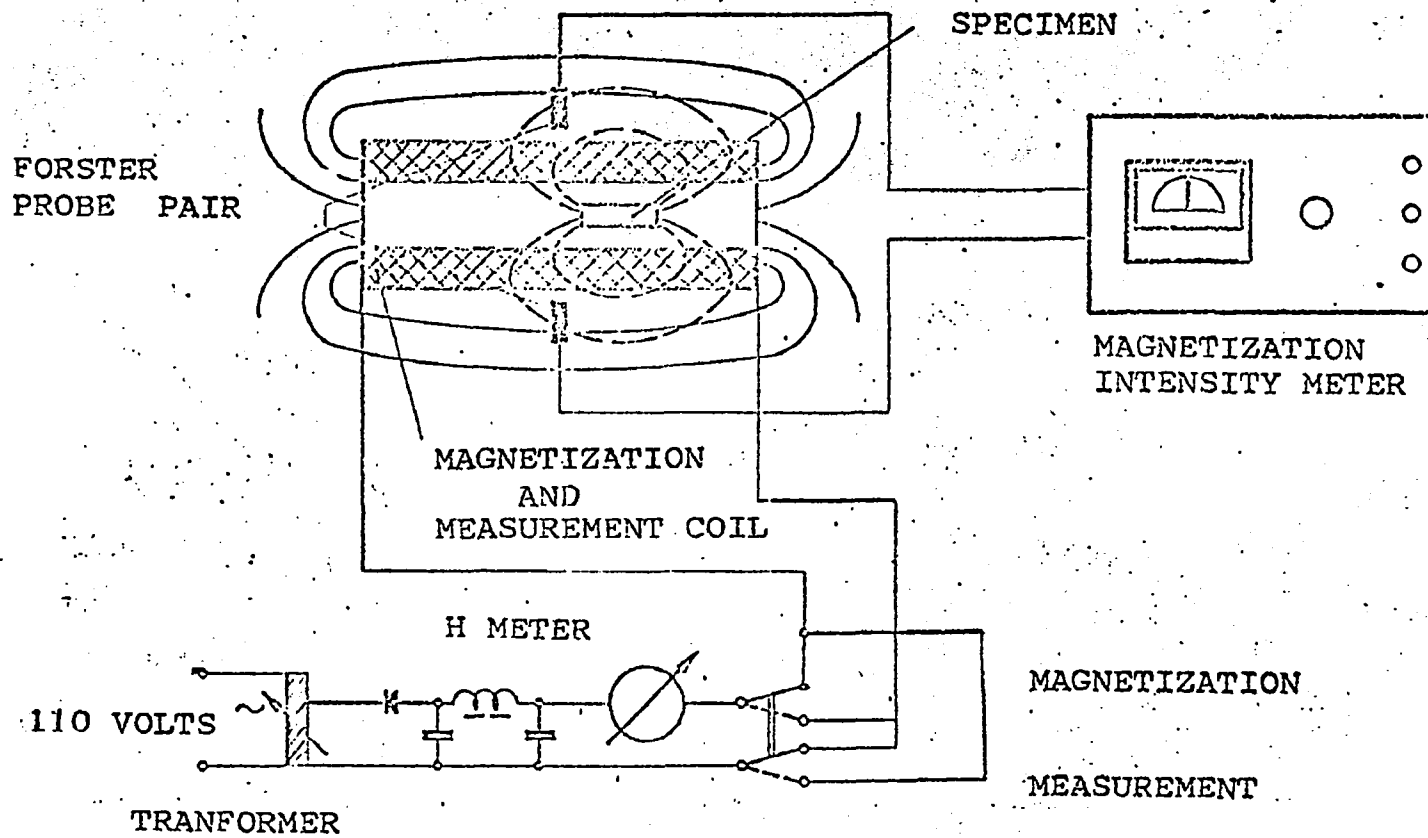


Fig. 3.3-1 . Schematic diagram of the coercimeter.

cores are placed in a D.C. magnetic field a secondary voltage containing even harmonics is developed. The resultant output voltage of the probe pair is proportional to the D.C. field (this equipment utilizes the second harmonic of the secondary). The probes are symmetrically placed on both sides of the field coil so that the magnetic field produced by the field coil is automatically compensated and the magnetic field emanating from the sample only, is indicated. The sensitivity of the instrument is 5 moe in the range of 0.5 Oe full scale deflection.

For the measurement of the temperature dependence of the coercive field, a tube furnace with a bifilar winding, surrounded by a cylindrical water jacket was built. This assembly was inserted into the field coil of the coercimeter. The temperature was uniform ( $\pm 5^{\circ}\text{C}$ ) for about 15 cm length of the furnace where the specimens were placed. The rate of temperature-rise was suitably adjusted so that a set of measurements from room temperature to  $700^{\circ}\text{C}$  could be made in about 10 minutes. This was necessary to avoid extensive recovery of the specimens during the period of a set of measurements.

The coercive field at  $-196^{\circ}$  and  $-78^{\circ}\text{C}$  was measured by placing the specimens in liquid nitrogen and in a mixture of dry ice and methanol respectively in a quartz boat. The boat of a suitable size was specially made for this purpose which could be placed inside the coil of the coercimeter.

### 3.4 MEASUREMENT OF INITIAL SUSCEPTIBILITY

The initial susceptibility ( $\chi_i$ ) is the slope of the linear and reversible part of the virgin magnetization curve of an ideally demagnetized specimen and is generally defined by the expression

$$\chi_i = \lim_{\Delta H \rightarrow 0} \frac{\Delta M}{\Delta H} \quad \left| \begin{array}{l} M = 0 \\ H = 0 \end{array} \right.$$

where  $\Delta M$  is the corresponding change in the magnetization brought about by a small field change  $\Delta H$ . The basis of the above equation defining  $\chi_i$  is that the measurement must be made at very small field and at low magnetization value i.e., near the origin of the magnetization curve. To measure the susceptibility of a material it is necessary to determine the magnetization as a function of the "internal" field and hence a closed magnetic circuit is required. The closed magnetic circuit can be obtained in the following ways:

(i) making a toroidal sample which creates no free poles when magnetized tangentially and hence no self demagnetization occurs, (ii) by using a suitable yoke as part of the magnetic circuit.

For most of the measurements at room temperature the second technique was employed. On a nonmagnetic former, 9 cm long, a primary winding of 20 turns and a secondary of 4000

turns , were wound. The specimen was put inside this coil and two semicircular permalloy yokes of relatively large cross-section of 2.25 sq. cm and very high permeability ( $\mu_r = 20,000$ ) were clamped to the two sides so as to make a complete magnetic circuit. Care was taken to obtain a good magnetic contact at the yokes. The initial susceptibility was measured ballistically and in all cases at field strength of 2.5 mOe. A Siemens super ballistic galvanometer was used ; this had a sensitivity of  $2.5 \times 10^{-9} \frac{\text{amp}}{\text{mm/m}}$  with 50 ohms damping resistance.

To study the temperature dependence of the initial susceptibility, the first technique was used so as to avoid the use of the yoke. Toroids were synthesized by stacking 2 cm wide strips of the material. These were approximately 40 mm and 45 mm inside and outside diameter respectively and were wound with two windings, a primary of 20 turns and a secondary of 150 turns using fibrefrax paper insulation ( a material of working temperature up to  $1200^\circ\text{C}$  available in liquid, powder and paper form made by Carborundum Co.) The measurements of initial susceptibility in this case were made at a field strength of 5 mOe which was well within the linear region of the magnetization curve.

Before each reading the specimen was demagnetized by passing an alternating current (60 Hz) of gradually diminishing amplitude through one of the windings. For the measurement of initial susceptibility at  $-78^\circ$  and  $-196^\circ\text{C}$  the

toroidal specimen was kept in a bath of the mixture of dry ice and methanol in the former case and in liquid nitrogen in the latter case. For the high temperature measurements, the toroids were put in a suitable resistance furnace having high heating rate. A set of measurements from room temperature to 700°C took around 45 minutes. The measurement of the specimen temperature was made by a thermocouple inserted into the toroidal specimen.

An error is introduced in the susceptibility measurement due to the use of yokes and unavoidable air gaps. However, for a comparatively large cross-section of the yoke (2.25 cm<sup>2</sup>) of high permeability ( $\mu_r=20000$ ) material and an air gap of few microns the error is less than 2% compared to a closed magnetic circuit.

## METALLOGRAPHIC STUDIES

### 3.5.1. EXPERIMENTAL

The specimens were wet-ground to 600 grit size and then a surface of about  $\frac{1}{2}$  cm<sup>2</sup> was electropolished with the Disa electropolishing machine using methanol-perchloric acid electrolyte. The actual composition of the polishing electrolyte used was:

perchloric acid	200 cc.
methanol	700 cc.
ethylene glycol monobutyl ether	100 cc.

The polishing time was 15 sec. at a current density of

3 amp/cm<sup>2</sup>. The polished surface was rinsed with water and then with methanol-1% hydrochloric acid solution for 15-20 seconds and finally with methanol and then dried. It was found that washing with methanol-HCl solution gives better etching results, probably by removing the top thin layer of the electrolytic products from the polished surface.

The specimens were then etched electrolytically.

The etching electrolyte was of the composition:

chromic acid (powder)	25gms.
acetic acid	33 cc.
water	7 cc.

The etching time in all cases was seven minutes at a current density of 20 ma/cm<sup>2</sup>. After etching, the surface was immediately washed with water and finally with alcohol and dried in a warm air stream. This etching electrolyte has been reported to have reliably revealed the dislocation structure in Fe-Si alloys [31-36].

A Leitz metallux microscope was used to study the microstructure of the specimens prepared in the manner described. For the estimation of the dislocation density microphotographs of different regions of the specimen within the polished area were obtained. In most cases the same region of the specimen was polished, etched and photographed for the dislocation density determination at two different stages of recovery. A large number of photographs was taken for different deformations and after various stages of annealing.

### 3.5.2. GENERAL REMARKS ON METALLOGRAPHIC TECHNIQUE

Numerous investigators [31] have demonstrated that certain reagents produce etch-pits on specific surfaces which are intensified at preferred sites, such as the points of emergence of dislocations on to the surface. The etch-pitting technique has been recently used extensively to study dislocation phenomena and has furnished valuable information. This technique is a powerful one, particularly in studying the annealing behaviour of dislocations. The method is non-destructive and the same region of the specimen can be repolished and re-etched to study the rearrangement and the changes in the density of dislocations at various stages of annealing. There are some limitations however, such as the information which can be gained from the etching studies is confined only to a plane section through the system of dislocations. This is a very serious limitation from the viewpoint of the interpretation of the results since it may be erroneous to deduce the behaviour of dislocations within the crystal from the observations made on the surface.

The optical microscope has the limitation that the dislocation density only in a certain narrow range can be determined with this instrument. The lower limit is set by the fact that at the lowest magnification used for the usual size of the etch pits, there should be at least a



few dislocations in the field of view to give a reasonable estimate of the dislocation density. The upper limit is fixed by the resolution at the maximum magnification available with the microscope. Thus the optical microscope can be used with reasonable accuracy only if the dislocation density lies between  $10^6$  to about  $2 \times 10^8$  lines per sq. cm.

The main limitation arises from the debatable question as to whether or not well defined etch pits are formed at and only at the dislocations. This depends critically on the orientation and state of the surface to be etched and precise composition of the etchant. The reasons as to why the emergence points of the dislocations are attacked preferentially are not very well understood so far. However, it seems established [31,35] that in metals some impurity segregation or atmosphere formation is necessary before dislocations can be reliably etched. Suits and Low [35] have shown that in Si-Fe the segregation of carbon atoms to dislocation sites due to an aging treatment is the necessary prerequisite for the production of etch pits. Various authors [31] have attempted to check the one to one correspondence between emergent dislocations and the etch pits--that is, whether every etch pit represents only an emergent dislocation and every dislocation terminus is etch pitted.

Vogel et al [40] obtained a satisfactory comparison between the spacing of etch pits with the angle of misfit across a pure tilt boundary in germanium ; Gilman and

Johnston [41] found a satisfactory correspondence between the etch pits on the matching cleavage surfaces of lithium fluoride. By introducing a known number of dislocations into crystals of germanium and Fe-Si alloy by bending them to a given radius of curvature, Vogel [42], and Dunn and Hibbard [33,34] compared the density of etch pits with the density of dislocations calculated from the radius of curvature [37-39], and confirmed the reliability of etch pitting technique.

In view of the above evidences in favour of one to one correspondence between the etch pits and dislocations termini, it is concluded that the observed values of the density of dislocations in the specimens of this work, are reliable and reasonably accurate for the scope of this study.

## CHAPTER IV

### EXPERIMENTAL RESULTS

#### 4.1. INTRODUCTION

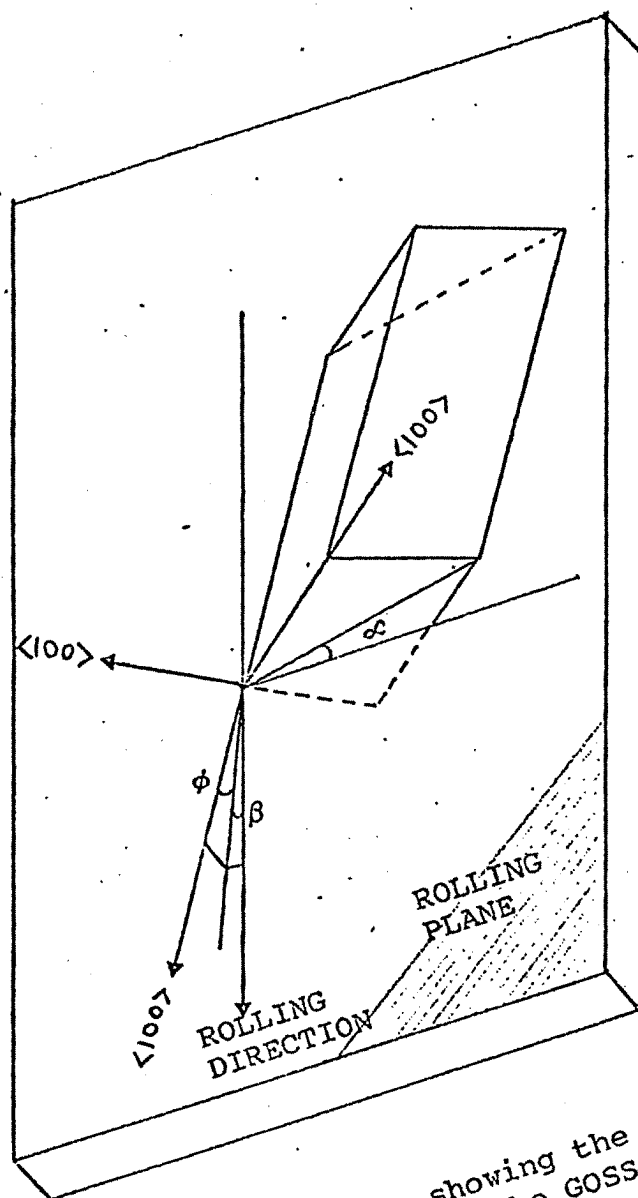
The theories of coercive field and initial susceptibility developed on the model based on single crystal specimens have the limitation that they cannot in general, be appropriately applied to polycrystalline specimens because of the effects of the presence of the grain boundaries. The grain boundaries in a polycrystalline specimen separate the regions of different crystallographic orientations, so that the direction of easy magnetization differs in different grains. At low field strengths, the magnetization vectors of neighbouring grains are not rotated from their easy magnetization direction into complete alignment. Consequently, there is a discontinuity across the grain boundary in the normal component of the magnetization vector. This causes the existence of magnetic poles at the grain boundaries, and magnetic energy is associated with these poles. This contribution to the energy of the system must be taken into account in the calculations of the coercive field strength and the initial susceptibility.

If  $\omega_1$  and  $\omega_2$  are the angles made by the spontaneous magnetization vector  $M_s$  of the neighbouring grains with the

normal to their common boundary, the surface pole density is proportional to  $(\cos \omega_1 - \cos \omega_2)$ . It has been shown [25] that, because of this effect the grain boundary contribution to the coercive field is proportional to  $(\cos \omega_1 - \cos \omega_2)^2$ .

However, this contribution of the grain boundaries in a polycrystalline specimen may be neglected for the case where  $(\cos \omega_1 - \cos \omega_2)$  is small, that is, if the specimen is highly grain oriented.

In a polycrystalline specimen of Si-Fe with grain oriented texture, the orientation of the various grains is found to have spread about the mean (110) [100] orientation, with the result that an individual crystal may differ from the intended orientation by angles  $\phi$ ,  $\beta$  and  $\alpha$  as shown in fig. (4.1-1). Here  $\phi$  is the smallest angle which one of the [100] directions makes with the rolling plane i.e., the surface of the specimen. The angle which the projection of [100] direction on the rolling surface makes with the rolling direction is  $\beta$  and  $\alpha$  measures the degree of [010] and [001] directions about the [100] direction. A position in which they make equal angles with the rolling plane is the reference position  $\alpha = 0$ . The information regarding the degree of misorientation may be obtained by studying the surface domain patterns of a large number of grains of the specimen.



A schematic diagram showing the orientation of a typical crystallite in the Goss textured silicon steel.

FIGURE - 4.1-1.

Reproduced with permission of the copyright owner. Further reproduction prohibited without permission.

The domain structure in single crystals of Fe-Si alloy with different orientations has been studied by many workers [43,44] and have been compared with those of the Goss textured sheet. In single crystals, with the surface of observation oriented parallel to (110) plane, the domain patterns are of simple  $180^\circ$  wall type; the patterns become more complex with an increase in the mis-orientation of the surface. The domain patterns on the surface of a Goss textured sheet with a very high degree of grain orientation have been found to be very similar to those of a single crystal. After the stress relief anneal, the specimens were electropolished. The surface domain structure was delineated by means of the conventional colloid techniques [44]. The domain structure of various grains was observed and photographed. Most of the grains showed simple  $180^\circ$  wall domains and others showed various kinds of  $180^\circ$  domain pattern fig. (4.1-2). It was inferred from the above result that the material used was highly grain oriented. This was evidenced further by the x-ray diffraction studies. The stereographic projection of 18 grains of the sample is given in fig. (4.1-3).

The only experimental evidence about the effects of grain boundaries on the coercive field is that of Yensen and Ziegler [5,45]. They found that the grain boundary contribution to the coercive field of iron is

$$H_c = 3.7 \times 10^{-3}/L$$

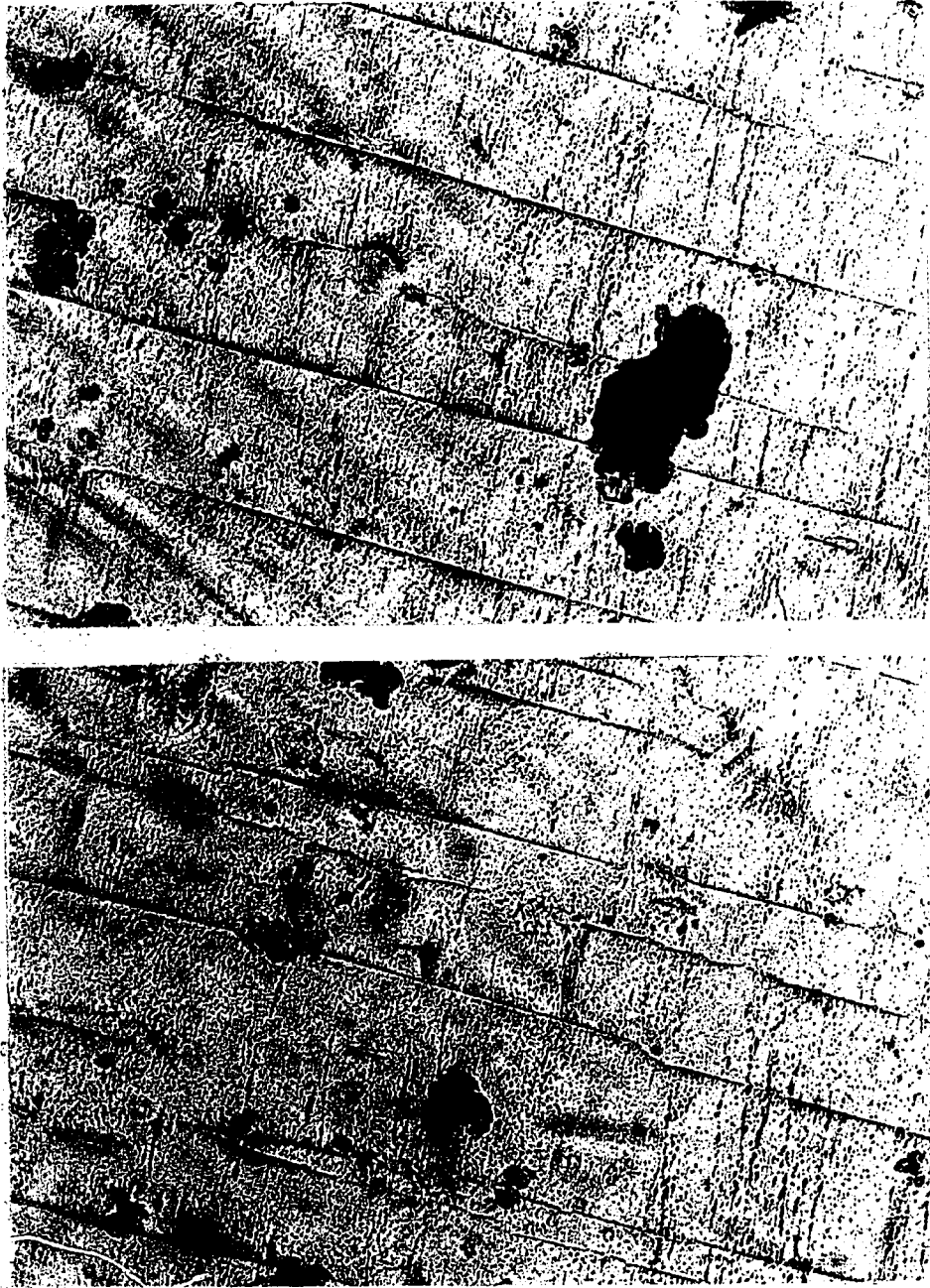


Fig. 4.1-2. Surface domain pattern in grain-oriented Fe-3.25% Si alloy.

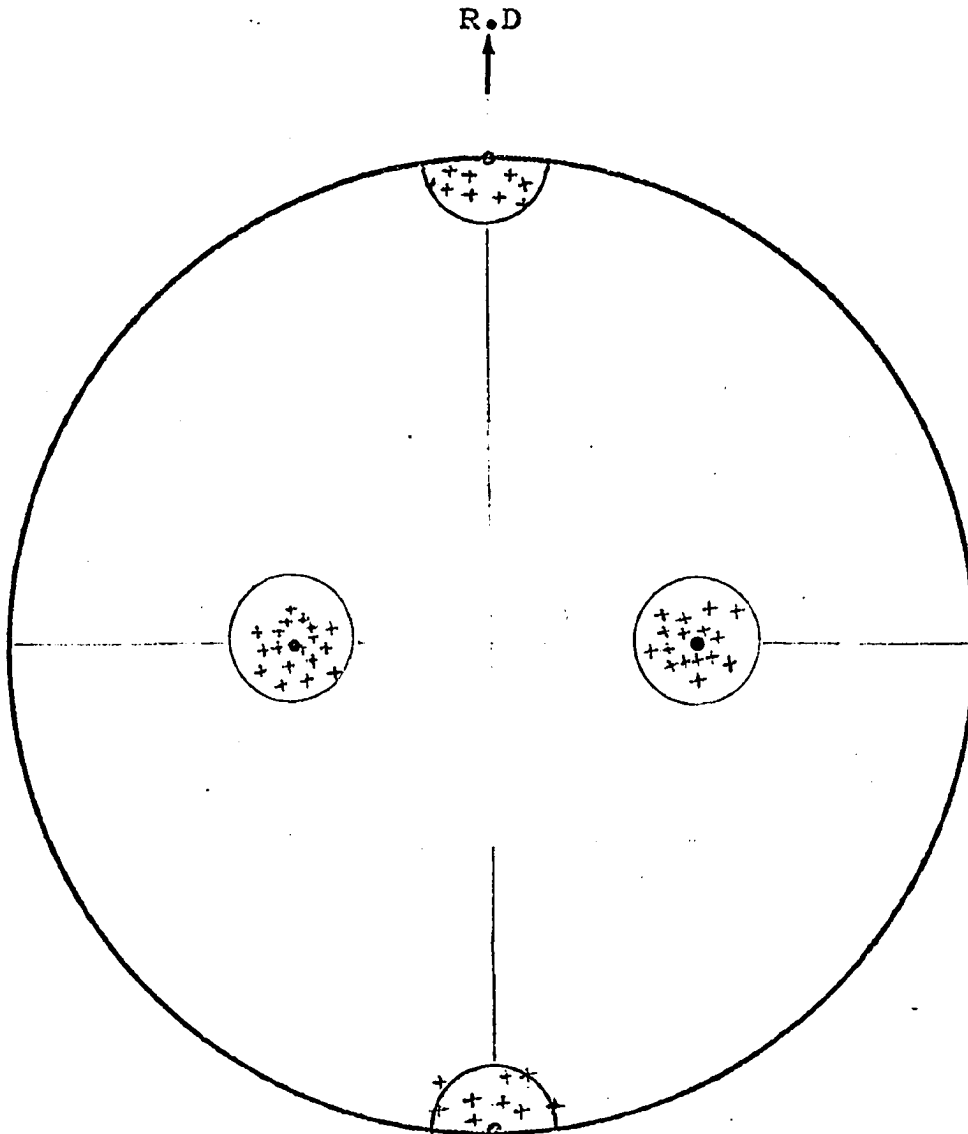


Fig.4.1-3. (110) [001] Stereographic projection of 18 grains in grain oriented silicon steel showing the orientation angles with respect to (110) [001] orientation.

- ideal (110) [100] orientation
- + typical orientation



where  $H_C$  is in Oe and  $L$  in cm, is the average grain diameter. Assuming that a similar relation holds in the case of Fe-Si alloy, the grain boundary contribution to  $H_C$  in these specimens (average grain diameter = 5 mm.) will be about 7 mOe, which is small compared to the range of  $H_C$  measured during this work (0.1 - 0.6 Oe).

In view of the above evidences it was concluded that these specimens were very suitable to be used for the present studies in making the quantitative comparison with the theories. In the following sections, the results of the various experimental investigations are discussed in detail.

#### 4.2 DEPENDENCE OF COERCIVE FIELD STRENGTH AND INITIAL SUSCEPTIBILITY ON DEFORMATION AND DENSITY OF DISLOCATION

##### (a) Plastic Deformation by Tension

Under the action of an applied stress, larger than a critical value, a crystal yields and plastic deformation occurs. For a ferromagnetic specimen, this results in a change in magnetic properties. The mechanism of macroscopic plastic strain is essentially the movement of dislocations introduced during the process of deformation [28, 29]. It is possible therefore, to relate the magnetic properties to plastic strain and hence indirectly to the density of dislocations.

The stress-strain curve (resolved shear stress versus resolved shear strain in the principal glide plane) of an intermediately oriented body-centered cubic single crystal such as iron, is characterized by three stages similar to that of a face-centred cubic single crystal [49]. In each of these regions the rate of change in dislocation density with strain is different. It is expected therefore, that at low deformations (region 1), the dislocation density  $N$  is linearly proportional to the resolved shear stress. In case of polycrystalline body-centred cubic metals, a parabolic relation between tensile stress and tensile strain is observed [28]. Therefore, on plastic deformation of the polycrystalline iron-silicon specimens in tension, the dislocation density  $N$  is expected to be proportional to the square root of the plastic tensile strain  $\epsilon$ .

or 
$$N = (\text{constant}) \epsilon^{1/2} \quad (4.2-1)$$

No experimental data on the variation of dislocation density in iron-silicon alloy with plastic tensile strain are available. In case of iron, the experimental results supporting this statement are those of Koster and Bangert [50]. According to their estimates, the dislocation density (based on the damping capacity measurement) varies as the square root of the plastic tensile strain. By transmission electron microscopy, Keh [51] and Keh and Weissmann [70] measured the changes in dislocation density with strain in single crystals of iron (strained by rolling) and polycrystalline iron (tensile strain). Their results show that the curves for the dislocation density vs. deformation in both cases are parabolic. On plotting the values of  $N$  against  $\epsilon^{1/2}$ , a linear relationship may be approximated within the accuracy of dislocation density measurements. (however for low strain region, a linear relationship between  $N$  and  $\epsilon$  is exhibited). In view of the above evidence it may be concluded that eqn.(4.2-1) is appropriate to describe the dependence of dislocation density on strain.

All the theories of coercive field  $H_c$  discussed in chapter II, eqns.(2.9),(2.11),(2.12) predict linear relation between  $H_c$  and the square root of the dislocation density  $N$

$$\text{or} \quad H_c = (\text{constant}) \sqrt{N} \quad (4.2-2)$$

Using relations (4.2-2) and (4.2-1), the expected dependence of coercive field  $H_c$  on the plastic strain  $\epsilon$  is given by

$$H_c = (\text{constant}) \epsilon^{1/4} \quad (4.2-3)$$

Kersten's model [8,9] for the initial susceptibility  $\chi_i$

leads to a relation of  $\chi_i$  with the dislocation density  $N$  from eqn. (2.24) as

$$\chi_i = (\text{const.})/N \quad (4.2-4)$$

According to Träuble's calculations [6], the dependence of initial susceptibility  $\chi_i$  is related to dislocation density  $N$  as [chap II eqn. (2.21)]

$$\chi_i = (\text{const.})/\sqrt{N} \quad (4.2-5)$$

Equations (4.2-4) and (4.2-5), using the relation between  $N$  and  $\mathcal{E}$  given by eqn. (4.2-1), yield the deformation dependence of the initial susceptibility  $\chi_i$  as

$$\chi_i = (\text{constant})/\mathcal{E}^{1/2} \quad (\text{Kersten}) \quad (4.2-6)$$

$$\chi_i = (\text{constant})/\mathcal{E}^{1/4} \quad (\text{Träuble}) \quad (4.2-7)$$

To obtain the deformation dependence of  $H_c$  and  $\chi_i$  experimentally, various specimens were strained from 1/2% to 7% at room temperature and their coercive field strength and initial susceptibility were measured. The values of  $H_c$  and the inverse initial susceptibility  $\chi_i^{-1}$ , are plotted as a function of the fourth root of the plastic tensile strain ( $\mathcal{E}^{1/4}$ ) in fig. (4.2-1). The values for 1, 3, 5 and 7% strain are obtained from the average of 15 measurements and for the remaining from 5 measurements. The experimental points for  $H_c$  and  $\chi_i^{-1}$  lie fairly well on straight lines.

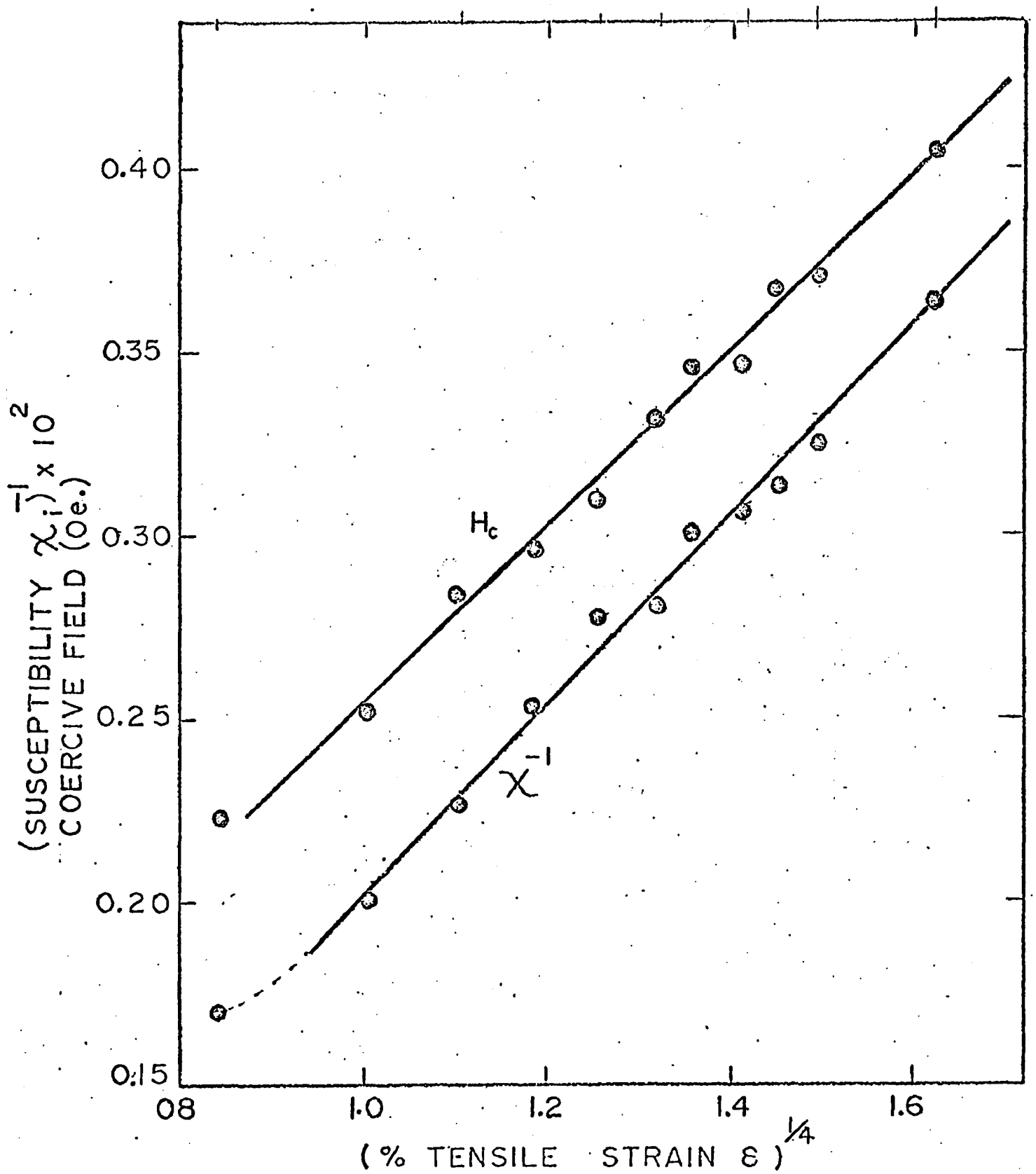


Fig. 4.2-1. Dependence of the coercive field and the initial susceptibility on tensile strain.

It is concluded on the basis of experimental results that the coercive field and the inverse initial susceptibility vary linearly with the fourth root of plastic tensile strain. The present results are in agreement with the deformation dependence expressed in eqns. (4.2-3) and (4.2-7). Relation (4.2-3) is predicted by all the theories of coercive field; relation (4.2-7) is based on Trauble's expression for  $\chi_i$ . The dependence of  $\chi_i$  on  $\mathcal{E}$  expressed by eqn. (4.2-6) does not hold true experimentally. This relation is based on Kersten's calculations for the initial susceptibility eqn. (4.2-4). The discrepancy in Kersten's formulation and agreement of the results with Trauble's statement are essentially due to the difference in models underlying their theories. Kersten has assumed an over simplified model in which the dislocations are distributed regularly lying parallel to each other at a constant distance 's' of a square lattice and in the plane of the Bloch wall. The initial susceptibility is caused by the reversible bending of the Bloch wall. Trauble [6] on the other hand, has taken into account the interaction of all types of randomly distributed dislocations, with the Bloch wall movement. It is not surprising to find that the present experimental results are in better agreement with the theoretical statements of Trauble. It is highly unlikely to find a regular geometric distribution of dislocations in real materials; in reality the dislocation distribution is

very random. Further supporting results are obtained in the following section where dislocations are introduced by a different technique.

(b) Plastic Deformation by Bending

Dislocations may also be introduced in a specimen during plastic deformation by bending. According to Cahn [37], Nye [38] and Gilman [39], the dislocation density  $N$  may be estimated from the radius of curvature according to the equation

$$N = \frac{1}{R b \cos \Psi} \quad (4.2-8)$$

where

$N$  = density of dislocations per unit area normal to the slip plane

$R$  = radius of the curvature of the neutral axis

$b$  = Burger's vector

$\Psi$  = angle between the slip plane and the neutral axis

It has been found experimentally [33-35,42] that for not too large strains, the dislocation density introduced by bending agrees with that given by the equation (4.2-8).

The above relationship assumes a single crystal slab with one active slip system ( $\Psi = \text{constant}$ ). In a polycrystalline material the values of  $\Psi$  will vary depending

on the orientation of the individual crystallites and the specific slip systems. However, for specimens having a high degree of grain orientation, the density of dislocations introduced in bending may be assumed, on the average, to be given by eqn. (4.2-8), i.e.,

$$N \sim 1/R \quad (4.2-9)$$

Using  $H_c \sim \sqrt{N}$ , the dependence of  $H_c$  on the radius of curvature  $R$  is given by

$$H_c \sim 1/\sqrt{R} \quad (4.2-10)$$

For an experimental verification of the relation (4.2-10), specimens were bent around circular cylinders of different radii, flattened, and their coercive field measured.

Five different values of radii were used. No attempt was made to ascertain the value of  $\psi$ , the angle between the slip plane and the neutral axis which was assumed to be constant in all the cases. For each radius of curvature five samples were used. The measured values of  $H_c$  are plotted in fig (4.2-2) as a function of  $1/\sqrt{R}$ . The experimental points lie fairly well along a straight line. This result indirectly indicates that within the approximation of the theory, the relationship  $H_c \sim \sqrt{N}$  is true for this mode of deformation as well.



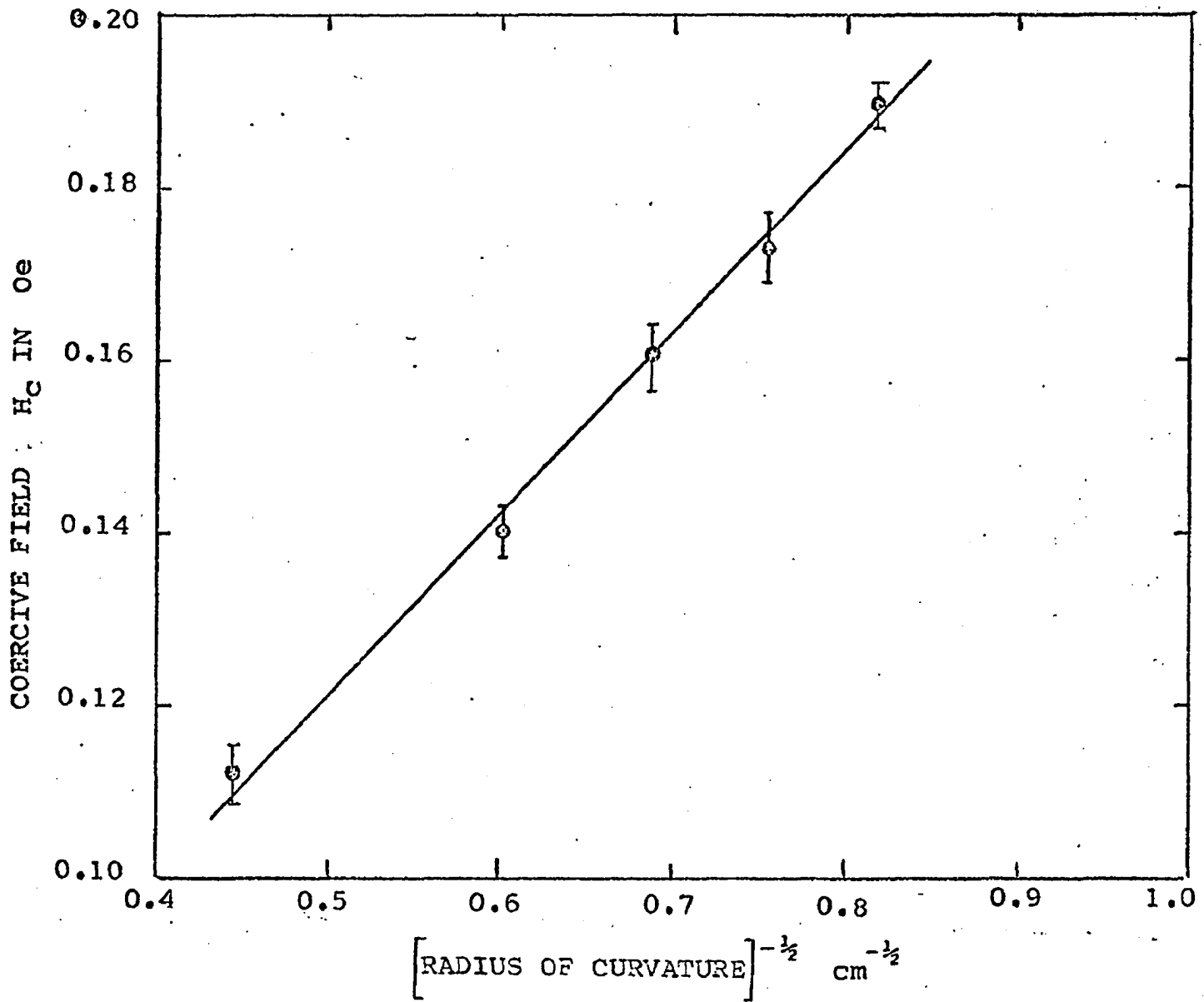


Fig. 4.2.2. Variation of the coercive field with the radius of curvature.

(c) Dependence of  $H_C$  and  $\chi_i$  on Dislocation Density

One of the most important aspects of the present investigations is the fact that attempts have been made to relate the coercive field strength, the initial susceptibility and the mechanical hardness directly with the density of dislocations determined metallographically. In the previous sections, the deformation dependence of  $H_C$  and  $\chi_i$  was measured and compared with their theoretical dependence on  $N$ . While the general agreement was quite satisfactory, the comparison was indirect--based on the theories of work hardening. In the following, the results of metallographic studies, in parallel to the measurement of  $H_C$ ,  $\chi_i$  and hardness are presented. To the author's knowledge, no such results relating  $H_C$ ,  $\chi_i$  and  $N$  based on direct measurement of  $N$  have been reported in literature.

The specimens with various plastic tensile strains were heat-treated at different temperatures. At various stages of recovery, using etch-pitting techniques, micrographs showing dislocation etch pits were obtained. The dislocation density  $N$  was determined from these micrographs by counting the etch pits. The values of coercive field, initial susceptibility and microhardness were also measured for specimens with identical history. The results of these measurements are given in fig. (4.2-3) where  $H_C$ ,  $\chi_i^{-1}$  and the micro-hardness have been plotted as a function of

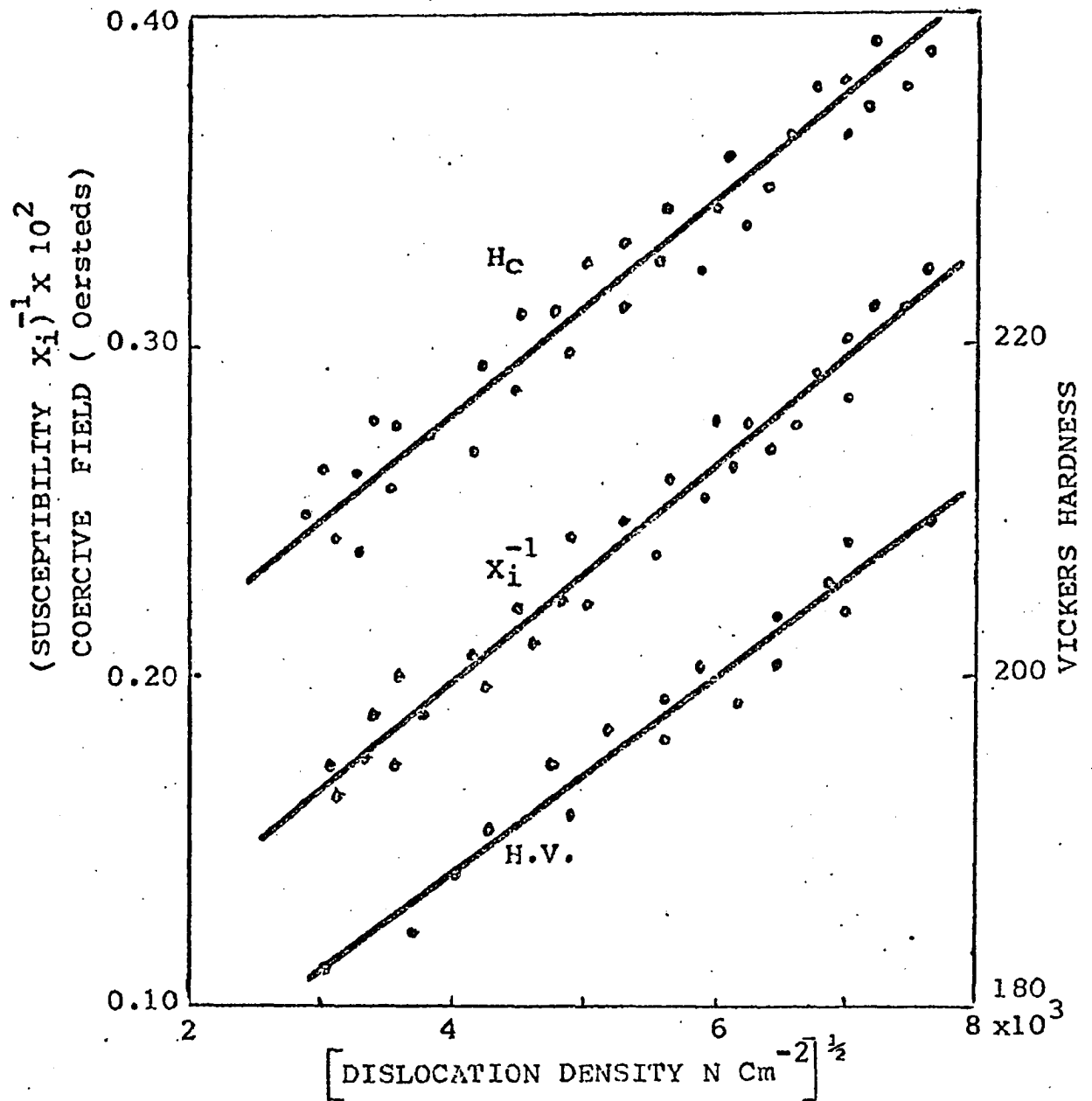


Fig. 4.2-3. Dependence of the coercive field , initial susceptibility and microhardness on the density of dislocations.



Fig. 4.2-4 (a) X 1000  
3% deformation ; 20 min. at 600 °C

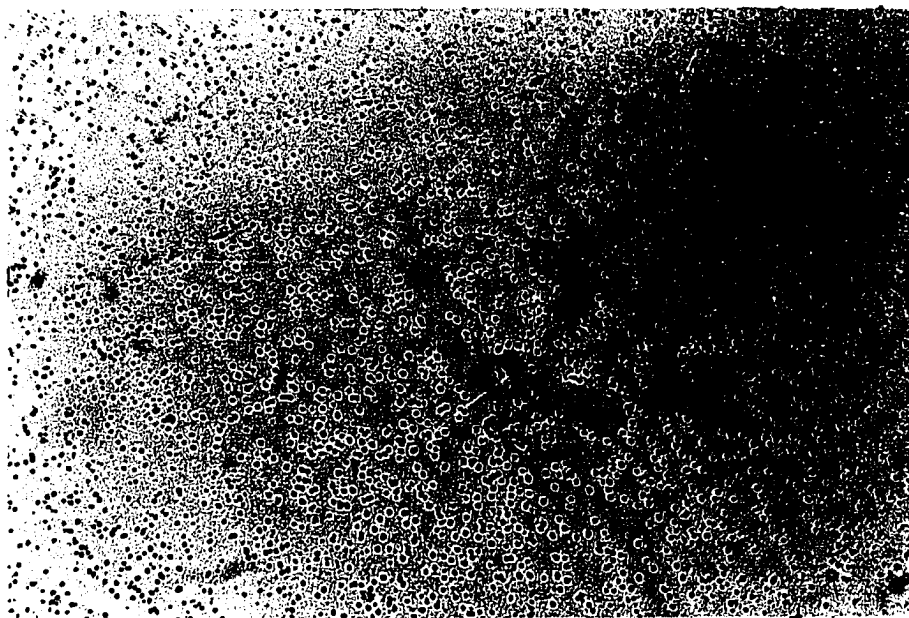


Fig. 4.2-4 (b) X 500  
3% deformation; 200 min. at 600 °C

Fig. 4.2-4. Micrographs showing dislocations in deformed Fe-3.25% Si alloy at various stages of recovery.

the square root of dislocation density. A few typical micrographs are shown in fig. (4.2-4).

The linear relationship of the coercive field strength, the inverse initial susceptibility and the mechanical hardness with the square root of dislocation density is evident. It may be concluded therefore, that the present experimental results are in a better agreement with the predictions of the theoretical statements by Träuble ( $\chi_i \sim 1/\sqrt{N}$ ). This agreement is probably the result of the nature of defects introduced which are random rather than regularly arranged. The interaction of dislocations with the Bloch wall movement must be treated statistically as considered by Träuble. These results also offer a further experimental verification of the assumption that Bloch wall displacements are responsible for the changes in magnetization in small fields. The theories of  $H_c$  and  $\chi_i$  will be examined later again when their temperature dependence will be explained.

### 4.3 STUDY OF THE PROCESS OF THERMAL RECOVERY

Recovery is the process whereby the crystal imperfections introduced into the material, are gradually eliminated and the physical properties are restored to that of perfect crystal. Imperfections such as point defects and dislocations are introduced during plastic deformation. These imperfections are in a state of thermodynamic inequilibrium and cause an increase in the free energy of the specimen. Many of the physical properties, e.g., mechanical hardness, coercive field and initial susceptibility are drastically altered. The imperfections may be gradually eliminated by the process of diffusion aided by thermal energy. With the reduction in the density of imperfections, the extra free energy of the system is reduced and the physical properties are recovered.

The rate of recovery is usually increased during annealing at higher temperatures because of increased rate of diffusion. A study of the mechanism of the recovery process, of some physical property, is expected to give valuable information on the behaviour of certain types of imperfections affecting that property. It is desirable therefore, to have a method by which a single type of defect may be introduced. Most methods designed to introduce an imperfection produce more than one type of defect and they all may have influence on the physical property to be

investigated. This in turn may render the analysis of the results more complicated. Annealing studies offer possible means of separating the effects of various defects. This is due to the fact that these defects are removed during annealing at different temperature ranges.

The activation energy for annealing of point defects is low and these are eliminated at comparatively lower temperatures. At these temperatures, the dislocations may interact with the point defects by acting as sinks or sources and may execute small scale rearrangement. The annealing of dislocations having higher activation energy takes place at higher temperatures when the thermal energy  $kT$  is large and the dislocations gain appreciable mobility and tend to rearrange and annihilate each other by glide or climb. Such large scale dislocation annealing eventually ends up in recrystallization of the specimen and this results in essentially complete removal of the strained structure. Thus the information regarding the annealing behaviour of dislocations can be obtained by studying the recovery characteristics of the magnetic properties such as  $H_c$  and  $\chi_i$  or the mechanical hardness, which are very sensitive to the internal stresses caused by the dislocations in the material.

#### Recovery of Magnetic Properties

In the present studies, the specimens after being strained to various degrees of deformation (1%, 3%, 5%, and 7%) were given isochronal and isothermal heat treatment. To obtain

the isochrones, the specimens were treated for 20 minutes at each temperature between  $100^{\circ}$  and  $800^{\circ}\text{C}$  at  $50^{\circ}$  interval. After each 20 minutes treatment, the specimens were quenched to room temperature and the coercive field strength and the initial susceptibility measured. The isothermal recovery was studied by annealing the specimens at various temperatures between  $550^{\circ}$  and  $720^{\circ}\text{C}$ . The coercive field and initial susceptibility were measured after interrupting the recovery process at various stages of annealing, by quenching the specimens to room temperature. In the following,  $H_{\text{CO}}$  and  $\chi_{\text{i0}}$  are the values of the coercive field and initial susceptibility respectively prior to heat treatment and  $H_{\text{C}}$  and  $\chi_{\text{i}}$  are the corresponding values at a certain stage of recovery.

#### Isochronal Annealing

Fig. (4.3-1) shows the results of isochronal recovery where the values of  $H_{\text{C}}/H_{\text{CO}}$  and  $\chi_{\text{i}}/\chi_{\text{i0}}$  at the end of each temperature pulse are plotted against the temperature of that pulse. The coercive field and the initial susceptibility remain almost constant up to about  $200^{\circ}\text{C}$ . Above this temperature the coercive field strength first increases to a maximum for all the specimens and then drops steadily below its initial value  $H_{\text{CO}}$ . The initial susceptibility drops to a minimum with increasing annealing temperatures and then steadily increases to values above  $\chi_{\text{i0}}$  during recovery at higher temperatures. The effect of the degree of deformation is apparent--with increased strain, the increase



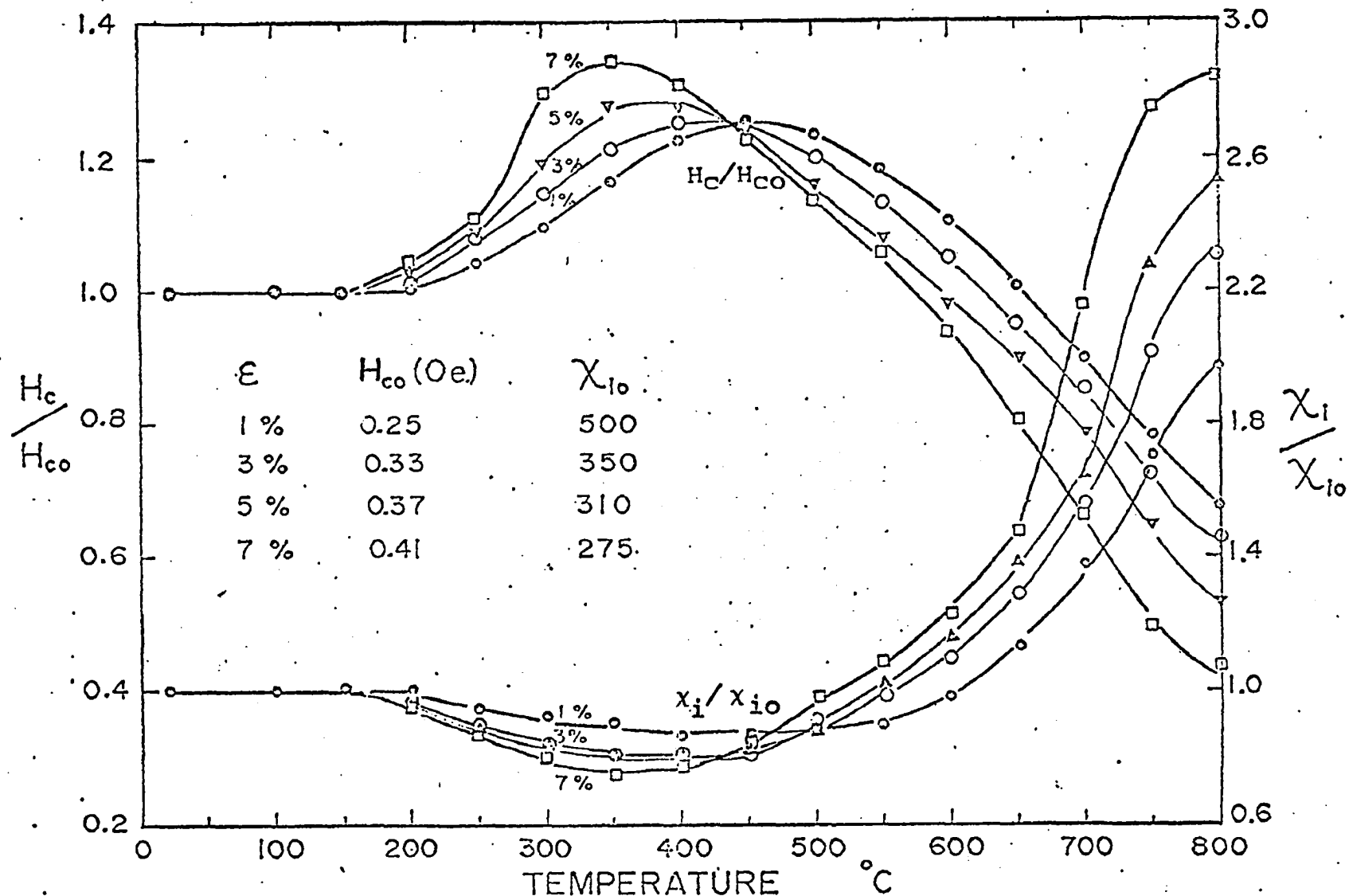


Fig.4.3-1. Isochronal recovery of the coercive field strength ( upper curves) and initial susceptibility (lower curves) of Fe-3.25%Si alloy specimens as a function of annealing temperatures after various degrees of deformation. ( t = 20 minutes at each temperature )

in the value of  $H_c/H_{c0}$  takes place at lower annealing temperature, the maximum value is increased and is attained at a lower temperature; after attaining the maximum the decrease is much faster than in the specimens with lower deformation.

### Isothermal Annealing

Fig. (4.3-2) to (4.3-9) show the results of isothermal recovery where the values of  $H_c/H_{c0}$  or  $[\chi_i/\chi_{i0}]^{-1}$  at the end of each recovery stage are plotted against the logarithm of total annealing time at that temperature. For 7% strained specimens the values of coercive field after aging at lower temperatures 200°-325°C are also given in fig. (4.3-2). The isothermal recovery curves shown in fig. (4.3-2) to (4.3-9) also reflect the initial rise in  $H_c$  and the drop in  $\chi_i$  at temperatures below 650° as exhibited by the isochrones of fig. (4.3-1). On aging at low temperatures, (200°- 325°C), the coercive field initially increases and then remains constant after achieving a maximum value. With increase in temperature of the isothermal heat treatment, the maximum achieved by the coercive field is damped to lower values followed by a gradual drop below its initial value. Finally, the isotherms of higher temperature (above 650°C) exhibit a steady drop in  $H_c$  without any initial rise. During the final stage of heat-treatment, the  $H_c$  and  $\chi_i$  approach to a constant value. In all the cases however, at least for the later stages, where the curves are approximately straight

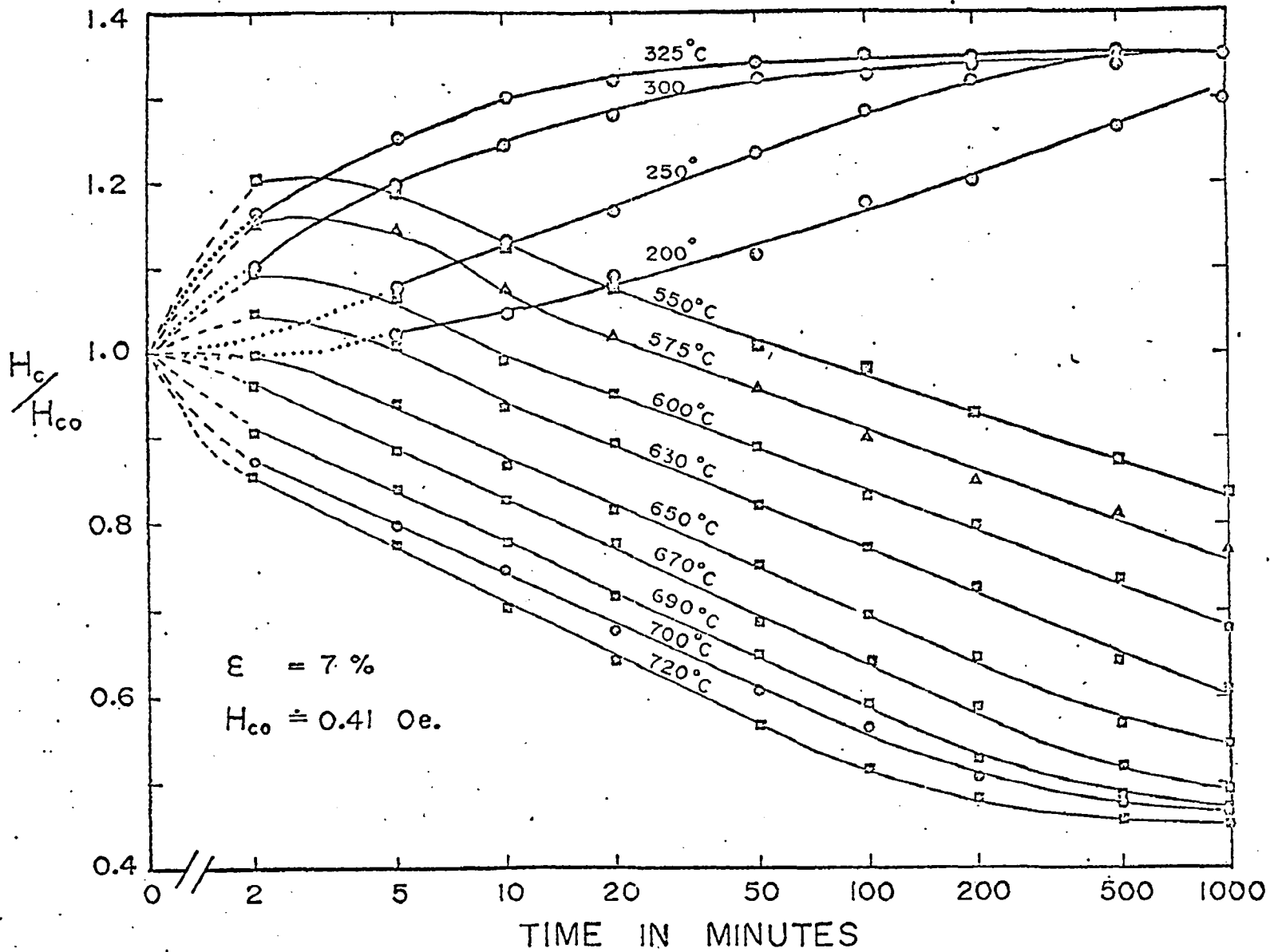


Fig.4.3-2. Isothermal recovery of the coercive field strength of 7% plastically deformed specimens as a function of annealing time at various temperatures.

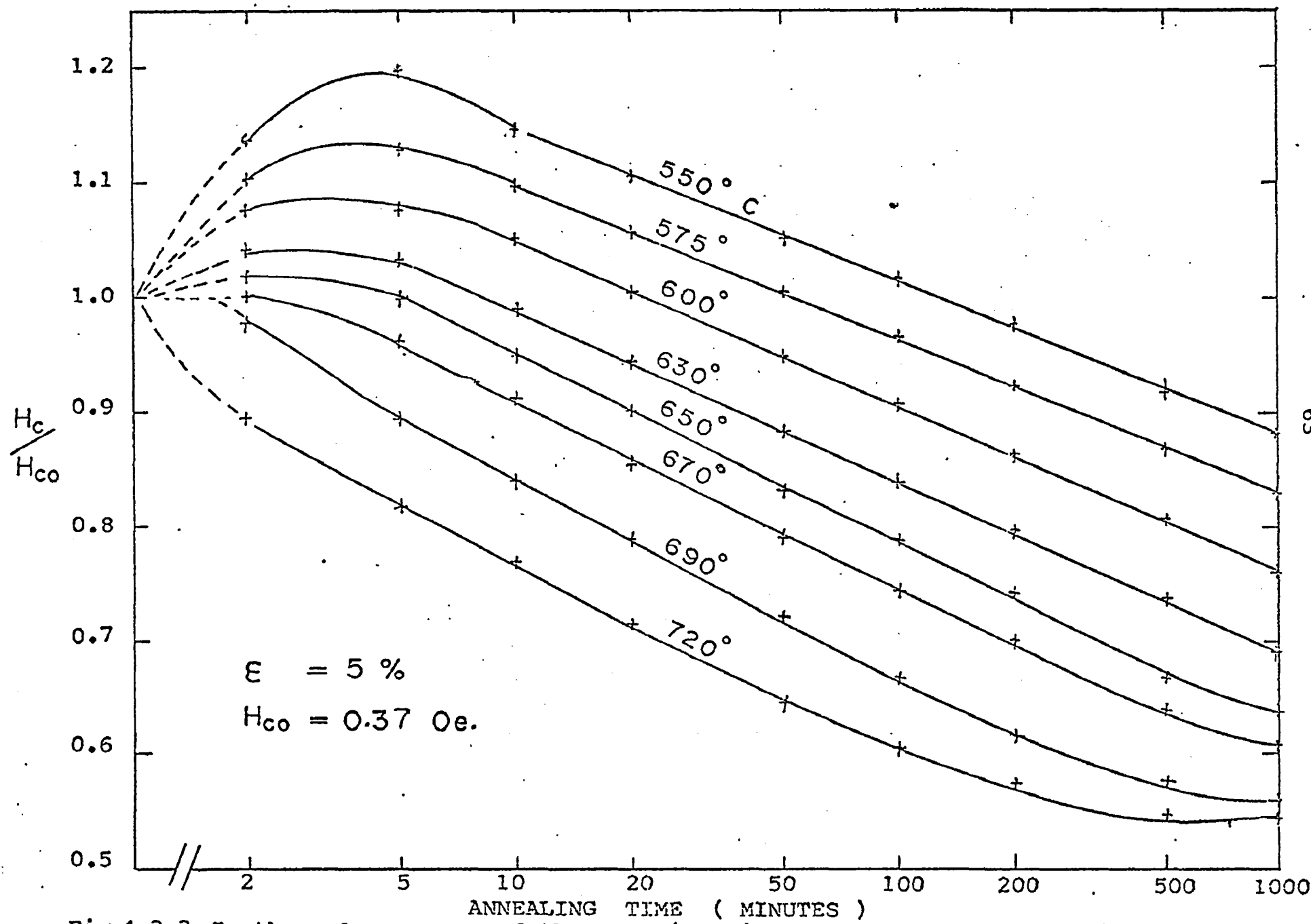


Fig.4.3-3 Isothermal recovery of the coercive field strength of 5% plastically deformed specimens as a function of the annealing time at various temperatures.

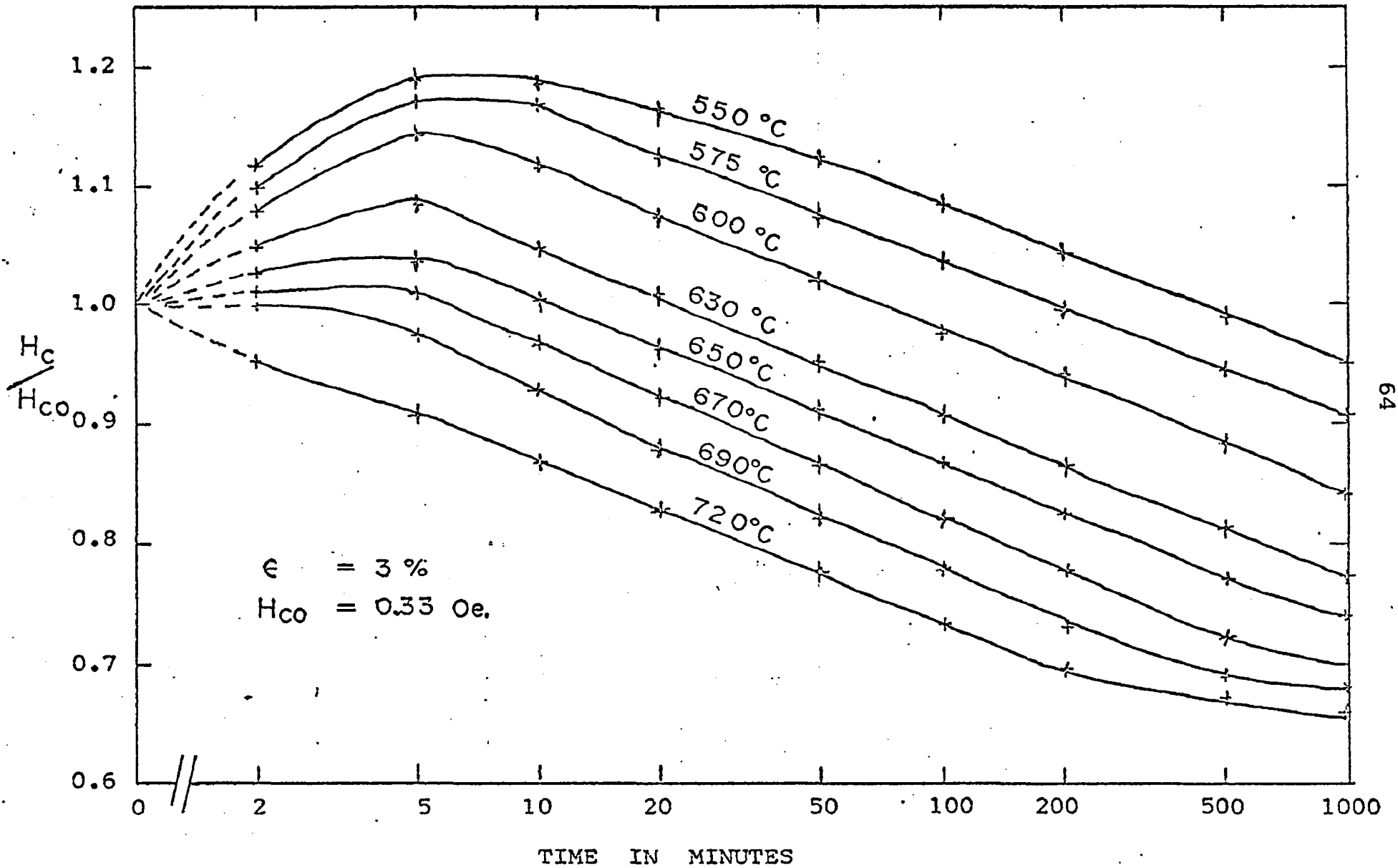
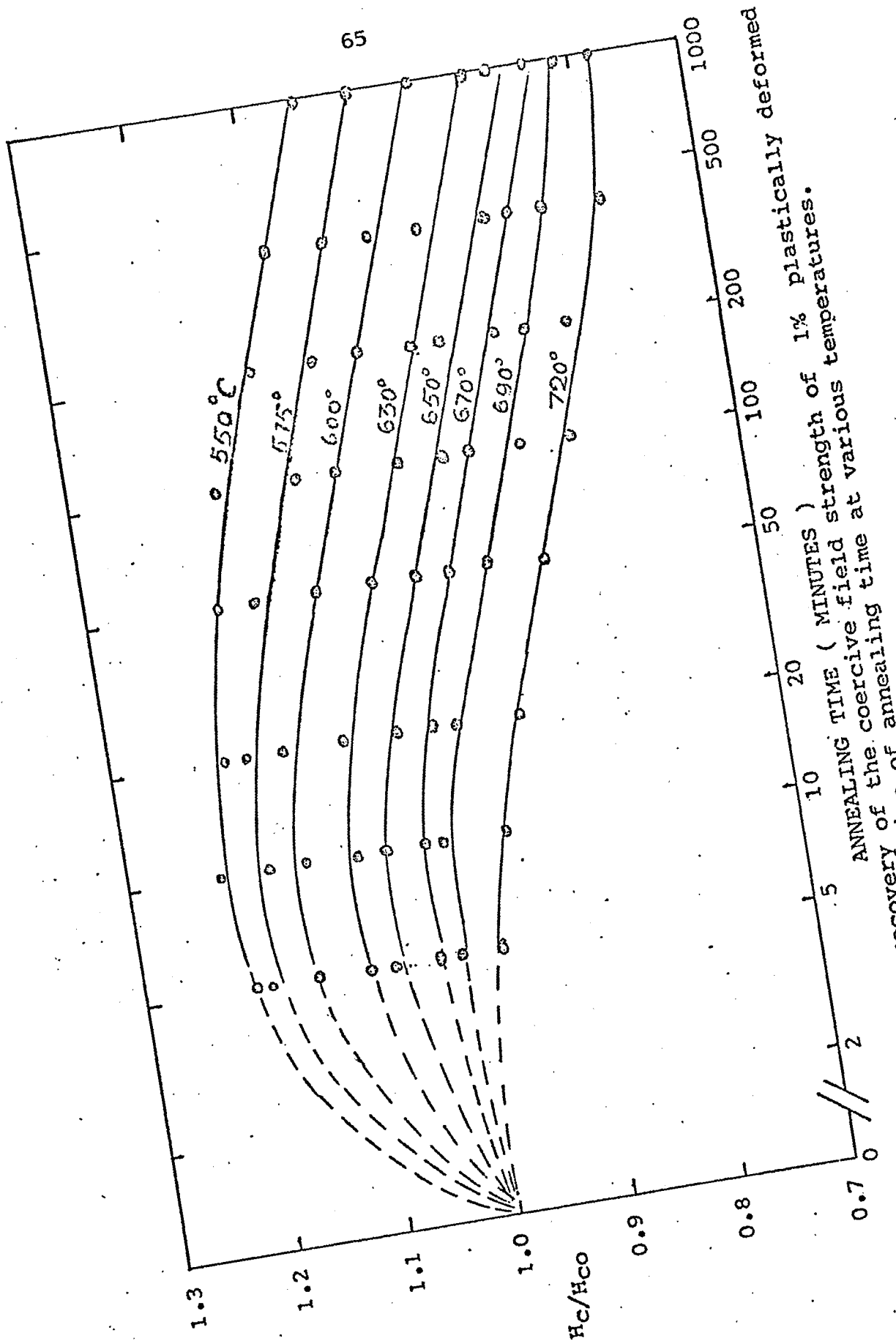


Fig.4.3-4. Isothermal characteristics of recovery of the coercive field strength of 3% plastically deformed specimens as a function of the annealing time at various temperatures.



ANNEALING TIME ( MINUTES )  
 1000 500 200 100 50 20 10 5 2

Fig.4.3-5. Isothermal recovery of the coercive field strength of 1% plastically deformed specimens as a function of annealing time at various temperatures.

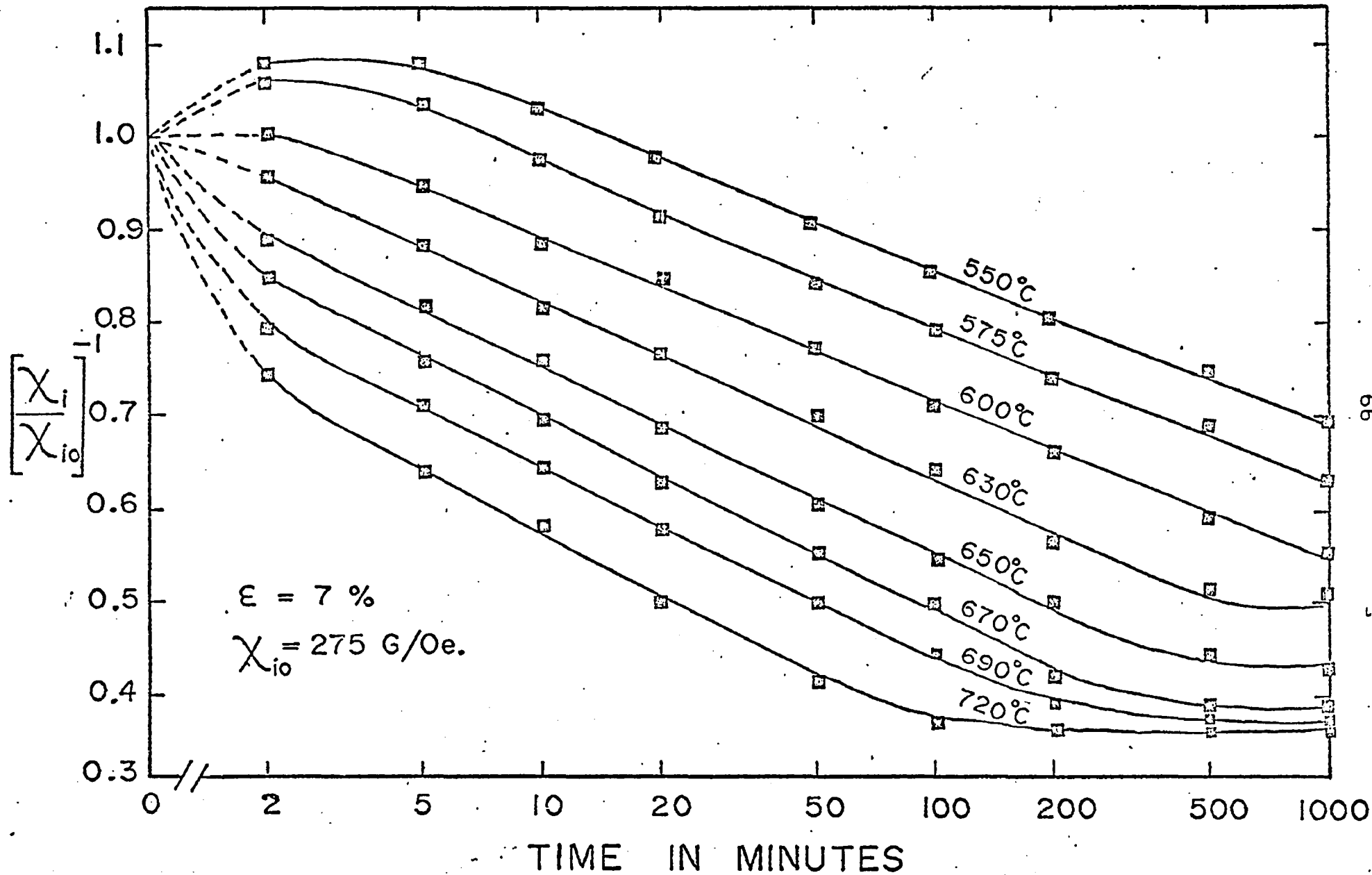


Fig.4.3-6 .Isothermal recovery of the initial susceptibility of 7% plastically deformed Fe-3.25%Si. alloy as a function of annealing time at various temperatures.

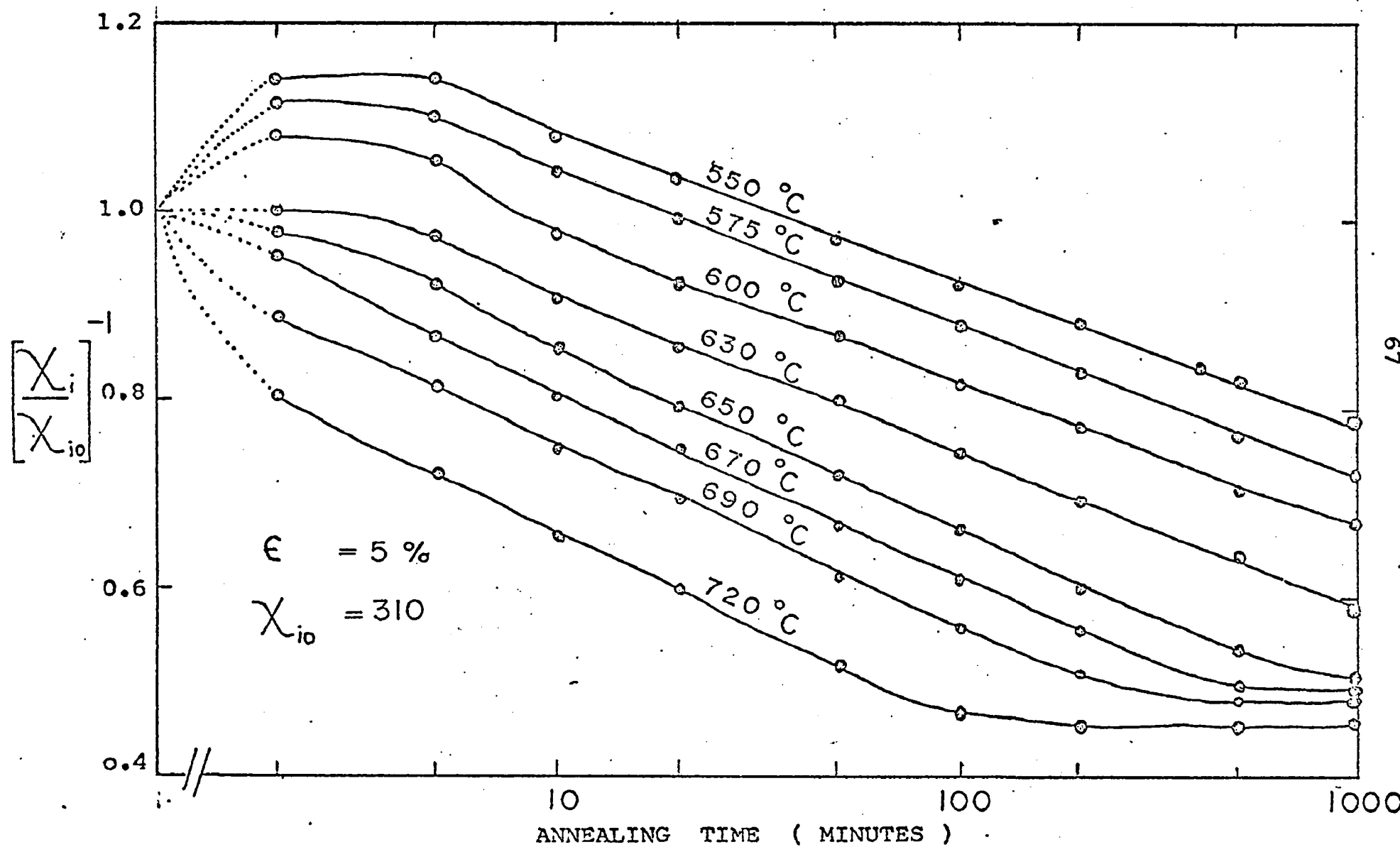


Fig.4.3-7. Isothermal recovery of the initial susceptibility as a function of the annealing time at various temperatures of 5% plastically deformed specimen.



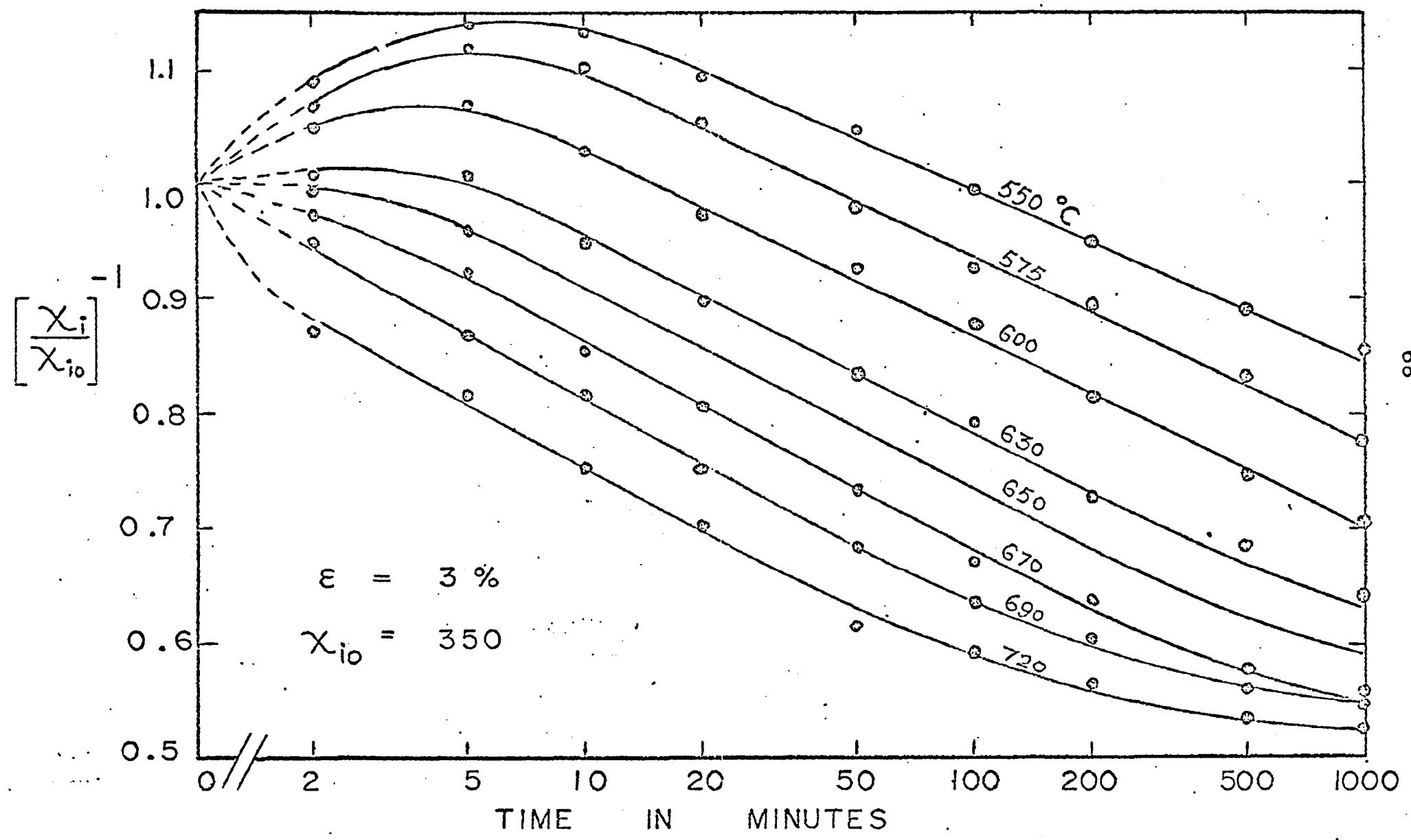


Fig.4.3-8 . Isothermal recovery of the initial susceptibility of 3% plastically deformed Fe-3.25%Si alloy specimens as a function of annealing time at various temperatures.

Reproduced with permission of the copyright owner. Further reproduction prohibited without permission.

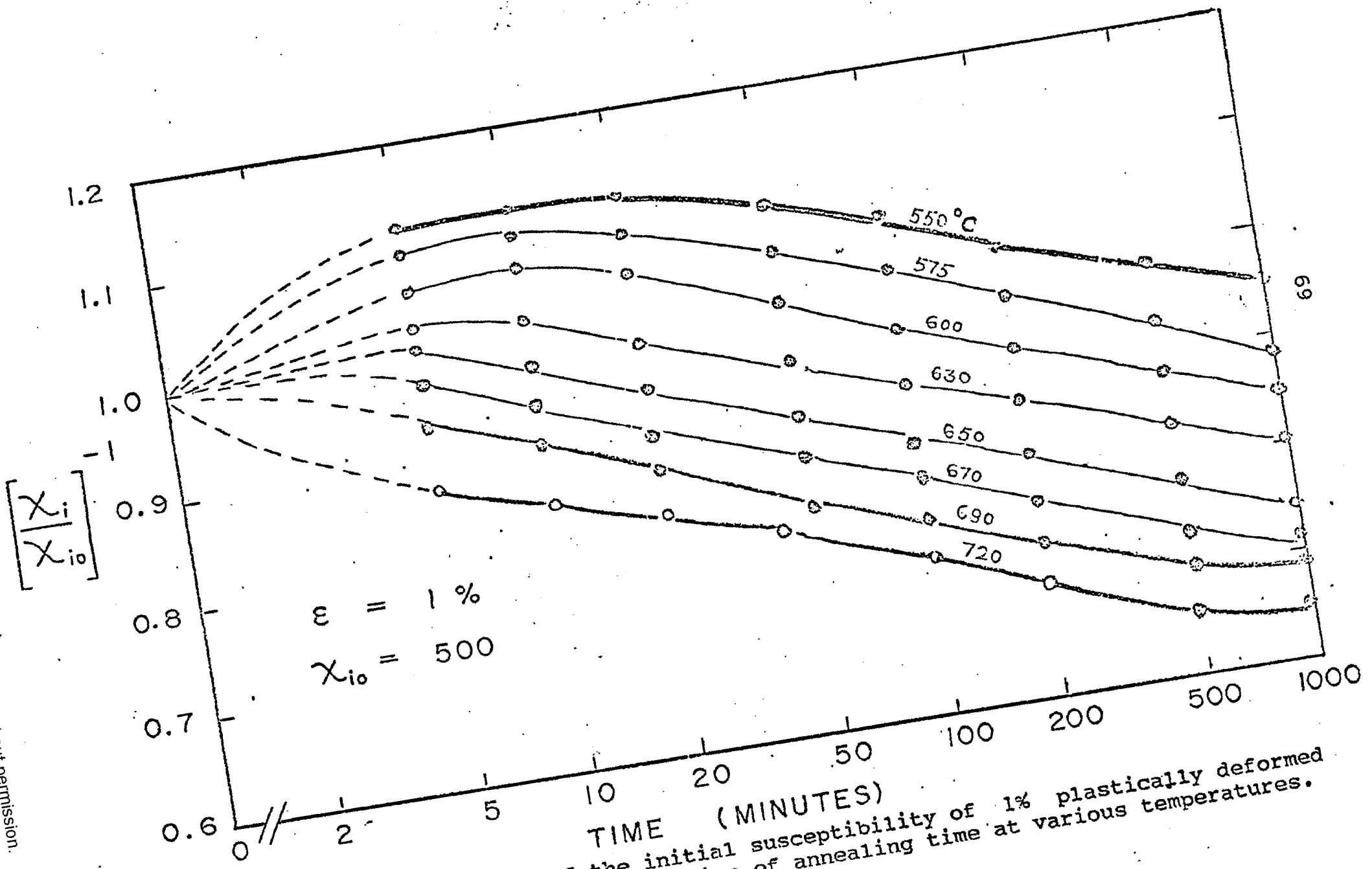


Fig.4.3-9 • Isothermal recovery of the initial susceptibility of 1% plastically deformed Fe-3.25%Si specimens as a function of annealing time at various temperatures.

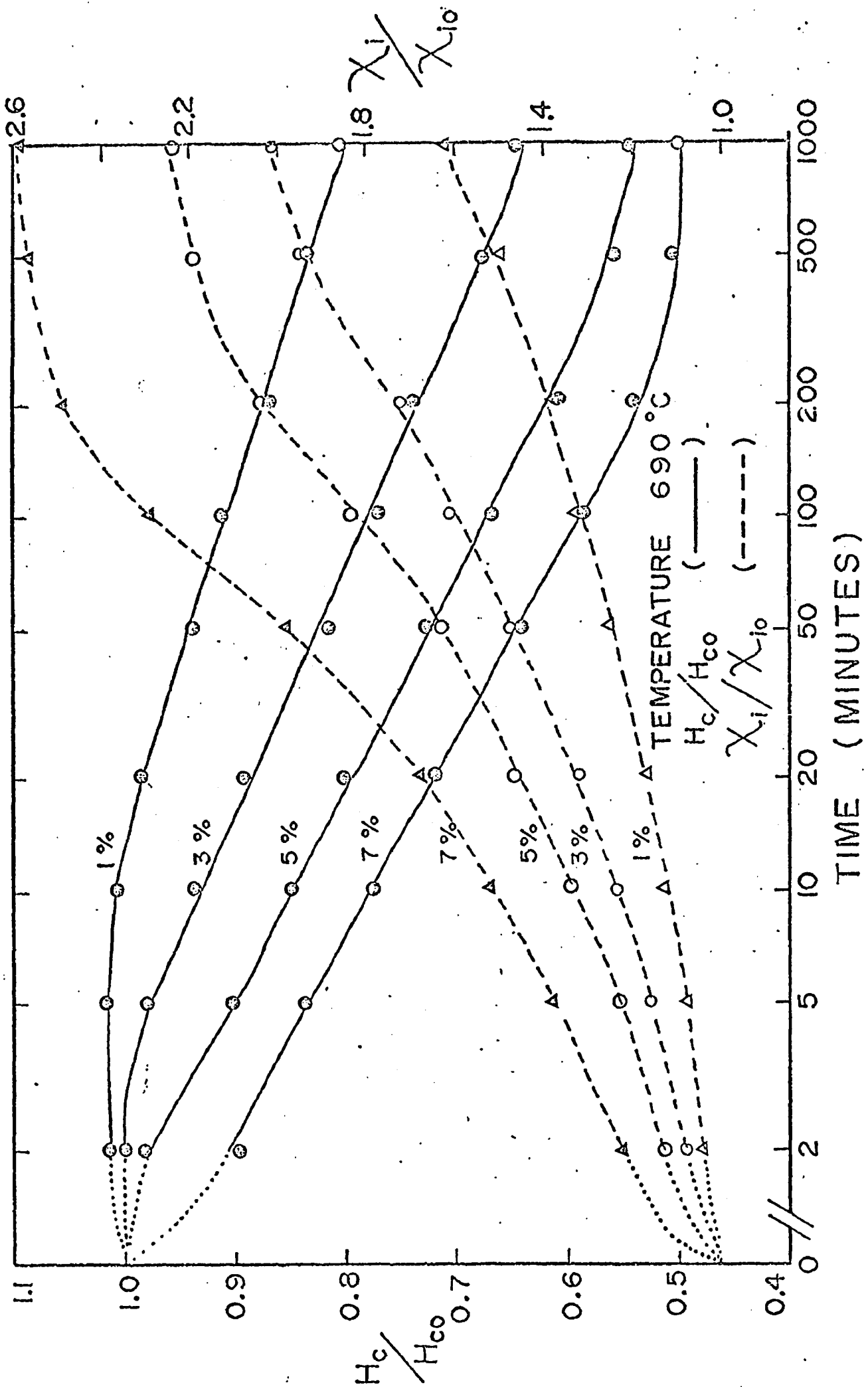
lines, the recovery is characterized by a logarithmic time dependence. In this temperature range the recovery of the coercive field (or that of inverse initial susceptibility) of a specimen with a certain pre-strain, at a constant temperature of annealing, may be described by equation of the form

$$\begin{aligned} H_c/H_{c0} &= B - A \ln t \\ \text{or } [\chi_i/\chi_{i0}]^{-1} &= B' - A' \ln t \end{aligned} \quad (4.3-1)$$

where  $B$ ,  $B'$  and  $A$ ,  $A'$  are constants dependent only on the annealing temperature and the degree of deformation.

The effect of strain on the rate of isothermal recovery, at a constant temperature, is shown in fig. (4.3-10), where the values of  $H_c/H_{c0}$  and  $[\chi_i/\chi_{i0}]^{-1}$  of specimens with various degrees of deformation are plotted against annealing time at  $690^\circ\text{C}$ . The values of  $H_c/H_{c0}$  and  $[\chi_i/\chi_{i0}]^{-1}$  after certain annealing time 't' are found to be smaller for 7% strained specimen and increases for 5%, 3% and 1% strain in that order. This means that the rate of recovery increases with increasing strains.

The recovery of various physical properties of many deformed metals have shown a logarithmic dependence on the time of isothermal annealing [46, 54, 55]. Michalak and Paxton [46] found a linear relationship between the flow stress  $\sigma$  in pure iron specimens and the logarithm of annealing time. If  $H_c$  or  $(\chi_i^{-1})$  is replaced by the flow stress  $\sigma$  using the linear relationship between  $H_c$  (or  $\chi_i^{-1}$ ),  $\sqrt{N}$  and  $\sigma$ , ( $H_c \sim \sqrt{N} \sim \sigma$ )



Reproduced with permission of the copyright owner. Further reproduction prohibited without permission.

equations (4.3-1) yield a result similar to theirs describing the recovery of flow stress. There is, however, a marked difference between the present results and those of Michalak and Paxton during the early phases of isothermal annealing where in contrast to their results, an increase in  $H_c$  and drop in  $\chi_i$  are observed (fig. 4.3-2 to 4.3-9). The laws and exact mechanism of annealing processes are still poorly known and a general analysis of the process is missing. In the following section, the present results are analysed to reveal further information on the mechanism of recovery.

#### Analysis of the Results

The recovery of the macroscopic magnetic properties  $H_c$  and  $\chi_i$  on annealing at a certain temperature is related to the disappearance of dislocations. The results show that the rate of recovery is dependent on the degree of cold work; it increases with increasing strains and higher dislocation densities. The internal stresses, whose sources are the dislocations themselves, aid in the process of annealing. It is expected therefore, that the rate of disappearance of dislocations is proportional to some function  $F(N)$  of the density of dislocations, i.e.,

$$dN/dt = -c F(N) \quad (4.3-2)$$

where 't' is the annealing time, and 'c' is a constant for the material and depends only on the temperature. Since during annealing, the potential barrier is overcome with the aid of thermal activation, the temperature dependence of

'c' should have the typical characteristics of the thermally activated processes, so that c will be of the usual form:

$$c = c_0 \exp(-U_a/kT) \quad (4.3-3)$$

where,  $c_0$  = a constant

$U_a$  = the apparent activation energy for the process

$k$  = Boltzmann constant

$T$  = the annealing temperature in  $^{\circ}K$

In the process of recovery, the energy stored in the internal stresses is released which reduces the necessary activation energy. The decrease in the activation energy can be considered to be given by some function  $f(N)$  of the dislocation density ( $N$ ). Therefore  $U_a$  may be taken as

$$U_a = U_i - f(N) \quad (4.3-4)$$

where  $U_i$  is the intrinsic activation energy. As the recovery progresses, the dislocation density  $N$  and therefore function  $f(N)$  decreases and the apparent activation energy  $U_a = U_i - f(N)$  increases. Using (4.3-3) and (4.3-4) the rate equation (4.3-2) can be written as

$$\frac{dN}{dt} = c_0 F(N) \exp. \frac{-[U_i - f(N)]}{kT} \quad (4.3-5)$$

The values of the functions  $F(N)$  and  $f(N)$  have to be evaluated from the analysis of the observed recovery characteristics of  $H_c$  and  $\chi_i$ . Denoting the ratio  $H_c/H_{c0}$  as  $\alpha$ , equation (4.3-1) may be written as

$$\alpha = H_c/H_{c0} = B - A \ln t$$

This gives on differentiation,

$$\begin{aligned} \frac{d}{dt} \left[ \frac{H_C}{H_{CO}} \right] &= \frac{d\alpha}{dt} = -\frac{A}{t} \\ &= -A \exp \frac{-(B-\alpha)}{A} \end{aligned} \quad (4.3-6)$$

The theoretical and the experimental results of section (4.2) relating  $H_C$  to  $\sqrt{N}$  give

$$H_C = (\text{const.})_1 \cdot \sqrt{N}$$

or

$$H_C/H_{CO} = (\text{const.})_2 \sqrt{N} \quad (4.3-7)$$

since  $H_{CO}$  is a constant for a certain strain value.

Substitution for  $\alpha$  in equation (4.3-6) gives

$$\frac{dN}{dt} = -(\text{const.})_3 \sqrt{N} \exp. \frac{-[B - (\text{const.})_4 \sqrt{N}]}{A} \quad (4.3-8)$$

A comparison of equation (4.3-8) with equation (4.3-5) suggests that the function  $F(N)$  and  $f(N)$  assumed in equation (4.3-5) are linearly related to  $\sqrt{N}$ , that is,  $F(N) \sim \sqrt{N}$  and  $f(N) \sim \sqrt{N}$ . On substituting for  $F(N)$  and  $f(N)$  in eqn.(4.3-5), the kinetic equation describing the rate of annealing of dislocations is given by

$$\frac{dN}{dt} = -(\text{const.})_5 \sqrt{N} \exp. \frac{-[U_i - (\text{const.})_6 \sqrt{N}]}{kT} \quad (4.3-9)$$

It is easy to show that eqn.(4.3-9) is the correct equation to describe the annealing kinetic. The substitution for  $N$  in eqn. (4.3-8) in terms of  $\alpha$  gives

$$\frac{d\alpha}{dt} = -C \exp - \left[ \frac{U_i - \beta\alpha}{kT} \right] \quad (4.3-10)$$

where  $C$  and  $\beta$  are constants. The origin of  $\beta$  may be traced back to equation (4.3-7) so that  $\beta$  depends on the many physical constants of the material relating  $H_c$  to  $\sqrt{N}$ . Equation (4.3-10) on integration yields the equation of recovery as

$$\alpha = \frac{U_i}{\beta} - \frac{kT}{\beta} \ln \left[ \frac{\beta C}{kT} \right] - \frac{kT}{\beta} \ln t \quad (4.3-11)$$

$$\text{or } \alpha \approx B - A \ln t \quad (4.3-12)$$

where

$$\frac{U_i}{\beta} - \frac{kT}{\beta} \ln \left[ \frac{\beta C}{kT} \right] = B = \text{intercept on the } t = 1 \text{ axis}$$

and  $\frac{-kT}{\beta} = A = \text{the slope of the line.}$

Equation (4.3-11) is exactly the same as equation (4.3-1), obtained directly from the experimental results. An analysis of the data of the recovery of the initial susceptibility on the above lines yields similar results.

The above analysis shows that by making only the magnetic measurements, the kinetics of the annealing of dislocations in ferromagnetic materials may be obtained. Further insight into the mechanism of recovery may be obtained by calculating the activation energy associated with the recovery process. Once the annealing kinetics have been determined, the method of calculation of activation energy has justifiable basis.



Calculation of Activation Energy

Rewriting the recovery equation,

$$\frac{H_c}{H_{co}} = \alpha = \frac{U_i}{\beta} - \frac{kT}{\beta} \ln \left[ \frac{\beta C}{kT} \right] - \frac{kT}{\beta} \ln t \quad (4.3-11)$$

one gets,

$$\frac{U_i - \beta\alpha}{kT} - \ln \frac{\beta C}{kT} = \ln t \quad (4.3-13)$$

In eqn. (4.3-13),  $\beta$  is a constant for the range of stresses involved; also the logarithmic term  $\ln (\beta C/kT)$  varies little for any change in  $T$  in the temperature range  $550^{\circ}$  to  $720^{\circ}$  C and may be treated as constant. Therefore, the values of  $\ln t$  plotted against  $1/T$  for constant values of  $\alpha$  ( $= H_c/H_{co}$ ) will yield straight lines. The slope  $(U_i - \beta\alpha)/k$  of such a line gives the value of apparent activation energy  $U_a = U_i - \beta\alpha$  for a particular value of  $\alpha$  or the fractional recovery of coercive field strength. In a similar way, the activation energies for various stages of recovery are calculated from the recovery characteristics of initial susceptibility.

The temperature dependence of the annealing time for various amounts of fractional recovery of the coercive field strength (solid lines) and the initial susceptibility (dotted lines) of 7% strained specimens is shown in fig. (4.3-11). The values of  $\ln t$  are plotted against  $1000/T^{\circ}K$  for constant

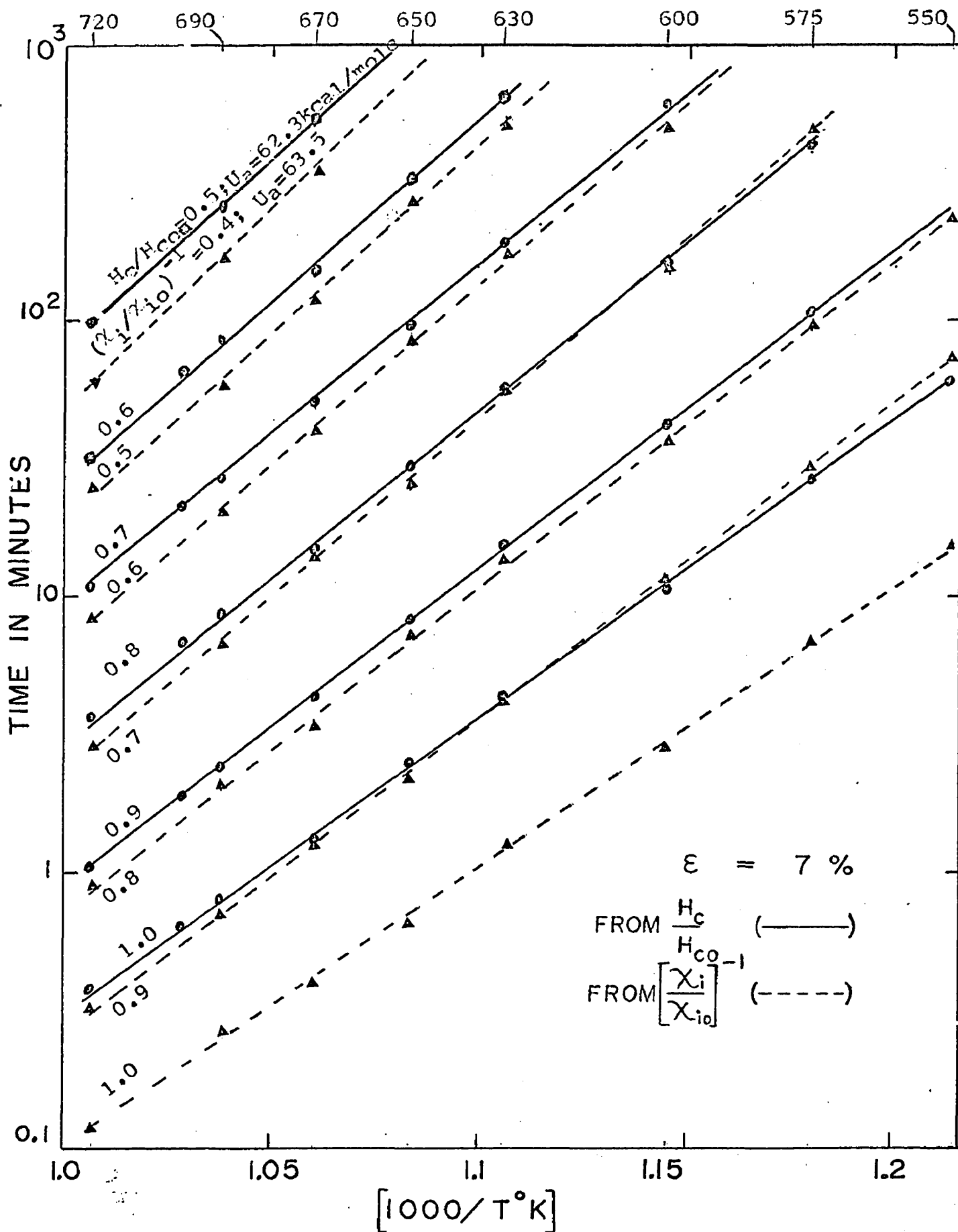


Fig. 4.3-11. Temperature dependence of the annealing time required for various amounts of fractional recovery of the coercive field strength (—) and the initial susceptibility (----) of 7% strained specimens.

value of  $H_C/H_{CO}$  and  $(\chi_i/\chi_{i0})^{-1}$ . The data for this figure are obtained from fig. (4.3-6) for  $H_C/H_{CO}$  and from fig.(4.3-6) for  $(\chi_i/\chi_{i0})^{-1}$ . The points corresponding to a certain stage of recovery lie approximately on a straight line; the slope of this line determines the activation energy for the process at that stage of recovery. The lines corresponding to different values of fractional recovery are not exactly parallel; the slope increases as the recovery progresses. This gives higher values of activation energy with the increase of recovery. Similar Arrhenius type plots are made and values of activation energies are calculated for other strain values (5%, 3%, 1%) as shown in figs. (4.-12) to (4.3-14). The complete result of the activation energy calculations are shown in fig. (4.3-15). The calculated values of apparent activation energy are plotted against the values of fractional recovery  $H_C/H_{CO}$  (solid lines) and  $(\chi_i/\chi_{i0})^{-1}$  (dotted lines), for all the strain values used (7%, 5%, 3%, 1%). The results show that for the same stage of recovery, The activation energy decreases with increasing strain.

The results of the present work are in disagreement with those of Michalak and Paxton [46] in which the activation energy associated with the recovery of flow stress in iron was found to be independent of prestrain. However, activation energy is a function of fractional recovery and increases as the recovery progresses. Kulhman [47] has discussed a

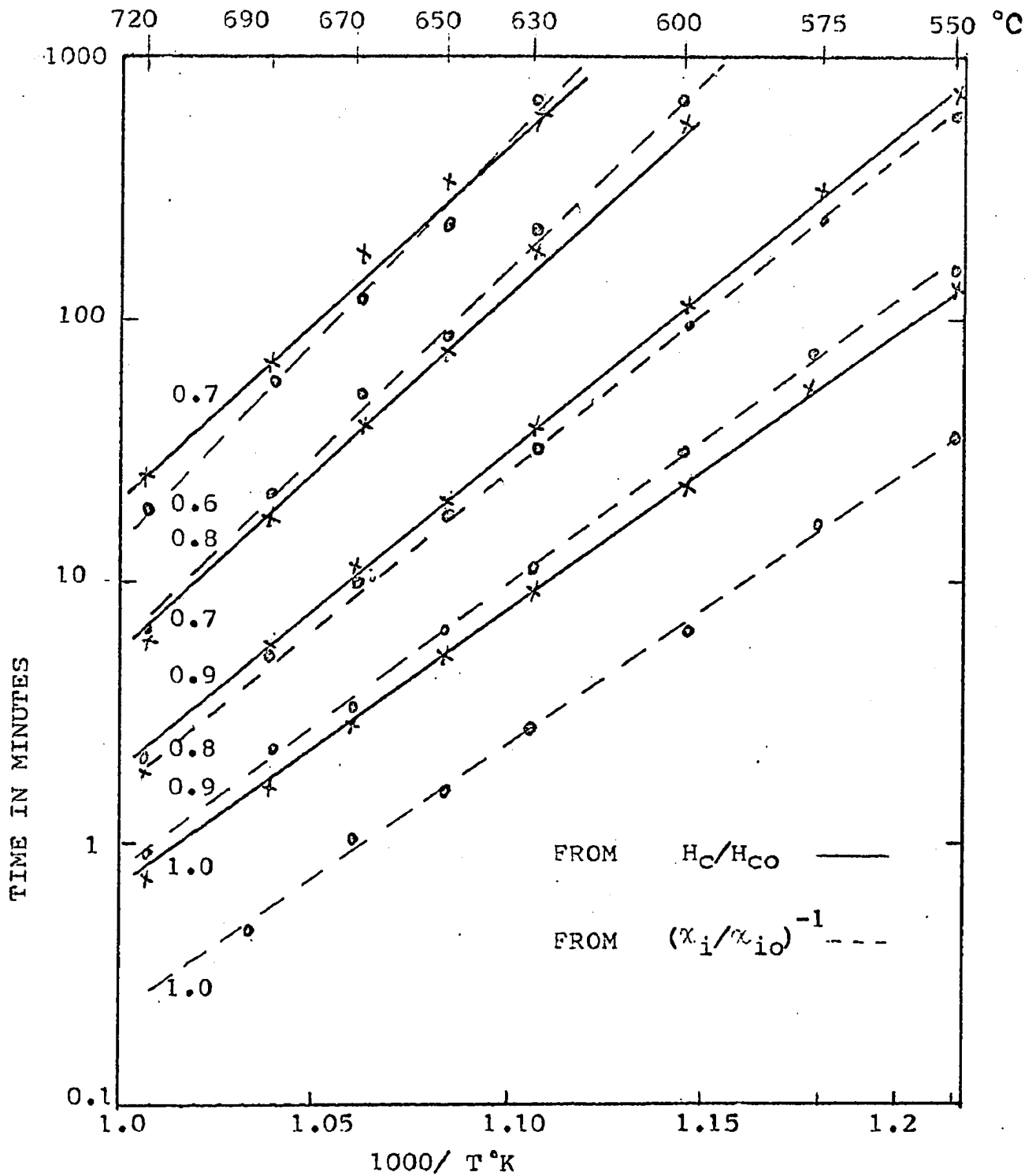


Fig.4.3-12. Temperature dependence of the annealing time required for various amounts of fractional recovery of the coercive field (solid lines) and initial susceptibility (dotted lines) of 5% deformed Fe-3.25%Si specimens.

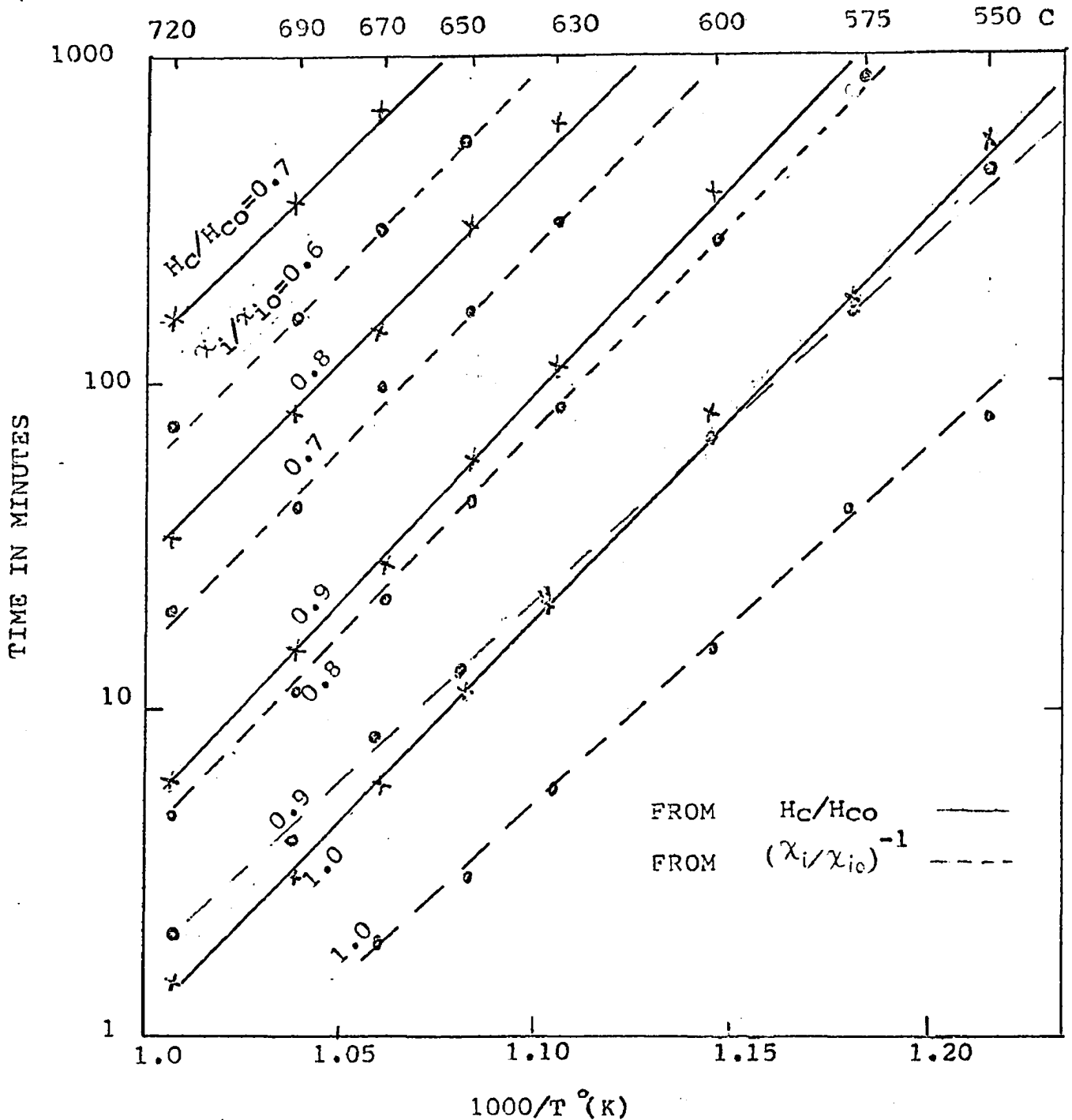


Fig.4.3-13, Temperature dependence of the annealing time required for various amounts of fractional recovery of the coercive field(solid lines) and initial susceptibility(dotted lines) of 3% deformed Fe-3.25% alloy specimens.

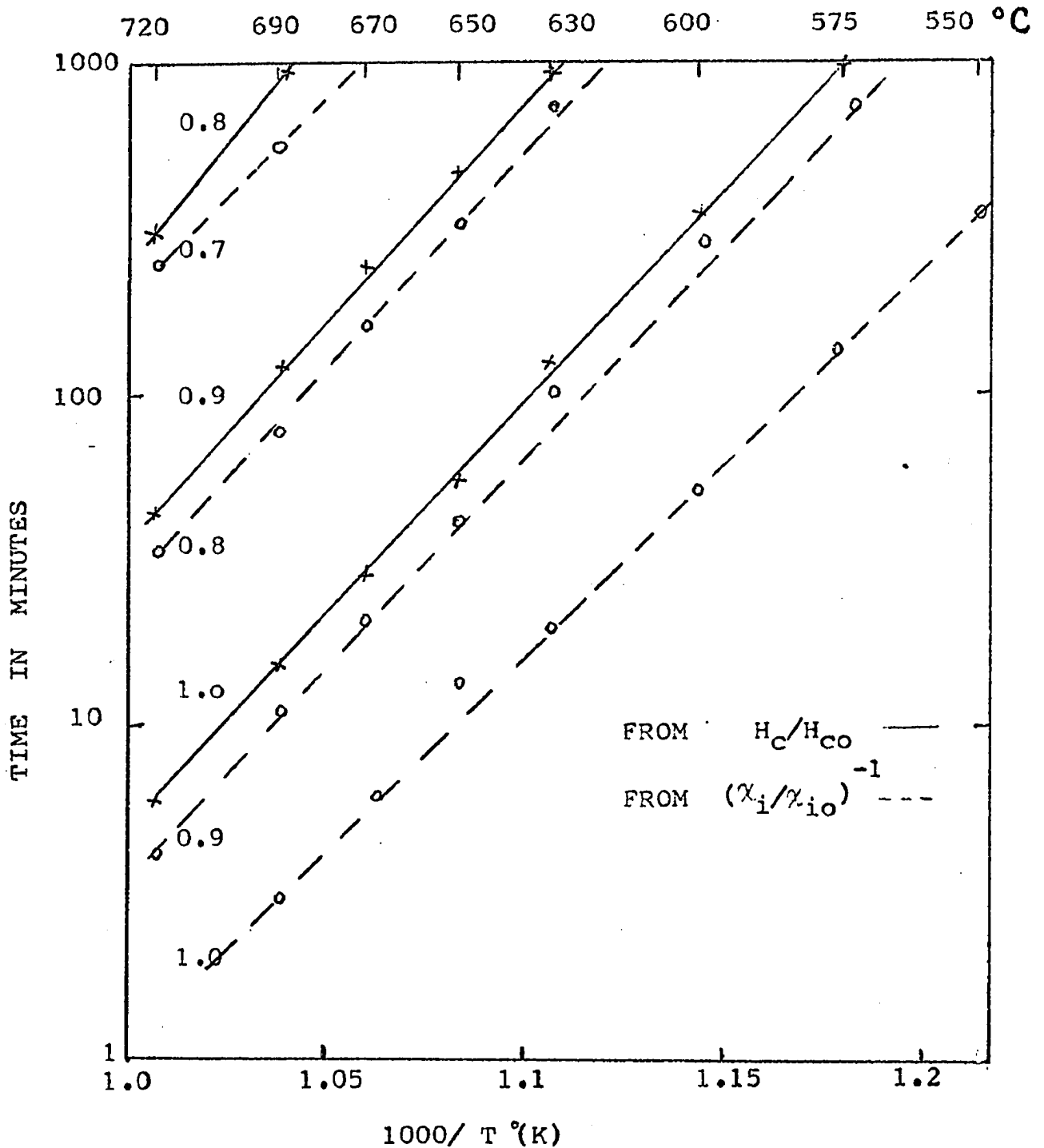


Fig. 4.3-14. Temperature dependence of the annealing time required for various amounts of recovery of the coercive field and initial susceptibility of 1% deformed Fe-3.25%Si alloy specimens.

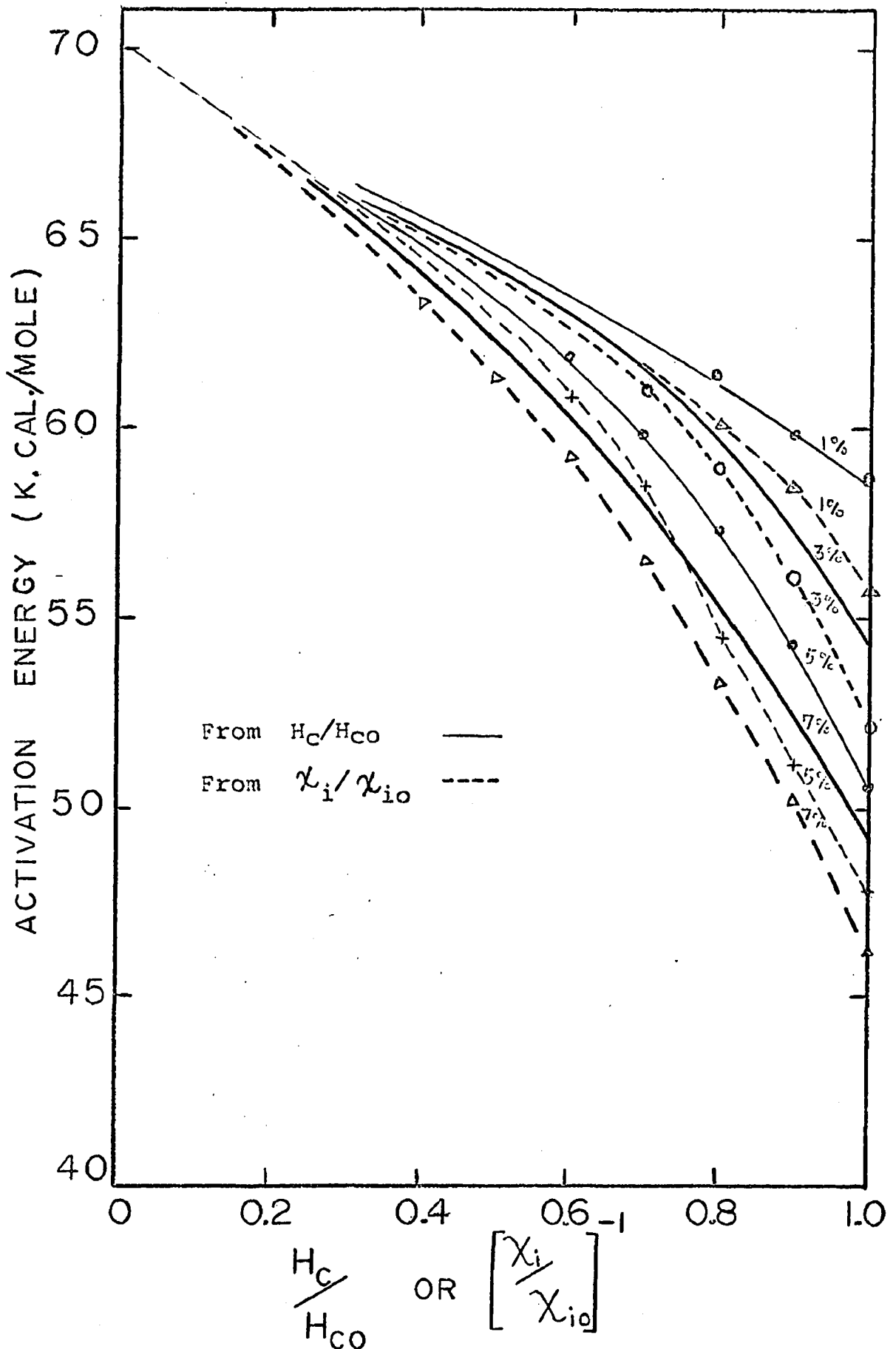


Fig. 4.3-15. The dependence of the apparent activation energy on the fractional recovery of the coercive field strength (solid lines) and of the initial susceptibility (dashed lines) for various degrees of plastic deformation.

mechanism of recovery process by assuming a model in which the recovery results by dislocations gliding over potential barrier with the aid of thermal activation. She made the assumption that the activation energy for recovery was a decreasing function of the mean internal stresses. If a linear relationship between internal stresses and square root of dislocation density be assumed, the present experimental results provide a basis for Kulhman's assumption.

#### Behaviour of Mechanical Hardness

Dislocations are introduced into a specimen during cold-work and its mechanical hardness is increased. The introduction of dislocations also increases the "magnetic hardness" of a ferromagnetic specimen -- an increase in the coercive field strength and a decrease in the initial susceptibility. In order to emphasize the relation between the mechanical hardness and magnetic hardness caused by dislocations, the recovery of microhardness of deformed specimens was studied in parallel to that of  $H_c$  and  $\chi_i$ .

The microhardness of 5% and 7% strained specimens was measured at various stages of recovery during isothermal and isochronal heat treatment. The results of the isothermal heat treatment are given in fig. (4.3-16) where the values of hardness are plotted as a function of the logarithm of annealing time at  $550^\circ$ ,  $575^\circ$  and  $600^\circ\text{C}$ . The results indicate



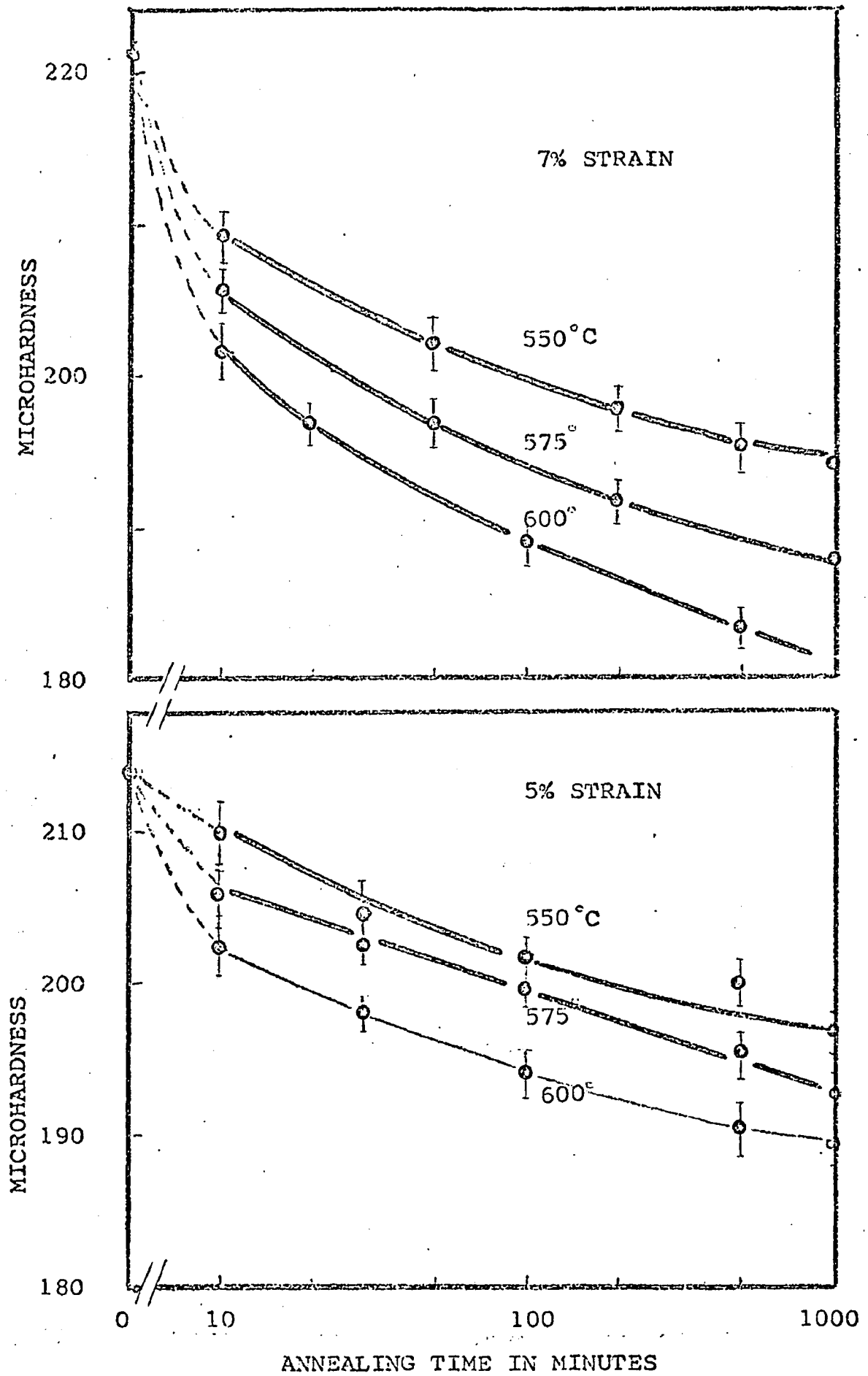


Fig.4.3-16. Isothermal recovery of microhardness of

Reproduced with permission of the copyright owner. Further reproduction prohibited without permission.

that in all cases, the hardness decreases almost linearly with the logarithm of annealing time. Similar logarithmic dependence is observed for  $H_C$  and  $\chi_i^{-1}$  during the later stages of isothermal annealing. This suggests a linear relationship between the mechanical hardness and the magnetic hardness in the later part of the recovery process. This agrees with the results of section(4.2) fig.4.2-3) based on the direct measurement of dislocation density and mechanical hardness at various stages of recovery. The results also show that at the same annealing temperature, the decrease in hardness for 7% strain is faster than that for 5% strain. This also is in agreement with the previous results on  $H_C$  and  $\chi_i^{-1}$  measurements. The results of isochronal annealing of 5% and 7% strained specimens, between 100° and 700°C at every 100° interval, are given in fig.(4.3-17); the specimens were treated for 30 minutes at each temperature.

There is however, a marked difference between the behaviour of  $H_C$  and  $\chi_i^{-1}$ , and the microhardness during the early stages of isothermal annealing. The microhardness sharply decreases within the first few minutes of annealing whereas at these temperatures an increase in  $H_C$  and  $\chi_i^{-1}$  are observed. The isochronal results support this fact. The hardness during isochronal recovery remains constant upto around 350°C and decreases sharply thereafter. This is again in contrast to the results of magnetic measurements during isochronal annealing where an increase in  $H_C$  and  $\chi_i^{-1}$  was observed. It can be concluded from the above results that up to the temperature of

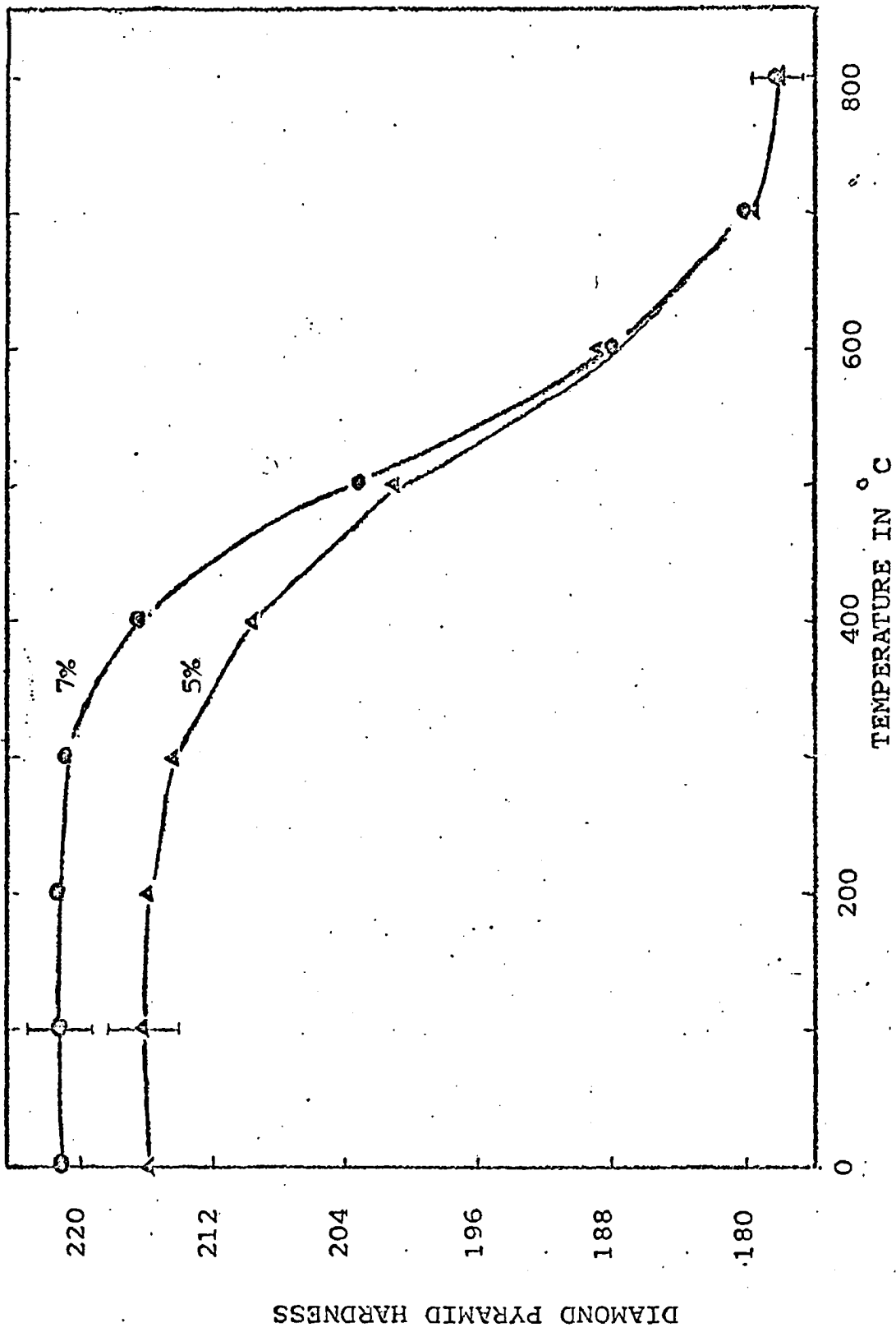


Fig.4.3-17. Isochronal recovery of microhardness of 5% and 7% strained specimens ( $\Delta t = 30$  min.)

350° C, no significant dislocation annealing takes place. The results also show that the increase in  $H_C$  and  $\chi_i^{-1}$  on aging at lower temperature is not consistent with hardness measurements.

### Interaction with Interstitial Atoms

During isochronal annealing of strained specimens, fig. (4.3-1), an increase in  $H_C$  and a decrease in  $\chi_i$  is observed. Similar behaviour is exhibited by  $H_C$  and  $\chi_i^{-1}$  during isothermal annealing at temperatures 550° C - 650° C. In order to obtain a better quantitative information about this phenomenon, 7% strained specimens were aged at temperatures in the range 200°-325° C and their  $H_C$  measured at various stages of aging process. The results are given in fig. (4.3-2) (top curves). The results show that  $H_C$  increases on aging, to values much higher than those prior to heat treatment and attains a maximum value which remains constant. At these temperatures there is no evidence of mobility of the dislocations; their density and arrangement remains unchanged. This is evidenced by the fact that on isochronal annealing, the hardness remains constant up to almost 350° C. Hence any increase in  $H_C$  can only be explained on the assumption that Bloch wall movement is comparatively more impeded by aged dislocations than the fresh ones.

In iron or iron silicon alloys, the impurities such as interstitial carbon and nitrogen are present. The interstitials

are known to have pronounced effects on domain wall mobility and magnetic aftereffects. The interstitials adept themselves to the direction of magnetization within the wall and its surrounding, causing the stabilization of the local magnetization and through this the position of the wall [71]. When dislocations are introduced into the specimen, the stress field of the dislocations exerts a dragging force on the interstitials and they move towards the dislocations with drift velocity which depends on the diffusion coefficient of the interstitials. The impurities will tend to form an enriched cloud around the dislocations. If the temperature is high enough to increase the diffusion rate, and if the concentration of the interstitials is sufficient, the dislocations will ultimately be saturated. Assuming that the increase in the coercive field is due to the diffusion of interstitial carbon atoms to dislocation, a maximum in the  $H_C$  value is expected. This maximum value will remain constant, even after prolonged aging, provided dislocation annealing is not taking place. This is shown in fig. (4.3-2).

Further evidence to the assumption that increase in  $H_C$  is caused by the diffusion of carbon atoms to dislocations is obtained by the knowledge of activation energy associated with the phenomenon. From the data in fig.(4.3-2) the aging time  $t$  at each temperature  $T$  in the range of 200-325°C necessary for a 20% increase in  $H_C$  ( $H_C/H_{C0} = 1.2$ ) is found. The logarithm of  $t$  is plotted against  $1000/T^{\circ}K$  in fig. (4.3-18) to yield a straight line. From the slope of this line

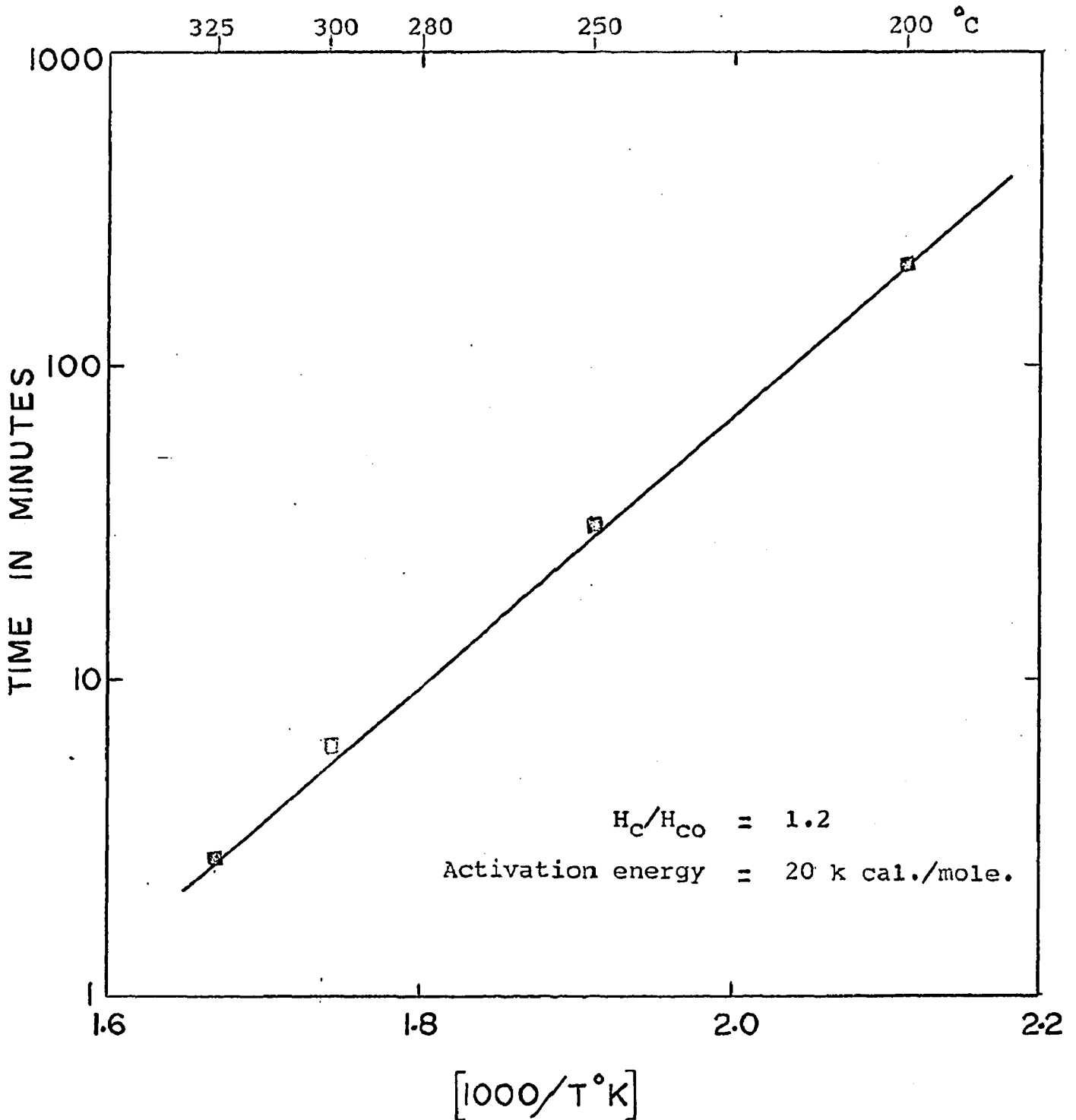


Fig.4.3-18. Temperature dependence of the time required for 20% increase in the coercive field strength for 7% strained specimen when annealed in the temperature range (200°C-325°C.)

value of activation energy associated with the process is calculated to be 20 kcal/mole. This value is almost the same as the value of the activation energy for the diffusion of carbon in  $\alpha$ -iron [52]. This confirms the assumption that the increase in  $H_C$  is caused by the diffusion of interstitial carbon atoms to dislocations.

On annealing in the temperature range  $550^\circ$  to  $650^\circ\text{C}$  the slip line arrangement of dislocations is disturbed and dislocation annealing takes place. This is evidenced by the decrease in mechanical hardness. Consequently the increase in  $H_C$  and the decrease in  $\chi_i$  is damped out as the temperature of heat treatment increases. At higher temperatures (about  $650^\circ$ ) the initial increase in  $H_C$  is not observed because the rate of dislocation annealing is much faster.

#### 4.4 TEMPERATURE DEPENDENCE OF COERCIVE FIELD STRENGTH

The present theories of coercive field strength based on dislocation model have been discussed in chapter II. These theories are developed on different models which make typical assumptions regarding the distribution of dislocations in the crystal and their specific interaction with the Bloch wall movement. At constant temperature, they all lead to a linear dependence of the coercive field strength  $H_C$ , on the square root of dislocation density  $N$  as

$$H_C = C N^{\frac{1}{2}} \quad (4.4-1)$$

Here the constant  $C$  symbolizes the proportionality constants in various expressions for  $H_C$  given by eqns (2.9), (2.11) and (2.12).

In all these expressions, the values of the constants differ numerically to a very large extent. This is because various material constants (e.g.,  $M_S$ ,  $\lambda$ ,  $K$ ,  $\delta$ ), enter the expressions for  $H_C$  in peculiar ways as a consequence of special assumptions made in the development of these theories. The experimental results discussed in section (4.2), based on direct measurement of  $H_C$  at room temperature and determination of dislocation density  $N$  by metallographic techniques, also confirmed the relationship given by (4.4-1). However, the measurements at room temperature are not enough exclusively to check the complete validity of these relationships. At room



temperature, only the effects of dislocation density varied by plastic deformation and annealing can be determined, while the material constants remain unchanged.

A conclusive check on the validity of the assumptions can be made only by studying the functional dependence of  $H_C$  on the material constants -- by varying them in a known way. This is possible by making measurements of  $H_C$  as a function of temperature since all these material constants are temperature dependent. As the values of all the material constants ( $M_S$ ,  $\lambda$ ,  $K$ ,  $\delta$ ) at room temperature and their temperature dependence are known, the value of the constant  $C$  in the expressions for  $H_C$  can be varied with temperature in a known way. For a true comparison with the theory, the dislocation density must remain strictly unchanged during the course of measurements. This can be achieved provided the measurements are made in a short time so that no appreciable annealing of dislocations takes place. In order to get a better insight into the mechanism of interaction between Bloch wall movement and dislocations, the study of the temperature dependence of  $H_C$  for undeformed and various deformed specimens were made. For further comparison, some iron-copper alloys, with the major portion of the available copper precipitated, were also used. The total duration of measurement of  $H_C$  between  $100^\circ$  and  $700^\circ\text{C}$  was about 10 minutes.

### Experimental Results

Fig. (4.4-1) shows the coercive field strength of iron-silicon specimens after various degrees of deformation as a function of temperature.

Fig. (4.4-2) shows the  $H_C - T$  behavior of undeformed iron-silicon alloy specimens together with that of three iron-copper alloys. The curves in this figure represent the ratio of the coercive field  $H_C$  at various temperatures to its value at  $20^\circ\text{C}$ ,  $H_C(20^\circ)$ . The iron-copper alloys containing 1%, 2%, and 3% copper were obtained by sintering from carbonyl iron and electrolytic copper. These specimens were annealed for 12 hours at  $875^\circ\text{C}$  in order to bring the copper in solution [17] and then aged at  $700^\circ\text{C}$  for 1000 minutes before their  $H_C - T$  behaviour was measured. It is known that during this treatment almost pure copper precipitates in the very early stages ( $\approx 10$  minutes) of aging, and further treatment causes the coagulation of the precipitated particles.

There is a striking difference between the  $H_C - T$  behaviour of deformed and undeformed specimens of Fe-Si alloy. In all the deformed specimens the coercive field strength as shown in fig. (4.4-1), first increases with rising temperature and subsequently falls rapidly after achieving a maximum. In the case of undeformed Fe-Si specimens, the  $H_C$  drops steadily with rising temperature.

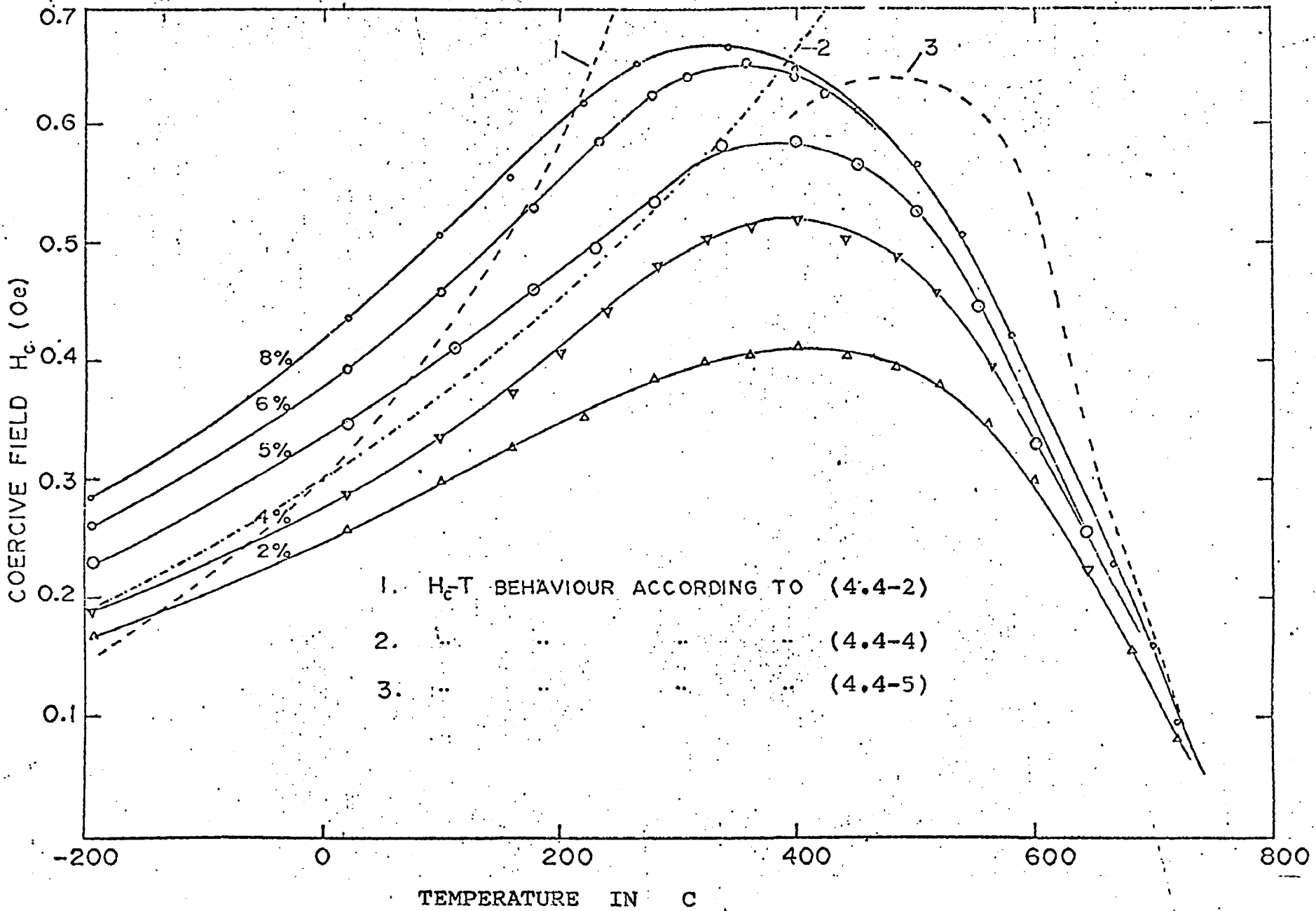


Fig.4.4-1. Coercive field  $H_c$  of deformed Fe-3.25Si alloy as function of temperature after various degrees of plastic deformation.

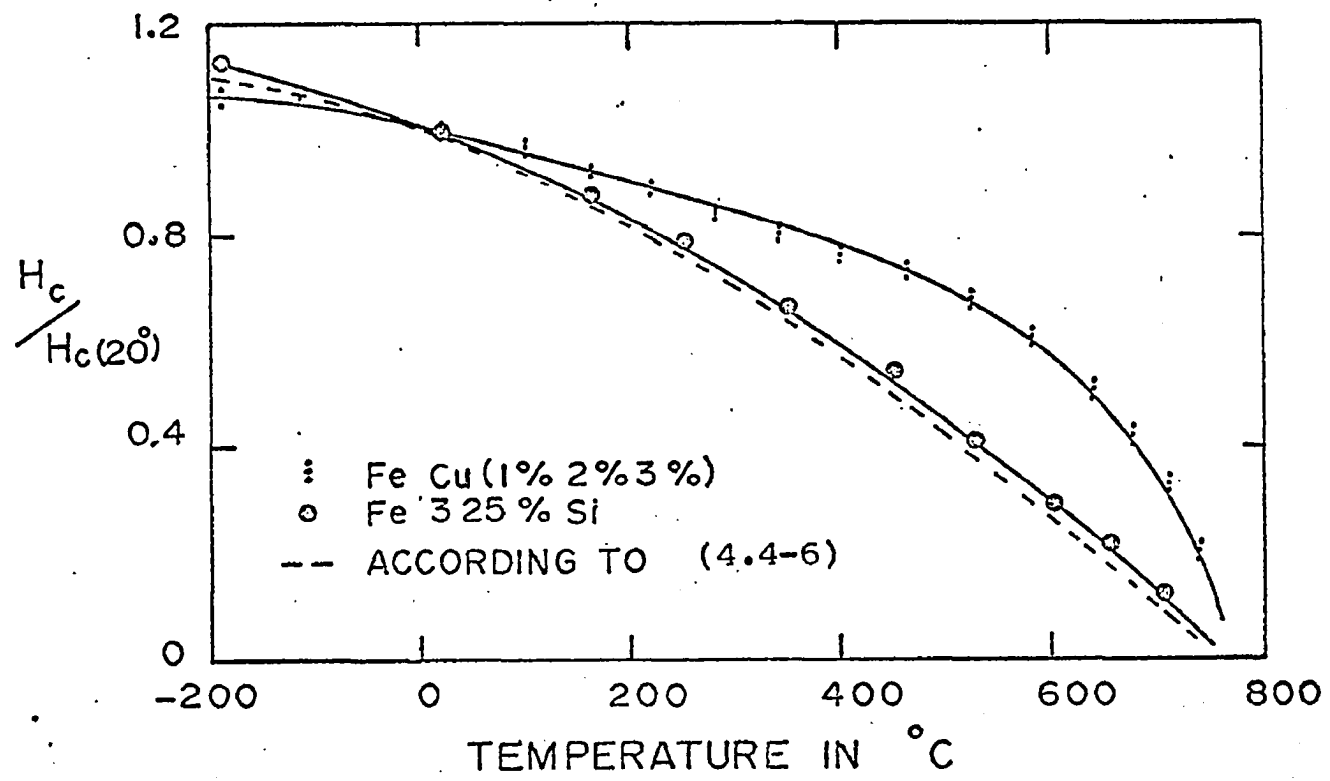


Fig.4.4-2 . Ratio of Coercive field  $H_c$  at various temperatures to its value at  $20^\circ\text{C}$   $H_c(20^\circ)$  as function of temperature of undeformed Fe-3.25%Si alloy, and of Fe-Cu alloys with up to 3 % Cu. The dashed curve represents H -T behaviour according to 4.4.6 normalised to  $H_c$  at  $20^\circ\text{C}$ .

With increasing deformation of the Fe-Si specimens the maximum in the  $H_c - T$  curve shifts towards lower temperatures. The experimental results are discussed in the following, in the light of predictions made by various theories of coercive field.

### Discussion

In iron-silicon alloys, at lower temperatures, the magnetocrystalline anisotropy energy  $\phi_K$  is considerably larger than the stress anisotropy  $\phi_S$  caused by the internal stresses. In this temperature range, there exists a well defined magnetic domain structure with  $[100]$  preferred magnetization direction. The theories of Vicena [7], Kersten [8], and Trauble [6] based on the interaction of Bloch wall with dislocations have been discussed in detail in chapter II. Vicena [7] calculated the coercive field by considering the effect of the stress field due to dislocations parallel to  $180^\circ$  Bloch wall on the wall movement in a cubic crystal. The temperature dependence of  $H_c$  from his model is given by

$$H_c = \frac{\lambda_{100}}{M_s K_1^{1/2}} \quad (4.4-2)$$

where  $M_s$  is the saturation magnetization,  $\lambda_{100}$  the saturation magnetostriction and  $K_1$  the anisotropy constant.

Kersten [8] based his model on a regular distribution of

dislocations located at equal distances and cylindrical bending of the Bloch wall under the influence of an external magnetizing field. This leads to the  $H_C - T$  behaviour expressed by

$$H_C = \text{const. } K_1^{\frac{1}{2}} \quad (4.4-3)$$

Trauble [6] assumed a statistical distribution of dislocations and the movement of large sections of Bloch walls. The model includes the interaction of all types of dislocation systems with the movement of  $90^\circ$  and  $180^\circ$  Bloch walls. For this case the  $H_C - T$  behavior obtained is

$$H_C = \text{const. } \frac{\delta \lambda_{100} (C_{11} - C_{12})}{M_S} \quad (4.4-4)$$

Here  $\delta$  is the Bloch wall thickness and  $C_{11}$  and  $C_{12}$  the constants of elasticity. All the above equations assume a constant density of dislocations.

The  $H_C - T$  behaviour expressed by equation (4.4-2) is shown by the dotted curve in fig. (4.4-1). The values of  $K_1$ ,  $\lambda_{100}$  and  $M_S$  at various temperatures are obtained from the works of Bozorth [1], Tatsumoto and Okamoto [62] and H. H. Patter [63] respectively. The curve is adjusted to an  $H_C$  value of 0.3 Oe at  $0^\circ\text{C}$ . It is evident that the rise in  $H_C$  with rising temperature as expected from Vicena's model does not agree with the experimental results. The

discrepancy may be due to the fact that the model represents a special case when the dislocations are located parallel to the  $180^\circ$  - Bloch wall, which is seldom encountered in nature. The Bloch wall movement would be much more restrained in the presence of dislocations parallel to its surface than if they were randomly distributed. The temperature dependence of  $H_C$  given by (4.4-3) also disagrees with the experimental results because  $K_1$  constantly decreases with rising temperature [1]. The failure of Kersten's model is because of its ideal nature, that is, regular distribution of dislocations, bending of Bloch wall free of stray fields. The experimental observations in fig.(4.2-4) suggest that the dislocation distribution in these specimens is far from ideal. Furthermore, the Bloch walls can not bend free of stray fields, which is contrary to the assumption in Kersten's theory.

The temperature dependence of  $H_C$  expected from eqn. (4.4-4) is shown by the dotted curve with the experimental results in fig. (4.4-1) for comparison. The results show that that the  $H_C - T$  behaviour up to about  $500^\circ\text{C}$  agrees reasonably with the theoretical model of Trauble [6]. The value of  $C_{11}$  and  $C_{12}$  used in eqn. (4.4-4) were taken from Lord and Beshers [64] and those for the Bloch wall thickness  $\delta$  obtained from a relation given by Kronmuller [3]. Here also the curve obtained from eqn. (4.4-4) is adjusted to an  $H_C$  value of 0.3 Oe at  $0^\circ\text{C}$ . In the evaluation of the

theoretical statements the values of the constants are of iron or of its alloys nearest in composition to Fe-3.25% Si. The error involved should not influence the  $H_C - T$  behaviour considerably and may be neglected.

Near the Curie temperature, the stress anisotropy  $\phi_s$  dominates the crystal anisotropy  $\phi_k$  in the deformed specimens. This is due to the rapid decrease in the crystal anisotropy with rising temperature while the stress anisotropy changes only little (due to some dislocation annealing and rearrangement). There is no well-defined domain structure and the preferred directions of magnetization are distributed irregularly. The magnetization changes occur predominantly due to rotational processes against the stress anisotropy energy. The coercive field  $H_C$  as a function of temperature is then approximately given by the expression [24]

$$H_C = \text{const.} \frac{\lambda_{100} G}{M_S} \quad (4.4-5)$$

where  $G$  is the modulus of elasticity in shear. The dotted curve (3) obtained from eqn. (4.4-5) is shown in fig. (4.4-1) where the values are adjusted to 0.3 Oe at 650°C. This seems to agree favourably with the experimental results near the Curie point.

The stress anisotropy is expected to increase with increasing degree of deformation while the crystal anisotropy is not affected. The maximum in the  $H_C - T$  curve



occurs at a temperature at which the stress and crystal anisotropies are approximately equal. Therefore, one would expect that a specimen with a higher degree of deformation, and thus with a greater stress anisotropy would exhibit an  $H_C - T$  maximum at a lower temperature than one with lower degree of deformation. The experimental results in fig. (4.4-1) confirm this observation. On the same basis one would expect that the  $H_C - T$  maximum in a highly deformed specimen would be shifted towards higher temperature if the temperature behaviour of  $H_C$  is measured at various stages of recovery. A specimen was annealed for 30 minutes at  $400^\circ\text{C}$  after 8% deformation and a shift in the  $H_C - T$  maximum towards a higher temperature was observed.

The results presented in Fig. (4.4-2) for undeformed iron-silicon and the iron-copper alloys with precipitated copper cannot be explained in the light of the above discussion. The predominant defect in the matrix of the iron-copper alloys is the copper precipitate as an impurity which is known to hinder the movement of Bloch walls [17]. The coercive field in the undeformed, well annealed iron-silicon specimens is influenced by minute traces of impurity and surface oxidation. Kersten [23] has calculated the coercive field due to stresses caused by nonmagnetic inclusions. His result leads to the  $H_C - T$  behaviour as

$$H_C = \text{const.} \frac{K_1^{1/2}}{M_s} \quad (4.4-6)$$

The dashed curve in fig. (4.4-2) represents the  $H_C - T$  behaviour according to eqn. (4.4-6) where values at various temperatures are normalized to  $H_C$  value at  $20^\circ\text{C}$ . This result almost exactly coincides with the experimental values for the Fe-3.25% Si specimen, and it is evident from fig. (4.4-2) that the  $H_C - T$  behaviour of the alloys with copper as impurity is quite similar to that given by eqn. (4.4-6).

The maxima in the  $H_C - T$  curve in fig. (4.4-1) correspond to the temperatures at which the crystal anisotropy energy  $\phi_k$  is equal to the stress anisotropy energy  $\phi_s$  for the strained specimens, i. e., when

$$\phi_k \approx \phi_s$$

since  $\phi_k \sim K_1$  and  $\phi_s \sim \lambda_{100} |\sigma_i|$

and also  $\sigma_i \sim \sqrt{N} \sim H_C$ ,

one expects  $\lambda_{100}^{(T)} H_C(\text{max.}) \sim K_1(T)$

where  $H_C(\text{max.})$  is the value of the coercive field at the maxima points occurring at temperature  $T$  in the  $H_C - T$  curves and  $K_1(T)$  and  $\lambda_{100}^{(T)}$  are the values of these constants at temperature  $T$ . The values of  $\lambda_{100} H_C(\text{max.})$  are plotted against  $K_1$  in fig. (4.4-3). The resulting straight line further supports the expectations of eqn. (4.4-4)

On the basis of the results of this section it may be concluded that in iron-silicon alloys, the magnetization changes occur by Bloch wall displacement up to around

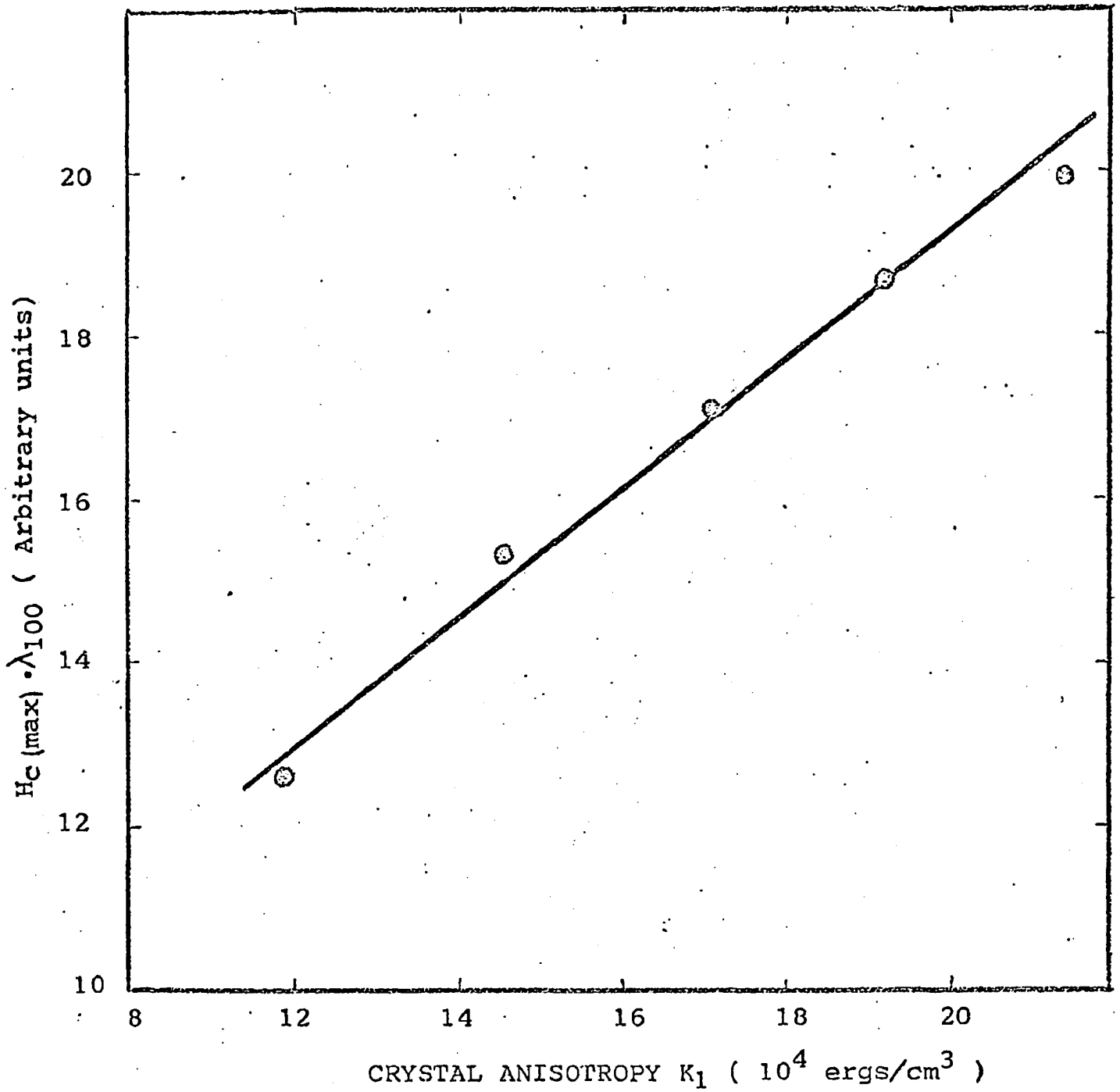


Fig. 4.4-3. Variation of  $H_c(\max) \cdot \lambda_{100}$  vs.  $K_1$  for Fe-Si alloy.

500° and above this temperature by rotational process. The experimental results are in agreement with the predictions of Trauble's theory of coercive field with respect to the dependence of  $H_c$  on deformation, dislocation, density, and temperature. Further information on the process of magnetization will be gained by studying the temperature dependence of initial susceptibility.

#### 4.5. TEMPERATURE DEPENDENCE OF INITIAL SUSCEPTIBILITY

The dependence of initial susceptibility on the density of dislocations was investigated and compared with theoretical models in section (4.2). In order to check the validity of those models further and complete the investigations, the dependence of the initial susceptibility of undeformed and deformed specimens was studied between  $-196^{\circ}$  and  $700^{\circ}\text{C}$ .

The results of the measurement of the initial susceptibility of iron-silicon specimens with various degrees of deformations are shown in fig. (4.5-1). In this figure, the ratio of the initial susceptibility  $\chi_i(T)$  at certain temperature  $T$  to its value at  $-196^{\circ}\text{C}$ , i.e.,  $\chi_i(-196^{\circ})$ , has been plotted against the temperature  $T$  of measurement. The  $\chi_i - T$  curve of the undeformed specimen passes through a minimum around room temperature and exhibits a second minimum around  $450^{\circ}\text{C}$ . These minima and the maximum are gradually flattened with increasing deformation until the specimen with 7% deformation shows an almost smooth curve. The  $\chi_i(T)$  values of specimens with higher degrees of deformation drop faster with temperature up to about  $450^{\circ}\text{C}$  than those with lower degrees of deformation. The maximum is shifted from  $350^{\circ}\text{C}$  to lower temperatures as the deformation increases.

The theoretical relation expressed by Kersten leads to a temperature dependence of  $\chi_i$  as

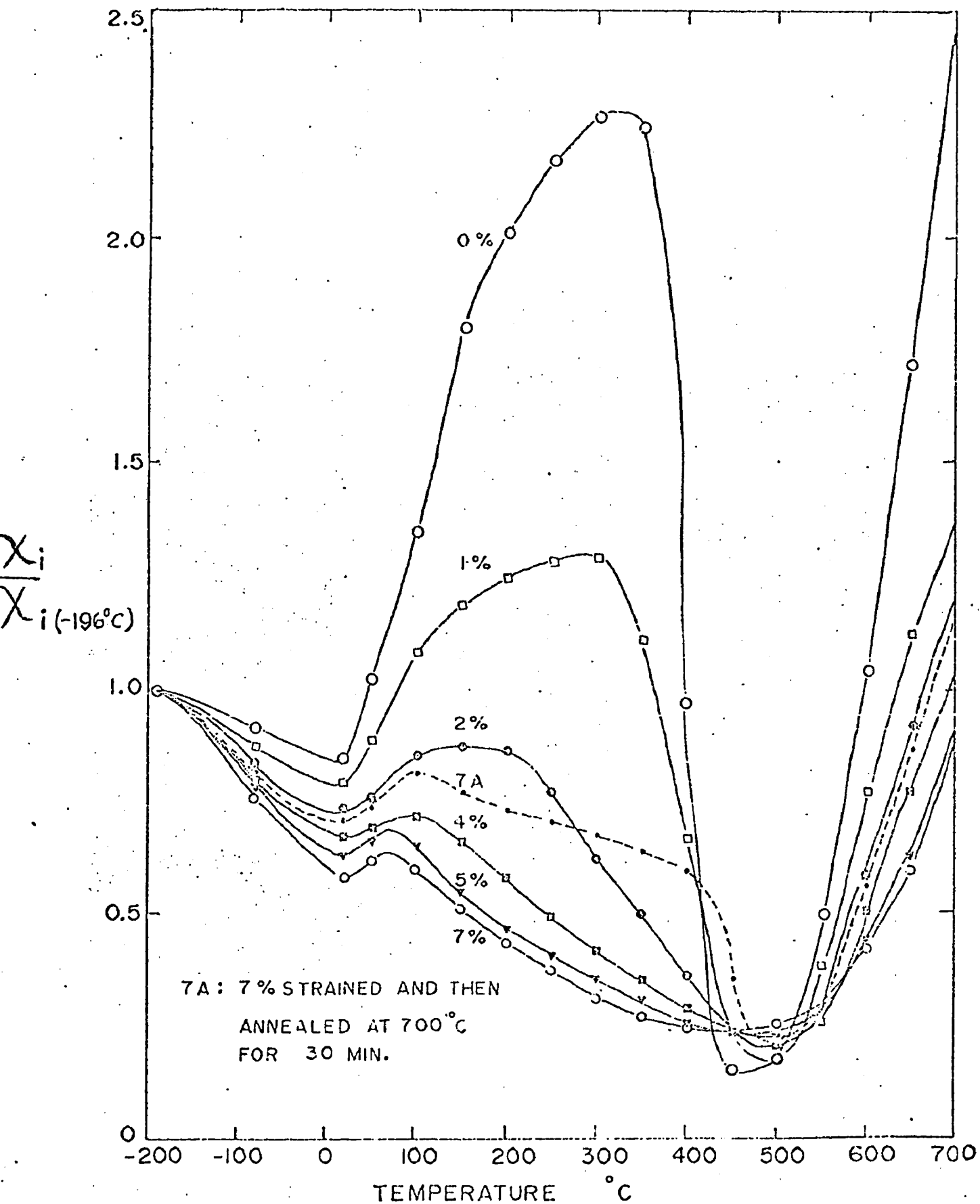


Fig.4.5-1. Ratio of the initial susceptibility  $\chi_i(T)$  at various temperatures to its value at  $-196^\circ\text{C}$   $\chi_i(-196^\circ\text{C})$  as a function of temperature of undeformed and deformed Fe-3.25%Si. alloy specimens.

$$\chi_i(T) = (\text{const.}) M_S / K_1^{1/2} d \quad (4.5-1)$$

where  $d$  = average domain width

Based on the interaction of Bloch wall movement with the dislocations, the temperature dependence of  $\chi_i$  according to Trauble is given by

$$\chi_i(T) = M_S^2 / G \lambda d K_1^{1/4} \quad (4.5-2)$$

According to equations (4.5-1) and (4.5-2),  $\chi_i$  would be expected to increase with rising temperature up to slightly below the Curie temperature. This is because the drop in  $K_1$  is much faster compared to  $M_S$  with rising temperature. With the approach of Curie temperature  $\chi_i$  steeply drops to zero. Kersten showed that several soft magnetic materials exhibit the  $M_S / K_1^{1/2}$  dependence of  $\chi_i$  on temperature when the domain width  $d$  in eqn. (4.5-1) is assumed to be independent of temperature. Certain ferromagnetic materials exhibit anomalous  $\chi_i$ -T behavior, much different from that expected theoretically. Snoek [65] found that the initial susceptibility of carbonyl iron is abnormally low between  $-50^\circ\text{C}$  and  $+50^\circ\text{C}$ . He associated this phenomenon to the diffusion of carbon and nitrogen. Anomalous behaviour of similar nature was observed in several materials and several temperature ranges [66-68]. An attempt is made to explain the present experimental results qualitatively as the existing theories fail to offer adequate explanation.

The number of dislocations and vacancies introduced in the specimens depends on the degree of plastic deformation. Both these defects interact with Bloch walls. However, the effect of dislocations is much stronger than that of vacancies. At lower temperatures the wall occupies a position of minimum energy and contains a certain number of these defects. As the temperature rises, the interstitial carbon atoms diffusing into the Bloch walls cause a gradual drop in the initial susceptibility and their combined effect on the mobility of the domain walls may be responsible for a faster drop in  $\chi_i$  in the deformed specimens than in the undeformed one. The flattening of the  $\chi_i - T$  maximum and its shifting towards lower temperature with increasing deformation indicates the role of stress anisotropy energy  $\phi_s$  in determining the  $\chi_i - T$  behaviour, since  $\phi_s$  increases with deformation. A gradual shift of the minimum from  $450^\circ\text{C}$  in the undeformed specimen towards higher temperatures in the deformed specimens is also observed. In this temperature region the stress anisotropy dominates over the crystal anisotropy and the magnetization is due to rotational processes. In fig. (4.5-1), curve 7A, shows the  $\chi_i - T$  behaviour of a specimen with 7% deformation followed by 30 minutes of annealing at  $700^\circ\text{C}$ . The behaviour is similar to that of a specimen with a lower degree of deformation and hence, low stress anisotropy.



The  $\chi_i - T$  behaviour of the undeformed specimen around room temperature may be associated with the diffusion of carbon atoms. The interstitial carbon atoms redistribute themselves around room temperature and according to Snoek [65] affect the susceptibility by migrating to Bloch walls. The anomaly at higher temperature could be due to vacancy migration. According to Dietze [67] the energy of a lattice vacancy depends on the direction of magnetization in its immediate neighborhood. The orientation of magnetization in a Bloch wall changes continuously from one crystallographic preferred direction to another one. This results in an interaction of the vacancies with the Bloch walls. The thermal energy facilitates the diffusion of the vacancies towards the Bloch walls and a new vacancy concentration is established inside the walls, which further hinders the wall movement and causes a drop in  $\chi_i$  above 300°C.

The assumption that domain width  $d$  in eqn. (4.5-1) remains constant is not quite valid; the domain width  $d$  is found to vary with temperature. Startseva and Shur [69] showed that  $d - T$  behaviour of iron-silicon specimens having 3.2 and 3.8% silicon, and crystallographic characteristics similar to the present specimens, exhibits a minimum around 350°C and a maximum around 450°C. If this behaviour of domain width  $d$  is taken into account in eqn. (4.5-1), a  $\chi_i - T$  behaviour similar to that in fig. (4.5-1) is expected.

Though the anomalies in the  $\chi_i - T$  behaviour have been reported in the literature, the present investigations had the objective to study the effects of dislocations and deformation on the magnetization at elevated temperatures. The present experimental results cannot be explained adequately in the light of the existing theories of magnetization. However they provide a basis for the improvement of the theories.

## CHAPTER VI

### CONCLUSIONS

The coercive field strength  $H_c$  and the initial susceptibility  $\chi_i$  of soft magnetic materials are strongly influenced by crystal imperfections such as dislocations. Dislocations are introduced on plastic deformation in tension and their density and arrangement are varied by heat treatment. The presence of dislocations has pronounced effects on the temperature dependence of the magnetic properties. The results show that:

(i) The coercive field strength  $H_c$  varies directly and the initial susceptibility inversely as the fourth root of the plastic tensile-strain.

(ii) The coercive field strength and the mechanical hardness are proportional directly, and the initial susceptibility inversely, to the square root of the dislocation density. These results are in agreement with Träuble's theoretical predictions.

(iii) On aging at lower temperatures ( $200^{\circ}$ - $325^{\circ}$ C) the coercive field strength of deformed specimens increases to a maximum and remains constant. The activation energy associated with this process is equal to that of the diffusion of carbon in alpha-iron. The increase in  $H_c$  and the decrease in  $\chi_i$  are attributed to the aging of dislocations.

(iv) During annealing at higher temperatures, (550°-720°C), the density of dislocations decreases. However, contrary to the expectations, during the initial stages of recovery up to 650°C, an increase in  $H_c$  and decrease in  $\chi_i$  was observed.

(v) For the later stages of isothermal recovery the coercive field strength  $H_c$  and the reciprocal of the initial susceptibility  $\chi_i$ , decrease showing a linear dependence on the logarithm of the annealing time; i.e., the recovery may be represented by an equation of the form  $H_c$  (or  $\chi_i^{-1}$ ) =  $b - a \ln t$  where  $b$  and  $a$  are constants depending on the degree of plastic deformation and the annealing temperature and 't' is the annealing time.

(vi) The activation energy associated with the recovery process is found to be strain-dependent. It decreases with increasing strain and increases during annealing as the recovery progresses.

(vii) On the analysis of the observed results an expression for the kinetics of annealing of dislocations is obtained. This also shows the applicability of magnetic measurements to metallurgical problems.

(viii) The coercive field strength of undeformed specimen decreases continuously with rising temperature. This temperature dependence is determined essentially by the interaction of the Bloch wall movement with the nonmagnetic inclusions.

(ix) The coercive field strength of deformed specimen increases considerably from its value at  $-196^{\circ}\text{C}$  to a maximum at about  $500^{\circ}\text{C}$  and then drops steeply to zero at the approach of the Curie temperature. It is concluded that below  $500^{\circ}\text{C}$  (magnetocrystalline anisotropy energy  $\phi_K \gg$  stress anisotropy energy  $\phi_S$ ), the change of magnetization takes place by the movement of Bloch walls and above this temperature where stress anisotropy predominates, by rotational process. This temperature dependence shows agreement with the results of the theoretical models developed for the various modes of magnetization.

(x) The temperature dependence of the initial susceptibility completely disagrees with all theoretical models. Certain anomalies are found in this case and an attempt has been made to explain the various maxima and minima which occur in the observed  $\chi_i - T$  behaviour.

The present investigations are an attempt to relate the magnetic properties to the density of dislocations determined metallographically. The results offer a test to the validity of the assumptions underlying the theories of hysteresis which is a complicated phenomenon. These results should prove useful in a better understanding and the modification of the theories of hysteresis.

An immediate extension of the work could be to study the effect of increased plastic deformation and higher dislocation density using optical and electron microscopy. Movement of Bloch walls in specimens having dislocations or

nonmagnetic inclusions may be studied in alternating fields of various frequencies and wave shapes. Optical techniques and high speed photography of domain walls in motion will give further clues towards the understanding of the phenomenon of hysteresis and help in verifying the assumptions on the interaction of defects with the domain walls. The anomalies found in the behaviour of  $\chi_i$  may be studied further in the light of magnetic aftereffects. It is possible that in the dynamic studies one may find the answer to some of the questions that have arisen from the present investigations.

## REFERENCES

- [1] R. M. Bozorth, "Ferromagnetism", 8th Printing, Van Nostrand, Princeton, N. J., 1964.
- [2] C. Kittel and J. K. Galt Rev. Mod. Phys. 21, 541 (1949), Solid state physics, 3, 439(1956).
- [3] H. Kronmüller in "Moderne Probleme der Metallphysik" (A. Seeger ed.) Vol. II, Springer, Berlin, 1965.
- [4] W. F. Brown Jr. "Micromagnetics", Interscience, Newyork 1963.
- [5] E. Kneller "Ferromagnetismus", Springer, Berlin, 1962.
- [6] H. Träuble in "Moderne Probleme der Metallphysik" (A. Seeger ed.) Vol. II, Springer, Berlin, 1963.
- in "Magnetism and Metallurgy", (A. Berkovitz and E. Kneller eds.) Vol II, Academic Press, 1969.
- [7] F. Vicena Czech. J. Phys. 5, 480 (1955), Czech. J. Phys. 9, 187 (1957).
- [8] M. Kersten Z. angew. Phys. 8, 313 (1956), Z. angew. Phys. 8, 382 (1956), Z. angew. Phys. 8, 496 (1956).
- [9] M. Kersten Ann. Phys. 20, 337(1957).
- [10] H. Bilger and H. Träuble Phys. Stat. Sol. 10, 755 (1965).
- [11] H. Bilger Phys. Stat. Sol. 18, 207 (1966).
- [12] H. Dietrich and E. Kneller Z. Metallk. 47 , 672 (1956) Z. Metallk. 47 , 716 (1956)
- [13] G. Rieder Abh. d. Braunsch. Wiss. Ges. II, 20, (1959), Z. angew. Phys. 9, 187 (1957), Z. angew. Phys. Math. U. Mech. 40, (1960).

- [14] K. H. Pfeffer            Phys. Stat. Sol. 19, 735 (1967)  
                               Phys. Stat. Sol. 20, 395 (1967)
- [15] A. Seeger, H. Kronmüller, H. Rieger  
       and H. Träuble            J. Appl. Phys. 35, 740 (1964)
- [16] L. J. Dijkstra            Phys. Rev. 79, 979 (1950)  
       and C. Wert
- [17] A. H. Qureshi            Z. Metallk. 52, 799 (1961)
- [18] Z. Malek                    Czech. J. Phys. 5, 613 (1959)
- [19] I. Ya. Dektyar            Fiz. Metal. Metall. 12, 97 (1961)  
       and D. A. Levina
- [20] L. Neel                    Ann. Univ. Grenoble 22, 299 (1946)  
                               Physica, 15, 225 (1949)
- [21] E. Kondorski            Soviet Phys. 11, 597 (1937)
- [22] M. Kersten in            "Probleme der technischen magnet-  
                               isierung Kurve", (R. Becker ed.)  
                               Springer, Berlin, 1938
- [23] M. Kersten              "Grundlagen einer Theory der  
                               Ferromagnetischen Hysterese Und  
                               der Koerzitivkraft", Hirzel,  
                               Leipzig, 1943
- [24] R. Beker and            "Ferromagnetismus", Springer, Berlin,  
       W. Döring              1938
- [25] J. B. Goodenough        Phys. Rev. 95, 917 (1954)  
                               Phys. Rev. 103, 356 (1956)
- [26] E. Kondorski            Dokl. Akad. Nauk SSSR 68, 37 (1949)
- [27] A. Cottrel                "Theory of Crystal Dislocations"  
                               Oxford Univ. Press, 1962
- [28] J. Fridel                 "Dislocations", Pergamon Press, 1964
- [29] A. Seeger                "Handbuch der Physik", Vol VII  
                               Springer, Berlin, 1958



- [30] H. G. Van Bueren "Imperfections in Crystals"  
North Holland, Amsterdam 1960
- [31] S. Amelinckx in "Direct observation of Dislocations"  
Suppl. 6, Solid State Physics  
Academic Press, 1964
- [32] C. E. Morris Metal Progress 56, 696 (1949)
- [33] C. G. Dunn and W. R. Hibbard Acta Met. 3, 409 (1955)
- [34] W. R. Hibbard and C. G. Dunn Acta Met. 4, 306 (1956)
- [35] J. C. Suits and J. R. Low Acta Met. 5, 285 (1957)
- [36] H. W. Pickering Acta Met. 13, 437 (1965)
- [37] R. W. Cahn J. Inst. Metals. 76, 121 (1953)
- [38] J. F. NYE. Acta Met. 1, 153 (1953)
- [39] J. J. Gilman Acta Met 3, 277 (1955)
- [40] F. L. Vogel, W.G. Pfann, E. E. Thomas and H. E. Corey Phys. Rev. 90, 489 (1953)
- [41] J. J. Gilman and W. G. Johnston J. Appl. Phys. 27, 101 S(1956)
- [42] F. L. Vogel Acta Met. 3, 95 (1955)
- [43] W.S. Paxton and T.S.Nilan J. Appl. Phys. 26, 494 (1955)
- [44] R. Carey and E.D.Isaac "Magnetic Domains and Techniques for their Observation"  
English Univ.Press,London,1966.
- [45] T. D. Yensen and M. A. Ziegler Trans. Am. Soc. Met. 23, 556 (1953)  
Trans. Am. Inst. Min. Met. Egrs. 116, 397 (1953)
- [46] J. T. Michalak and H. W. Paxton Trans. AIME 221, 850 (1951)
- [47] D. Kuhlmann A. Phys. 124, 468 (1947)

- 48 S. Mader in "Moderne Probleme der Metallphysik" (A. Seeger ed.) Vol. I, Academic Press Newyork, 1969.
- 49 A. S. Keh Phil. Mag. 12, 9 (1965)
- 50 W. Koster and L. Bangert Acta Met. 3, 274 (1955)
- 51 A. S. Keh in "Direct Observation of Imperfections in Crystals" Inter Science, 1962
- 52 C. Zener and C. Wert Phys. Rev. 76, 1169 (1949)
- 53 B. A. Lilley Phil. Mag. 41, 792 (1952)
- 54 H. Bilger Phys. Stat. Sol. 18, K-135 (1966)
- 55 M. Asanuma J. Phys. Soc. Japan 15 1469 (1960)
- 56 H. Scharf and P. Klimanek Phys. Stat. Sol. 11, K-145 (1965)
- 57 R. J. Borg and E. E. Birchenall Trans. Met. Soc. AIME, 218, 980 (1960)
- 58 D. Krause Z. Phys. 168, 239 (1962)
- 59 H. Rieger Phys. Stat. Sol. 8, 283 (1965)
- 60 E. Köster Phys. Stat. Sol. 19, 153 (1967)
- 61 A. Schauer Z. angew. Phys. 15 90 (1963)
- 62 E. Tatsumoto and T. Okamoto J. Phys. Soc. Japan, 14, 1588, (1959)
- 63 H. H. Patter Proc. Roy. Soc. (London), A 146, 362 (1934)
- 64 A. E. Lord and D. M. Bishers J. Appl. Phys. 36, 1620 (1965)  
J. Appl. Phys. 36, 1620 (1965)
- 65 J. L. Snoek Physica, 5, 663(1938)  
Physica, 6, 161(1939)
- 66 H. Fahlenbrach and G. Sommerkorn Tech. Mitt. Krupp 15, 161 (1957)

- [67] H. D. Dietze            A. Phys. 149, 276 (1957)  
Tech. Mitt. Krupp. 17, 67 (1959)  
Phys. Stat. Sol. 3, 2309 (1968)
- [68] H. Kronmüller        "Nachwirkung in Ferromagnetika",  
Springer, Berlin, 1968
- [69] I. Ye. Startseva       Fiz. Metal. Metall. 25, 298 (1968)  
and Ya. S. Shur
- [70] A.S.Keh and            in "Electron Microscopy and Strength  
Weissmann               Crystals" Wiley, New York, 1963.
- [71] G.W.Rathenau         "Magnetism and Metallurgy"  
and G.De Vries         (A.Berkovitz and E.Kneller eds.)  
Academic Press, New York, 1969.

## VITA AUCTORIS

The author was born in Makandpur (Bhagalpur), India, in 1936. He passed the Matriculation examination of Patna University ( T.N.J.Collegiate School Bhagalpur) in 1950. He received the B. Sc.(Hons.) degree from Bihar University in 1955, the Diploma of the Indian Institute of Science Bangalore, in 1959, and M. Sc. degree from the University of Keele, England in 1965.

From 1959 to 1964 he was Lecturer at Bihar College of Engineering, Patna University, Patna, India. From 1965 to 1967 he was with the Radio and Space Research Station, Slough, England. Currently he is a candidate for the Ph. D. degree at the University of Windsor, Windsor, Ontario.

\* \* \*

Parts of this work have been published in the following journals ;

1. J. Appl. Phys. 41, 1042 ( 1970 )
2. I.E.E.E. Trans. on Magnetics, vol. Mag 6, 705 ( 1070)
3. J. Appl. Phys. 42, 1785 ( 1971 )
4. I.E.E.E. Trans. on Magnetics, vol. Mag 7, no. 3. (1971).

\* \* \*